MINISTÉRIO DA CIÊNCIA, TECNOLOGIA, INOVAÇÕES E COMUNICAÇÕES
INSTITUTO NACIONAL DE PESQUISAS ESPACIAIS

sid.inpe.br/mtc-m21b/2017/09.12.20.07-TDI

SYNCHRONIZATION AND CONTROL IN NETWORKS WITH STRONGLY TIME-DELAYED COUPLINGS

Marcos Daniel Nogueira Maia

Doctorate Thesis of the Graduate Course in Applied Computing, guided by Drs. Elbert Einstein Nehrer Macau, and Tiago Pereira da Silva, approved in October 03, 2017.

URL of the original document:
<http://urlib.net/8JMKD3MGP3W34P/3PKDKT8>

INPE
São José dos Campos
2017

PUBLISHED BY:

Instituto Nacional de Pesquisas Espaciais - INPE
Gabinete do Diretor (GB)
Serviço de Informação e Documentação (SID)
Caixa Postal 515 - CEP 12.245-970
São José dos Campos - SP - Brasil
Tel.:(012) 3208-6923/6921
E-mail: pubtc@inpe.br

COMMISSION OF BOARD OF PUBLISHING AND PRESERVATION OF INPE INTELLECTUAL PRODUCTION (DE/DIR-544):
Chairperson:
Maria do Carmo de Andrade Nono - Conselho de Pós-Graduação (CPG)
Members:
Dr. Plínio Carlos Alvalá - Centro de Ciência do Sistema Terrestre (CST)
Dr. André de Castro Milone - Coordenação de Ciências Espaciais e Atmosféricas (CEA)
Dra. Carina de Barros Melo - Coordenação de Laboratórios Associados (CTE)
Dr. Evandro Marconi Rocco - Coordenação de Engenharia e Tecnologia Espacial (ETE)
Dr. Hermann Johann Heinrich Kux - Coordenação de Observação da Terra (OBT)
Dr. Marley Cavalcante de Lima Moscati - Centro de Previsão de Tempo e Estudos Climáticos (CPT)
Silvia Castro Marcelino - Serviço de Informação e Documentação (SID) **DIGITAL LIBRARY:**
Dr. Gerald Jean Francis Banon
Clayton Martins Pereira - Serviço de Informação e Documentação (SID)
DOCUMENT REVIEW:
Simone Angélica Del Ducca Barbedo - Serviço de Informação e Documentação (SID)
Yolanda Ribeiro da Silva Souza - Serviço de Informação e Documentação (SID)
ELECTRONIC EDITING:
Marcelo de Castro Pazos - Serviço de Informação e Documentação (SID)
André Luis Dias Fernandes - Serviço de Informação e Documentação (SID)

MINISTÉRIO DA CIÊNCIA, TECNOLOGIA, INOVAÇÕES E COMUNICAÇÕES
INSTITUTO NACIONAL DE PESQUISAS ESPACIAIS

sid.inpe.br/mtc-m21b/2017/09.12.20.07-TDI

SYNCHRONIZATION AND CONTROL IN NETWORKS WITH STRONGLY TIME-DELAYED COUPLINGS

Marcos Daniel Nogueira Maia

Doctorate Thesis of the Graduate Course in Applied Computing, guided by Drs. Elbert Einstein Nehrer Macau, and Tiago Pereira da Silva, approved in October 03, 2017.

URL of the original document:
<http://urlib.net/8JMKD3MGP3W34P/3PKDKT8>

INPE
São José dos Campos
2017

Cataloging in Publication Data

Maia, Marcos Daniel Nogueira.
M28s Synchronization and control in networks with strongly time-delayed couplings / Marcos Daniel Nogueira Maia. – São José dos Campos : INPE, 2017.
xvi + 107 p. ; (sid.inpe.br/mtc-m21b/2017/09.12.20.07-TDI)

Thesis (Doctorate in Applied Computing) – Instituto Nacional de Pesquisas Espaciais, São José dos Campos, 2017.
Guiding : Drs. Elbert Einstein Nehrer Macau, and Tiago Pereira da Silva.

1. Synchronization. 2. Complex networks. 3. Time-dalay. I.Title.

CDU 004.93'1

Esta obra foi licenciada sob uma Licença Creative Commons Atribuição-NãoComercial 3.0 Não Adaptada.

This work is licensed under a Creative Commons Attribution-NonCommercial 3.0 Unported License.

Aluno (a): ***Marcos Daniel Nogueira Maia***

Título: "SYNCHRONIZATION AND CONTROL IN NETWORKS WITH STRONGLY TIME-DELAYED COUPLINGS"

Aprovado (a) pela Banca Examinadora em cumprimento ao requisito exigido para obtenção do Título de ***Doutor(a)*** em ***Computação Aplicada***

Dra. Margarete Oliveira Domingues
Presidente / INPE / SJCampos - SP

Dr. Elbert Einstein Nehrer Macau
Orientador(a) / INPE / São José dos Campos - SP

Dr. Tiago Pereira da Silva
Orientador(a) / USP / São Carlos - SP

Dr. Lamartine Nogueira Frutuoso Guimarães
Membro da Banca / INPE / SJCampos - SP

Dr. Solon Venâncio de Carvalho
Membro da Banca / INPE / SJCampos - SP

Dr. Takashi Yoneyama
Convidado(a) / ITA / SJCampos - SP

Dr. José Roberto Castilho Piqueira
Convidado(a) / USP / São Paulo - SP

Este trabalho foi aprovado por:

( ) maioria simples

(x) unanimidade

São José dos Campos, 03 de outubro de 2017

ACKNOWLEDGEMENTS

I thank the Lord for the gift of life. I thank the support of my family, especially my wife Lidiana Aquino who sacrificed her work and personal projects to be with me and take care of me whenever we go.

I thank also to the professors that I have met during the several courses, seminars, etc, not only at INPE but also at USP, Humboldt, and TU Berlin, that passed a fraction of their knowledge to me. In special, I thank my supervisors Elbert Macau, Tiago Pereira, and Serhiy Yanchuk. Through their guidance, advice, and teaching I could accomplish several aims traced at the beginning of my Ph.D. and gain/improve my skills regarding the study, research, and several aspects of the common life.

I will not cite names but I also thank my colleagues at the upper cited institutions, to whom I could chat not only about mathematics, science and so on but also about our personal life.

My work was supported by CAPES and, during my stay at Humboldt/TU Berlin, while in the Ph.D. sandwich period, by CNPq grant 233718/2014-1. Therefore, at last, but not least important, I thank those institutions for the financial support.

ABSTRACT

The stability of synchronization and control in networks of dynamical systems with strongly delayed connections is investigated. Strict conditions for both, synchronization of stable periodic and equilibrium solutions , and control of unstable equilibrium are obtained. With a network model including self-feedback delay, the existence of a critical coupling strength κ_c is demonstrated, which is related to the network structure, isolated vector field and coupling function, such that for large delay and coupling strength $\kappa < \kappa_c$ the network undergoes to stable synchronization. Moreover, it is derived that for heterogeneous networks, $\kappa_c \to 0$ as the network size grows to infinity, unless the coupling parameter scales with the maximum degree. In contrast, for random networks, the interval of coupling strengths that leads to stable synchronization is the maximum possible when the connectivity threshold is crossed making the network connected. Based on the network structure, the scaling of the coupling parameter, which allows for a synchronization, is derived. And, with a network model consisting of instantaneous self-connections, it is shown that it is possible to stabilize synchronous equilibrium that is unstable in an isolated system. Such a control close to a Hopf bifurcation is studied in details and strict conditions for the stability are obtained. In particular, it is demonstrated that the stabilization domains in parameter space are reappearing periodically and decreasing in size with the increase of time-delays. Also, the frequency of the reappearance of the control domains and the number spectral roots of the adjacency matrix are closely dependent, for instance, the number of cycle multi-partitions of the graph indicates the reappearance frequency of the control domains.

SINCRONIZAÇÃO E CONTROLE EM REDES COM ACOPLAMENTO DE ATRASO TEMPORAL LONGO

RESUMO

Nesta tese investiga-se a estabilidade da sincronização e o controle em redes de sistemas dinâmicos onde o acoplamento se dá com atraso grande. São obtidas condições analíticas para ambos, a saber, sincronização de soluções periódicas e equilíbrios estáveis e controle de equilíbrio instáveis. Com um modelo de rede que inclui atraso com auto-alimentação, mostra-se a existência de um parâmetro crítico de acoplamento, κ_c, que depende apenas da estrutura da rede, do campo de vetores e da função de acoplamento, tal que para atraso grande e parâmetro de acoplamento $\kappa < \kappa_c$ a rede apresenta uma sincronização estável. Além disso, mostra-se que para redes heterogêneas, $\kappa_c \to 0$ ao passo que o número de nós da rede cresce ao infinito, a menos que o parâmetro de acoplamento κ é escalonado com o grau máximo da rede. Em contrapartida, evidencia-se que para redes aleatórias, o intervalo de parâmetros de acoplamento que induzem sincronização estável é o máximo possível quando o limiar de conectividade da rede é atingindo fazendo com que a mesma se torne conectada. Baseando-se na estrutura da rede, propriedades de escalonamento do parâmetro de acoplamento são derivadas, permitindo sincronização estável. E, com um modelo de rede consistindo de auto-alimentação instantânea, verifica-se que é possível estabilizar soluções de equilíbrio que são instáveis no sistema isolado. Este cenário de controle quando o sistema isolado está próximo da bifurcação de Hopf é estudado em detalhes e então condições analíticas para a estabilidade são obtidas. Em particular, demonstra-se que os domínios de estabilização no espaço de parâmetros são periódicos e decrescentes ao passo que o atraso cresce. Além disso, evidencia-se como a frequência de reaparecimento de tais domínios é influenciada pelo número de raízes espectrais da matriz de adjacência do grafo, que por sua vez está relacionado com, por exemplo, as multipartições cíclicas do grafo.

LIST OF FIGURES

Pág.

2.1 Example of directed graph 14
2.2 A regular directed graph. 21
2.3 Illustrations of BA and ER networks. 22

3.1 Solutions of a DDE for different history functions. 26
3.2 Numerically computed spectrum of two Stuart-Landau oscillators. 30
3.3 The spectrum and the asymptotic continuous spectrum for a scalar DDE. 35
3.4 Average of consecutive points of the spectrum against the time-delay for a scalar DDE. 37
3.5 Area between the fitting curve of the spectrum and the asymptotic continuous curve against the time-delay. 38

4.1 A directed ring network. 48
4.2 Solutions of the Stuart-Landau oscillators in a network (equilibrium case). 50
4.3 The asymptotic continuous and the pseudo-continuous spectrum for the periodic Stuart-Landau. 53
4.4 Solutions of the Stuart-Landau oscillators in a network (periodic case). . 54
4.5 Synchronization map. 55
4.6 Characteristic time. 57
4.7 Comparative of the critical parameter's order. 59

5.1 A non-directed ring graph and a directed ring graph. 66
5.2 Comparison of the stability regions. 67
5.3 The spectrum for two coupled oscillators with showing the impossibility of controlling both parts of the spectrum. 74
5.4 Position of the eigenvalues. 76
5.5 Schematic control strategy. 77
5.6 Control region for two coupled Stuart-Landau oscillators. 81
5.7 Fitting of the difference between analytically boundary and true spectrum. 82

LIST OF SYMBOLS

κ – Overall coupling parameter
λ – Eigenvalues (root of the characteristic equation)
Γ_A – Asymptotic continuous spectrum
Γ_{SU} – Strongly unstable spectrum
Γ_I – Instantaneous spectrum
n – Number of nodes in the network
mod – Modulus (equivalence class)
τ – Time-delay
det – Determinant
$:=$ – By definition equal to
$\mathbb{I}_q$ – Identity matrix of dimension q
$\mathbb{R}^{q\times q}$ – The space of real and square matrices of dimension q
$\mathbb{i}$ – Imaginary unity
ln – Natural logarithm
$\|\cdot\|$ – Norm
$\Re(\cdot)$ – Real part
$\Im(\cdot)$ – Imaginary part
$\mathcal{D}f(x)$ – Jacobian matrix of f at x
sup – Supremum
inf – Infimum
ρ_L – Spectral radius of the matrix L
arg – The argument or angle of a complex number
$\mathcal{O}(\cdot)$ – Big O notation
$\otimes$ – Kronecker product
$\sigma(H)$ – Eigenvalue of the matrix H
$W(\cdot)$ – Lambert W function

CONTENTS

Pág.

1 INTRODUCTION 1
1.1 Dynamical time-delay network models 5
1.1.1 NDSF Model: delay-coupled systems with self-feedback 5
1.1.2 NID Model: delay-coupled systems with instantaneous self-feedback . . 6
1.2 Heuristic discussion on the main results 7
1.3 The structure of the Thesis 10

2 GRAPH THEORY 13
2.1 Graph Matrices 14
2.2 Partitions of Regular Graphs 15
2.2.1 Non-directed Regular Graphs 15
2.2.2 Directed Regular Graphs 16
2.2.2.1 Strongly connected graphs 16
2.2.2.2 Cycle multipartite graphs 17
2.3 Complex Networks 19

3 THEORY OF DELAY DIFFERENTIAL EQUATIONS 23
3.1 The general theory of DDE 23
3.1.1 Existence and uniqueness of solutions 24
3.2 Some general properties of DDEs 24
3.3 Linear DDE Theory for Large Delay 25
3.3.1 Description of the Spectrum 28
3.3.2 The Case of Equilibrium Solution 29
3.3.3 The Case of Periodic Orbits 31
3.4 Small delay versus large delay 32

4 SYNCHRONIZATION IN NETWORKS WITH STRONGLY DELAYED COUPLINGS 39
4.1 Main Results 39
4.2 Variational equation, conditions for synchronization 42
4.2.1 The persistence of equilibrium solution 44
4.2.2 The case of synchronous periodic orbits 46
4.3 Example: Coupled Stuart-Landau systems 48

4.3.1 Persistence of equilibrium 49
4.3.2 Synchronous Periodic Orbit 51
4.3.3 Characteristic time 55
4.4 Synchronization loss versus network structure 56
4.4.1 Synchronization of BA and ER networks when coupling strength is scaled with n 60

5 STABILIZATION OF STEADY STATES IN REGULAR NETWORKS 63
5.1 Main Result 63
5.1.1 Illustration 65
5.2 Variational equation 68
5.3 More of the same: description of the spectrum 69
5.3.1 Controlling the strongly unstable spectrum 70
5.3.2 Controlling the asymptotic-continuous spectrum 71
5.4 Proof of Theorem 5.1: The case of two coupled oscillators 75
5.4.1 Computing the stability region for two coupled oscillators 80
5.5 Proof of Theorem 5.1: Extension 81
5.5.1 Validity of Assumption 5.1 for strongly connected graphs 83
5.5.2 Validity of Assumption 5.1 for cycle multi-partite graphs 84

6 CONCLUSIONS 85
6.1 Perspective of future research 86

APPENDIX A 89
A.1 On the approximation of the eigenvalues from pseudo-continuous spectrum 89

APPENDIX B 95
B.1 Deduction of the Transcendental Equation Solution 95
B.2 Deduction of the Block-diagonal Variational Equation 96

REFERENCES 99

1 INTRODUCTION

Coupled systems and networks with time-delayed interactions emerge in different fields including laser dynamics (JAVALOYES et al., 2003; FIEDLER et al., 2008; ERNEUX, 2009; SORIANO et al., 2013; YANCHUK; GIACOMELLI, 2017), neural networks (WU, 1998; FOSS; MILTON, 2000; IZHIKEVICH, 2006; CAMPBELL et al., 2006), traffic systems (OROSZ et al., 2010), and others. Time delays in these systems are caused by finite signal propagation or finite reaction times. In many cases, especially for the applications in optoelectronics, delays are longer than the other time scales of the system, and they play a major role in studying the system's dynamics. For neural systems, strong delays may emerge as a lump effect of a signal propagation along a feed-forward chain of neurons (LÜCKEN et al., 2013).

Synchronization is a natural feature in coupled systems. The word synchronization comes from Greek and it means "occurrence at the same time" (PIKOVSKY et al., 2003). The idea is that subsystems that interact with each other may adjust their rhythms to a common behavior in time. This process may emerge naturally in the cited systems and many others, for example in pendulum clocks (ROSENBLUM; PIKOVSKY, 2003), collective animal behavior (MILLER et al., 2013), cognitive tasks (BRÁZDIL et al., 2013), neuronal illness (PETSCHE; BRAZIER, 2012), chemical oscillators (RAMIREZ et al., 2016), climatological processes (RIAL et al., 2013), power grids (THOMPSON, 2012), and many others. For more examples see (ARENAS et al., 2008). The main ingredient for observing synchronization is the coupling between the subsystems. This coupling can be seen as the "communication road" which may lead to the delayed interactions. The time delay may influence significantly the synchronization and its stability in coupled systems, leading to several possible different scenarios such as destabilization, multi-stability, bifurcations, etc (PENG; YUAN, 2007). Therefore, the subject of study in this Thesis, namely, synchronization in time-delayed coupled systems is of major importance in applied sciences.

In this context, one of our basic assumptions is that the network possesses a synchronous solution, where all subsystems constituting the network behave identically. Such a situation is quite common and appears in systems of identical (similar, in practice) coupled oscillators with some kind of symmetry in the coupling (GOLUBITSKY; STEWART, 2005). Then, an important question arises about the stability of the synchronous solutions, which determines whether the real system can achieve the synchronization in practice. The importance of this question follows from many applications. For instance, neural synchronization is known to be involved in the brain functioning (SINGER, 1993), synchronization of lasers is used for communication purposes (COLET; ROY, 1994; ARGYRIS et al., 2005), etc.

Also, several natural systems exhibits in their intrinsic dynamics, unstable solutions and the stabilization of them might be of interest for applications. The stabilization of unstable equilibrium solutions has applications, for instance, in semi-conductor lasers (TRONCIU et al., 2006), in nanoeletronics (PRIVAT; TRELAT, 2015), in medicine (DIBROV et al., 1982), and others.

In (FLUNKERT et al., 2010) the authors derived a neat synchronization condition for networks with delayed self-feedback term in the limit of large delay. They showed that the synchronizability is related in a simple way with the spectral properties of the network structure. Here, this condition is studied for the cases of periodic and equilibrium dynamics and the novelty is the study of how the synchronizability condition changes when the network topology changes. Another subject of study is the stabilization of unstable equilibrium dynamics. In (YANCHUK et al., 2006) the authors obtained conditions for stabilization of equilibrium in a single normal form of the Hopf bifurcation system with large delay self-feedback. And, here, these strict conditions for stabilization are extended for regular network and its relation to the network structure is investigated.

Hence, in this Thesis, two closely related topics are investigated: the stability of synchronization in networks of coupled dynamical systems with a self-feedback term and large delayed connections; and conditions for stabilization of equilibrium in networks of coupled dynamical systems without self-feedback term. In order to not get the reader confused, let's for now, write the two different models that are considered as Model A and Model B, with and without self-feedback term, respectively. Two different models are considered since

- the delay might be an inner property of the isolated dynamical system (HART et al., 2015; FLUNKERT et al., 2010; KINZEL et al., 2009; CAMPBELL et al., 2006) and also
- the delay might come from the "communication lag" among the elements of the network (OGUCHI et al., 2008; GRZYBOWSKI et al., 2012).

Thus, Model A will take into account these above two properties and Model B will take into account only the second property.

With the model A, a network model in which all connections are time-delayed is studied, in particular, this means that the nodes of the network possess a self-feedback loop. The uncoupled units of the network are assumed to have an attractor, which is an equilibrium or a periodic orbit. With strong enough delay, there is a critical coupling parameter that leads to one of the scenarios:

(1) synchronization of the stable units if the coupling parameter is positive and smaller than the critical one;

(2) destabilization of coupled nodes if the coupling term is larger than the critical one.

So, the critical parameter represents a bifurcation point.

In particular (considering the model A), from the network structure point of view, the synchronization condition is shown to be related to the maximal network's degree. This allows studying how the synchronizability of strongly delayed coupled units is associated with the coupling structure.

As a consequence of the relation of the synchronization condition to the graph structure, the synchronizability is studied for regular networks and complex ones such as Barabási-Albert scale-free (BA) and Erdös-Réniy (ER) random networks. More specifically, it will be showed that both BA and ER networks do not possess a stable synchronization in the limit of large network size, however ER networks, loses stable synchronization at a slow rate compared to BA networks. Moreover, for random networks, it will be shown that the synchronization interval is the wider possible when the network crosses the connectivity threshold becoming connected, i.e., when the degree is the minimum possible to have a connected network.

Considering model B, it will be shown to be useful studying synchronization in the case the isolated systems possess unstable steady state solutions. In such a scenario, the synchronization is achieved by controlling the unstable solutions. The word control, in our context, can also be referred to the concept of amplitude death in coupled limit-cycle oscillators (MIROLLO; STROGATZ, 1990) which were also observed in coupled oscillators with time-delay (REDDY et al., 1998).

An efficient strategy to control unstable periodic orbits embedded in chaotic attractors, which is also applied to stabilization of equilibrium, is to introduce a self-feedback delayed term. This approach is non-invasive since the feedback term does not alter the original solutions. In particular, for stabilization of periodic orbits, the usual approach is to consider the delay equal or close to the period of the orbit, a method known as Pyragas control (PYRAGAS, 1992).

For stabilization of equilibrium, with also a suitable choice of delay, the aim can be achieved (YANCHUK et al., 2006; HÖVEL; SCHÖLL, 2005). Hence, for the model B, oscillators with an unstable equilibrium, coupled through long delay interaction is considered. Then, from the network point of view, the nodes are "distant" from each other and then, only for the network Model B, the delay is not an inner property of the isolated system but it is due to network coupling.

Therefore, the Model B approaches the case in which the self-connections of the nodes of the network are non-delayed (instantaneous). Moreover, diffusive coupling is considered, that is, for a fixed node j, the coupling function depends on the difference of the state variables $x_\ell(t-\tau) - x_j(t)$, where node ℓ is adjacent to j and $\tau > 0$ is the time-delay (the Model A brings also a diffusive coupling but the difference is that the coupling function depends on the difference of the state variables $x_\ell(t-\tau) - x_j(t-\tau)$). This means that the information that arrives at node j coming from its ℓ neighbors arrives with a delay τ. This approach might be more realistic rather than considering models with delayed self-feedback interactions (OGUCHI et al., 2008). In other words, depending on the application, the Model B might be more realistic in comparison to Model A. Therefore, stabilization of steady states will be showed to be possible not with self-feedback delay term, but with the delay coming from long adjacent nodes of the network.

Such a control close to a Hopf bifurcation is studied in details and necessary and sufficient conditions for stability is obtained. The effects of the network structure of the control are investigated as well. In particular, it will be shown that the stabilization domains are reappearing and shrinking with the increase of time-delays. Also, it is studied here how the frequency of the reappearance of the control domains is influenced by the number of spectral roots of the graph adjacency matrix, which in particular, can be associated with the number of cycle multi-partitions of the graph.

In the next section, it is described the two dynamical network model with time-delay that we will be studied.

1.1 Dynamical time-delay network models

For what follows, some definitions might be needed, mainly for the readers who have no previous knowledge of graph theory and/or differential equations. However, those definitions will be given in Chapters 2 and 3.

1.1.1 NDSF Model: delay-coupled systems with self-feedback

The following system of n identical coupled oscillators with self-feedback time-delayed interactions (HART et al., 2015; FLUNKERT et al., 2010; KINZEL et al., 2009; STEUR et al., 2014; DAHMS et al., 2012; CAMPBELL et al., 2006) is considered

$$\dot{x}_j(t) = f(x_j(t)) + \kappa \sum_{\ell=1}^{n} A_{j\ell} h(x_\ell(t-\tau) - x_j(t-\tau)), \tag{1.1}$$

where $x \in C([-\tau, 0], \mathbb{R}^q)$ is continuous function, $j = 1, \cdots, n$, $\kappa > 0$ is the coupling strength, A is the *Adjacency matrix* with the elements defined as $A_{j\ell} = 1$ if there is a *link* from ℓ to j and $A_{j\ell} = 0$ otherwise. For now on, Eq. (1.1) will be called for the acronym NDSF (Network with Delayed Self-Feedback).

The function $f : \mathbb{R}^q \to \mathbb{R}^q$ describes the isolated node dynamics. The coupling function $h : \mathbb{R}^q \to \mathbb{R}^q$ describes interactions between nodes and $h(0) = 0$. The initial conditions of (1.1) are history functions $\phi_j : [-\tau, 0] \to \mathbb{R}^q$ and it is assumed that ϕ_j is continuous for all $j = 1, \cdots, n$.

The NDSF possess a self-feedback term in the coupling. This kind of coupling is widely studied and physically it is justified, for example, in semiconductors lasers models (SORIANO et al., 2013; HART et al., 2015), where the self-feedback interaction, which stands for the optical feedback, is an inner property of the laser.

The time-delay $\tau > 0$ will be considered to be a large parameter. Physically, this means that the interaction time is much larger than the typical time scale of an uncoupled system, which also often occurs in, e.g. coupled laser systems (SORIANO et al., 2013; YANCHUK; GIACOMELLI, 2017).

Due to the diffusive nature of the coupling, the coupling term vanishes identically if the states of all oscillators are identical. This ensures that the globally synchronized state $x_j(t) = s(t)$ for all $j = 1, 2, \ldots, n$ is invariant for all coupling strengths κ, that is, the coupling term vanishes inside since $x_j(t) = s(t)$ for all $j = 1, 2, \ldots, n$.

The following assumptions under the vector field f and coupling function h restrict the NDSF to the studied synchronization scenarios.

Assumption 1.1. *The function* f *is of class* C^p, $p \geq 2$ *and there exists* $s(t) \in \mathbb{R}^q$, *solution of the uncoupled system* $\dot{s}(t) = f(s(t))$ *(*$\kappa = 0$ *in Eq. (1.1)). Moreover,* $s(t)$ *is either an* equilibrium solution *or a* periodic orbit solution which is orbitally exponentially stable*.*

Assumption 1.2. *The coupling function* h *is bounded and differentiable,* $h(0) = 0$, $H = \mathcal{D}h(0)$ *is the Jacobian matrix at* 0 *and* $\det(H) \neq 0$*.*

Consider $U \subset \mathbb{R}^q$ a neighborhood of $s(t)$, the same solution specified in Assumption 1.1 such that U belongs to the basin of attraction of $s(t)$. The subspace

$$\mathcal{S} := \{x_j \in U \subset \mathbb{R}^q : x_1 = \cdots = x_n\}$$

is called the *synchronization manifold.* The local stability of $\mathcal{S}$ determines the stability of the synchronization, and it depends, in particular, on spectral properties of *Laplacian matrix* L defined as $L = D - A$, where D is the diagonal matrix containing in its diagonal the *degrees* of the nodes and A is the adjacency matrix, as introduced in NDFS.

1.1.2 NID Model: delay-coupled systems with instantaneous self-feedback

The second object of our study is the network without delays in self-connections, i.e., the delays emerge only in the interactions with the other subsystems. More specifically, the following network model (OGUCHI et al., 2008; GRZYBOWSKI et al., 2012; GRZYBOWSKI et al., 2017) is considered

$$\dot{z}_j(t) = f(z_j(t)) + \kappa \sum_{\ell=1}^{n} A_{j\ell} h(z_\ell(t - \tau) - z_j(t)), \tag{1.2}$$

where $z_j \in \mathbb{C}$, $\kappa > 0$ is the overall coupling strength, n is the number of nodes in the network, $f, h : \mathbb{C} \to \mathbb{C}$, the adjacency matrix $A = [A_{j\ell}]_{j,\ell=1}^{n}$ describes the structure of the network with $A_{jl} = 1$ if there exists a link from ℓ to j and $A_{j\ell} = 0$ otherwise, and also time-delay $\tau > 0$ will be considered to be a large parameter. For now on, Eq. (1.2) will be referred as the acronym NID (Network model with Instantaneous self-feedback Delay).

A specific dynamics $f(z)$, namely f, is considered. It represents the normal form of the *Hopf bifurcation*, known also as the Stuart-Landau (SL) system. It reads

$$f(z_j) = (\alpha + \beta i)z_j - z_j|z_j|^2, \tag{1.3}$$

where i stands for the imaginary unit. As stated, the SL system represents the normal form of the Hopf bifurcation, therefore, it has one equilibrium at the origin, which is asymptotically stable for $\alpha < 0$, and a stable periodic orbit (with period $T = 2\pi/\beta$) for $\alpha > 0$, which emerges from the Hopf bifurcation at $\alpha = 0$. A specific dynamics on the NID model is considered since the result that this second model brings, namely, stabilization of unstable steady states is valid for systems that possess this type of behavior (Hopf bifurcation).

Assumption 1.3. *The case where the uncoupled systems possess an unstable equilibrium is take into account. This case is characterized by* $\alpha > 0$*. Moreover, the system is near the Hopf bifurcation, that is,* $\alpha \ll 1$*.*

Assumption 1.4. *The coupling function* $h : \mathbb{C} \to \mathbb{C}$ *is smooth, bounded, and it is assumed to fulfill the following properties:* $h(0) = 0$ *and the Jacobian* $H = \mathcal{D}h(0)$ *(taking partial derivatives with respect to real and imaginary parts) is a positive-definite matrix.*

A natural candidate for h is the sine function. In such a case, $H = \mathbb{I}_2$, the *identity matrix* in $\mathbb{R}^{2\times 2}$, the space of real and square matrices of dimension 2. Many times, the index of $\mathbb{I}_2$ (or $\mathbb{I}_q$) may be omitted in the case it is clear.

1.2 Heuristic discussion on the main results

In this section, it is discussed, informally and in short, the possible main frequently asked questions about this Thesis.

The problem tackled in this Thesis. One of the approached problems consists of studying how the synchronization of stable coupled units depends on the elements of the network model, that is, how it depends on the vector field, the coupling function, the network structure and the time-delay. And, how the synchronization region is affected by changing the network type and its size. Considering now that the units of the network are unstable steady states, then the extended problem consists on studying whether these units can be stabilized in the network and how the stability region depends on the network structure and the time delay.

The main challenges on approaching the discussed problem. The main challenge on approaching this problem is to understand and connect different fields of study. This Thesis does not produce new mathematical tools but uses the existing ones, in a novel way, to provide new insights on the problem of synchronization and control in complex networks with long delay interactions.

The results that this thesis brings. The main results concerning NDSF model are the obtainment of conditions for synchronization and desynchronization which depends on the network dynamics.

(i) (Persistence of equilibrium) With strong enough delay, there is a critical coupling parameter κ_c, which depends on the dynamics, coupling function and network structure, such that the equilibrium solution in the network remains stable if $|\kappa| < \kappa_c$; and the destabilization of coupled nodes occurs if $|\kappa| > \kappa_c$ (see Theorem 4.1). For this case, κ_c is independent of the delay.

(ii) (Synchronization of periodic orbits) It is in sharp contrast to equilibrium case. It is shown to be always desynchronized for long enough time-delay. However, for long but finite delay the synchronization is attained for an interval that is shrinking as the delay grows to infinity, that is, for this case the critical coupling parameter depends also on the delay, $\kappa_c = \kappa_c(\tau)$, and $\kappa_c(\tau) \to 0$ as $\tau \to \infty$. See Theorem 4.3 for the precise statement.

Fixing the vector field f, the coupling function h and the delay τ, it is studied how the network structure affects the critical coupling κ_c. The results elucidate this dependence. For instance, it will be shown that

- For Barabási-Albert scale free network, $\kappa_c \sim \mathcal{O}\left(1/\sqrt{n}\right)$.
- For Erdös-Réniy (ER) random networks, $\kappa_c \sim \mathcal{O}\left(1/\log n\right)$.

This shows that having a large number of connections is detrimental, and close to percolation threshold is optimal for synchronization. This is in contrast to the non-delayed case (MAIA et al., 2016; PEREIRA et al., 2014) – best synchronization scenario happens for homogeneous networks and as large the degrees as better.

The main results concerning NID model are the obtainment of the analytical expression for the stability region in the $\tau \times \kappa$ plane which provides control of unstable nodes close to a Hopf bifurcation. The following points summarize the results for the referred network model.

- For all large enough $\tau > 0$, there exists a non-empty approximated control interval
$$\kappa_1(f, \mathcal{G}) < \kappa < \kappa_c(f, \mathcal{G}, \tau),$$
where f is the dynamics given in Eq. (1.3) and $\mathcal{G}$ is the graph which is assumed regular. Moreover, fixing the parameters of the dynamics f and the graph $\mathcal{G}$ then
$$\kappa_c \sim \mathcal{O}\left(1/\tau^2\right),$$
that is, the control interval shrinks at a rate of order $1/\tau^2$.
- Fixing the delay and the parameters of f accordingly to Assumption 1.3, the effect of the network size n can be derived. Table 1.1 summarizes the results for some regular graphs.

Table 1.1 - Results on the NID Model summarized to some regular graphs.

Graph	**lower bound**	**upper bound**
Complete	$\alpha/(n-1)$	$\kappa_c \sim \mathcal{O}\left(1/n\right)$
Ring (non-directed)	$\kappa_1 = \alpha/2$	does not depend on n
Ring (directed)	$\kappa_1 = \alpha$	$\kappa_c \sim \mathcal{O}\left(1/n^2\right)$
Cycle multi-partite	$\kappa_1 = \alpha/d$, where d is the degree of the graph	$\kappa_c \sim \mathcal{O}\left(1/m^2\right)$, where m is the number of multipartitions of the graph.

The relevance of the results. The results give new insights on the role of the network structure to the synchronization and control in complex networks with strongly delayed connections. It also shows the contrast to the non-delayed case. Moreover, the control of unstable units in a network scenario with long delay interaction might have wide applications in engineering systems, for instance, controlling distant agents (PALEY et al., 2007).

Techniques used to overcome the challenges. It is used in this Thesis the theory of functional differential equations (HALE; LUNEL, 1993; SMITH, 2010), elements of the spectral theory for graphs (FIEDLER, 1973; BEINEKE; WILSON, 2004; BROUWER; HAEMERS, 2011), as well as a spectral theory for delay differential equations with strong delays (WOLFRUM et al., 2010; LICHTNER et al., 2011; SIEBER et al., 2013; YANCHUK; GIACOMELLI, 2017). Some important ideas from Ref. (FLUNKERT et al., 2010) on the synchronization of strongly delayed networks are used as well. Moreover, some important ideas from Ref. (YANCHUK et al., 2006) on control of unstable equilibrium are used. In particular, the results obtained in the cited reference is extended here for regular networks.

1.3 The structure of the Thesis

All environments (equations, theorems, lemmas, etc) in this Thesis are named accordingly the chapter they are placed in.

The two considered models have been presented in Section 1.1. The Chapters 2 and 3 brings the basic concepts used throughout this Thesis. Namely, the basic theory of graphs (and networks) and the theory of delay differential equation, respectively. More specifically, examples of the main concepts about graph theory are given, they are: graph matrices (in Section 2.1), graph partitions (in Section 2.2) and complex networks (in Section 2.3). The problems on synchronization and control of steady states are tackled by using the properties of the asymptotic spectrum of the variational delay differential equation. Hence, in Chapter 3 the basic properties of Delay Differential Equations (DEE) are defined (Section 3.1) and details on the asymptotic spectrum of a general linear DDE (Section 3.3 and 3.4) is given.

In the Chapters 4 and 5 the main results are stated and developed. More specifically, Chapter 4 brings the results considering the NDSF Model and Chapter 4 regarding the NID Model.

In Section 4.1 the main theorem concerning the synchronization condition using the NDSF Model is stated. Considering various complex networks, such as random, scale-free, regular, the synchronization condition will be related to the structure of the graph and how the synchronization is affected in the limit of large networks is studied. These results are place in Section 4.1 and discussed in Section 4.4. Also, it is discussed, in Section 4.4.1, how scaling properties of the coupling parameter influences the synchronization interval.

In Section 5.1 the main result concerning the NID Model is presented. It gives necessary and sufficient condition to achieve stabilization of the equilibrium and how this condition depends on the particular network structure. Also, in the same section, an illustration of our main result is depicted, comparing how small changes in the network structure gives dramatic changes in the control domain. In the Section 5.4 and 5.5 the proofs of the main result to the specific case of two coupled oscillators and for the general case, respectively, are presented.

An essential ingredient to prove the main result of Chapter 5 is to estimate the location of the spectra in the complex plane as the delay grows. Hence, in Appendix A.1 the precise estimation of the asymptotic spectrum is given.

Some deductions and proofs are placed on the subsequent appendices. Chapter 6 brings the conclusion of this Thesis, summarizing the main new scientific achievement in the field of synchronization and control in networks with large delay couplings, and also future research topic is pointed out, that is, a possible continuation of this Thesis.

2 GRAPH THEORY

Throughout this chapter one gives several definitions associated to graphs that are necessary for the study of complex networks. For the definitions and some subsequent results one follow several different classical textbooks such as (BONDY; MURTY, 2007; BEINEKE; WILSON, 2004; BROUWER; HAEMERS, 2011; BOLLOBÁS, 2001).

The complex networks are seen and modeled as graphs in which the nodes are the vertices and the links between them are the edges. That is, a *graph* $\mathcal{G}$ is a pair $(\mathcal{V}, \mathcal{E})$ in which $\mathcal{V}$ is a non-empty set of vertices, $\mathcal{V} \cap \mathcal{E} = \emptyset$, and $\mathcal{E}$ is the set of edges that connect the vertices.

Each edge is represent by a pair $e_{jk} = (v_j, v_k)$. If the edge e_{jk} has a direction from v_j to v_k then it said to be *directed*. By convenience, if e_{jk} is directed then its direction is from v_j to v_k. Therefore $e_{jk} \neq e_{kj}$, unless it is non-directed.

The graphs that is considered throughout this manuscript are *simple*, *connected* and, possibly, *directed*.

Definition 2.1 (Simple Graph). *A graph is said to be simple if the vertices vertices do not possess self-connections or if there are no two or more edges with the same direction between two vertices.*

Definition 2.2 (Directed Graph). *A graph is said to be directed if at least one of its edges is directed.*

A *path* in a graph is a directed (or not) trail between any two vertices such that the middle vertices are all distinct.

Definition 2.3 ((Weakly) Connected Graph). *A graph is said to be (weakly) connected if for any two vertices v_j and v_k of the graph and disregarding the directions of the edges, there is a path between v_j and v_k and the other way around.*

Another concept about direct graphs is also relevant for our study.

Definition 2.4 (Strongly Connected Graph). *A graph $\mathcal{G}$ is said to be strongly connected if for any two vertices of $\mathcal{G}$ there is a directed path between them.*

The Fig. 2.1 brings illustrations of the definitions stated so far.

Figure 2.1 - Example of simple, (weakly) connected and directed graph. The graph is not strongly connected because there is no directed path from the vertice 4 to vertice 3, for instance. The edge $e_{23} = e_{32}$ is non-directed.

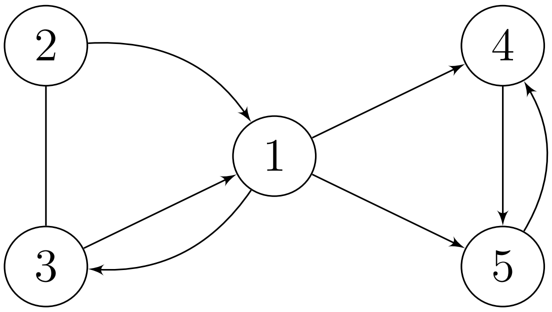

2.1 Graph Matrices

Let $\mathcal{G} = (\mathcal{V}, \mathcal{E})$ be a directed (or not) graph with n vertices with, by simplicity, $\mathcal{V} = \{1, \cdots, n\}$. Then, $\mathcal{G}$ can be described (regarding the set of edges) by an *Adjacency matrix* $A = [A_{j\ell}]$, $j, \ell = 1, \cdots, n$, defined as

$$A_{j\ell} := \begin{cases} 1, & \text{if there is an edge from } \ell \text{ to } j \\ 0, & \text{otherwise.} \end{cases}$$

A non-directed graph has a symmetric adjacency matrix whilst in directed graphs, this is not necessarily the case.

Each vertex of the graph has a basic measure called *degree*. The *inner degree* d_j of a vertex i is the number of edges arriving at j. The *outer degree* of j is the number of edges going out from j. For example, in Fig. 2.1 the inner degree of the vertex 5 is $d_5 = 2$ whereas its outer degree is 1.

Remark 2.1. *The degree of a vertex j is defined to be the inner degree d_j.*

In terms of the adjacency matrix, one has

$$d_j = \sum_{\ell=1}^{n} A_{j\ell}.$$

Another important matrix associated to the graph connectivity structure is the *Laplacian matrix* $L = [L_{j\ell}]$ defined as

$$L_{j\ell} = \begin{cases} d_j, \text{ if } j = \ell; \\ -1, \text{ if there is an edge from } \ell \text{ to } j; \\ 0, \text{ otherwise.} \end{cases}$$

If $D = \text{diag}(d_1, \cdots, d_n)$ is the diagonal matrix in which the diagonal elements are the degrees of each vertex, then the Laplacian matrix L reads

$$L = D - A.$$

By construction, the graph Laplacian matrix has zero row sum. Therefore, the eigenvector $\mathbf{1} = (1, \cdots, 1) \in \mathbb{R}^n$ corresponds to the zero eigenvalue. The Laplacian matrix is assumed to be diagonalizable, i.e., for simplicity, it is assumed that its eigenvalues are simple.

Spectral properties of the Adjacency and Laplacian matrices have an important role in the description of the synchronization properties in networks (MAIA et al., 2016; PEREIRA et al., 2014; ARENAS et al., 2008). In particular, the spectral radius of those matrices (the largest eigenvalue in modulus) is the main interest.

2.2 Partitions of Regular Graphs

In Chapter 5, one restricts the analysis that will be developed there to regular graphs. More specifically, one will be interested in the eigenvalues of the Adjacency matrix os such graphs.

Definition 2.5 (Regular Graph)**.** *A regular graph is a graph in which every vertex has the same degree $d \geq 1$. In this case, the graph is said to be d-regular.*

Examples of d-regular graph are: complete graph, ring graph with d neighbors, d-random graph, etc.

2.2.1 Non-directed Regular Graphs

Let $\mathcal{G}$ be a d-regular non-directed graph of n vertices. Then, it is known (see Ref. (BROUWER; HAEMERS, 2011)) that the eigenvalues σ_j, $j = 1, \cdots, n$, of the adjacency matrix of such graph are real (since the adjacency matrix is symmetric) and they satisfy

$$d = \sigma_1 > \sigma_2 \geq \sigma_3 \geq \cdots \geq \sigma_n \geq -d.$$

Moreover, $\sigma_n = -d$ if and only if the graph is bipartite.

A graph $\mathcal{G} = (\mathcal{V}, \mathcal{E})$ is said to be *bipartite* if the set of vertices $\mathcal{V}$ can be portioned into two disjoint sets such that every edge connects vertices from a different set, that is, vertices in the same set cannot be adjacent.

Remark 2.2 (On the existence of regular graphs)**.** *It is known that a regular and non-directed graph with n vertices of degree d exists if and only if either n or d is even. If n and d are both odd, then it's not possible to construct such a regular graph. A proof of this result can be found in (BROUWER; HAEMERS, 2011). For directed graphs, if both n and d are odd, such a graph may exist. For example, a clockwise directional ring with an odd number of vertices is a directed* 1*-regular valid graph.*

2.2.2 Directed Regular Graphs

Two characterizations of directed d-regular graphs are given, for which the spectral radius of the adjacency matrix is known.

2.2.2.1 Strongly connected graphs

The first characterization is given in terms of the Perron-Frobenius theory for non-negative matrices. It says that if the graph is strongly connected then the eigenvalues of the adjacency matrix that are on the spectral circle always rise up uniformly distributed on it.

A *non-negative matrix* $A \in \mathbb{R}^{n \times n}$ (with short notation $A \geq 0$) is a matrix in which the elements $A_{j\ell}$ are non-negative. For example, the adjacency matrix of a graph (directed or not) is a non-negative matrix. If $\mathcal{G}$ is a strongly connected graph with adjacency matrix A, then A is said to be an *irreducible matrix.*

Definition 2.6 (Primitive and imprimitive matrices)**.** *A non-negative and irreducible matrix A is said to be primitive if it has only one eigenvalue, $d = \rho_A > 0$, on its spectral circle. If it has $m > 1$ eigenvalues on its spectral circle, A is called imprimitive, and m is referred to as index of imprimitivity of A. The algebraic multiplicity of an eigenvalue $\sigma_k(A)$, denoted by* alg mult(σ_k)*, is the number of times this* *eigenvalue repeat.*

Theorem 2.1. *Let $A \geq 0$, $A \in \mathbb{R}^{n\times n}$, be an irreducible matrix with m eigenvalues $\sigma_1, \cdots, \sigma_m$ on its spectral circle. Then each of the following statements is true.*

(I) alg mult$(\sigma_k) = 1$ *for $k = 1, \cdots, m$ and*

(II) for $k = 1, \cdots, m$, the eigenvalues σ_k reads

$$\sigma_k = d \exp\left(\frac{2\pi k \mathbb{i}}{m}\right) \tag{2.1}$$

where $d = \rho_A > 0$ and $\mathbb{i} = \sqrt{-1}$.

Naturally, a d-regular strongly connected graph fulfills the conditions of the Theorem 2.1 which means that the eigenvalues on the spectral circle read accordingly with Eq. (2.1).

A proof of the Theorem 2.1 can be found in Ref. (MEYER, 2000). In a general scenario, it is not possible say what is the imprimitivity index of the spectral radius of a strongly connected graph just by looking at its structure. However, Lemma 2.1 (see (MEYER, 2000)) shows how the index of imprimitivity can be found from the characteristic polynomial of the adjacency matrix.

Lemma 2.1 (Index of Imprimitivity). *If $p(\sigma) = \sigma^n + c_{k_1}\sigma^{n-k_1} + c_{k_2}\sigma^{n-k_2} + \cdots + c_{k_s}\sigma^{n-k_s} = 0$ is the characteristic equation of an imprimitive matrix $A \in \mathbb{R}^{n\times n}$ in which only the terms with nonzero coefficients are listed (i.e., each $c_{k_j} \neq 0$, and $n > n - k_1 > \cdots > n - k_s$), then the index of imprimitivity m, of the spectral radius ρ_A, is the greatest common divisor of $\{k_1, k_2, ..., k_s\}$.*

2.2.2.2 Cycle multipartite graphs

The second characterization of the d-regular directed graph does not require the graph to be strongly connected. It is based on the number of cycle multi-partitions which are defined as follows.

Definition 2.7 (Cycle multi-partition of a graph). *Let $m \geq 2$ be an integer. A graph $\mathcal{G} = (\mathcal{V}, \mathcal{E})$ is called cycle m-partite if $\mathcal{V}$ admits a partition into m classes such that every class k couples only with the class $k+1$ where modulus m is applied to the classes, that is, every edge outgoing from class k has its end at class $k+1$. In* *particular, it means that vertices in the same partition class must not be adjacent.*

Note that this definition of m-partite graph is more restrictive than the usual one (see Ref. (BROUWER; HAEMERS, 2011) for a definition) which requires only that the vertices at the same partition class do not couple with each other. Note also, that when a graph admits a cycle multi-partition, this multi-partition is not necessarily unique. See Fig. 2.2 for an illustration of an 1-regular cycle 4-partite graph.

If the graph is cycle m-partite it is possible to assert about its eigenvalues in terms of the number of partitions m.

Theorem 2.2. *Let $\mathcal{G}$ be a d-regular graph so that $\mathcal{G}$ is cycle m-partite. Then, the adjacency matrix A of $\mathcal{G}$ has m eigenvalues on its spectral circle. Moreover, they are simple and read*

$$\sigma_k = d \exp\left(\frac{2\pi k \mathbb{i}}{m}\right), \quad k = 0, \cdots, m-1. \tag{2.2}$$

The complete proof of Theorem 2.2 can be found in Ref. (LEHNERT, 2015). The idea of the proof is to notice that if the graph $\mathcal{G}$ is cycle m-partite, then the adjacency matrix is of the form

$$A = \begin{pmatrix} 0 & \cdots & \cdots & 0 & A^{(2)} \\ A^{(1)} & 0 & \cdots & \cdots & 0 \\ 0 & A^{(2)} & 0 & \cdots & 0 \\ 0 & \ddots & \ddots & \ddots & 0 \\ 0 & \cdots & 0 & A^{(m)} & 0 \end{pmatrix}$$

where each block $A^{(j)}$ is the adjacency matrix of the edges that connects partition j to $j+1$. And then notice that the complete adjacency matrix to the power m is a block-diagonal matrix turning easier to compute the eigenvalues of A^m and then associate them with the eigenvalues of A.

A simple example of a d-regular graph which is both, strongly connected and cycle multipartite, is the unidirectional ring of n vertices, where each vertex k connects only with the vertex $k+1$ applying modulus n. In this case $d = 1$ and the graph is cycle n-partite. Therefore its eigenvalues are $\exp(2\pi k \mathbb{i}/n)$ with $k = 1, \cdots, n$. See Figure 2.2 for another illustration.

Fig. 2.2 gives an illustration of a graph which is also both, strongly connected and cycle multipartite. Since it is strongly connected, one can compute the characteristic equation $p(\sigma) = \det(A - \sigma I) = 0$ which is a polynomial in terms of σ and then use Lemma 2.1 to find the index of imprimitivity. Getting $p(\sigma) = \sigma^{12} - 16\sigma^{8} = \sigma^{12} - 16\sigma^{12-4}$. Therefore, the the index of imprimitivity is 4, which means that the eigenvalues of the adjacency matrix on the spectral circle are simple and reads $2\exp(2\pi k \mathbb{i}/4)$, $k = 1, \cdots, 4$. This is confirmed by the structural cycle 4-partition of the graph (right of Fig. 2.2).

2.3 Complex Networks

Informally, networks are the graphs that often appear, for instance, in nature, in technology. The neurons, the birds, the internet, the transportation systems, and so on, are some examples of complex networks (NEWMAN, 2003).

In this section one approach some example of complex networks, how they are constructed and some of their properties. The complex network models are characterized by some probability function that gives birth to the links between nodes. In particular, the main interest is two examples of complex networks that are related to the degree distribution, namely, homogeneous and heterogeneous networks.

Homogeneous networks are characterized by a small disparity in the node degrees (BOCCALETTI et al., 2006). A canonical example is the Erdös-Rényi (ER) random network: Starting with n nodes the graph is constructed by connecting nodes randomly. Each edge is included in the graph with probability $p = p_0 \log n/n$ independent from every other edge, where n is the number of nodes in the network and $p_0 > 1$ is constant. Any other probability function can be used to connect the nodes of an ER network, for instance, $0 < p < 1$ could be just fixed constant. Here, one considers the referred probability because it represents a bifurcation scenario in which the condition $p_0 > 1$ ensures that the ER network is almost surely connected while the condition $p_0 < 1$ ensures that the ER network is almost surely disconnected (BOLLOBÁS, 2001). Therefore, one use $p_0 > 1$ in order to have a connected network as the same step that the probability $p = p_0 \log n/n$ makes it not densely connected, unless p_0 is to large.

Heterogeneous networks have the property that some nodes have a high disparity in their degrees (BOCCALETTI et al., 2006). An example is the Barabási-Albert (BA) scale-free network. In this type of network, there are some nodes (called hubs) that are highly connected whereas most of the nodes have only a few connections. A simple way to construct this network is to start with two nodes and a single edge that connect them. Then at each step, a new node is created and it is connected with one of the preexisting nodes with a probability proportional to its degree. This process is called preferential attachment. BA networks presents a node's degree distribution following a power law, in particular, the asymptotic proportion of vertices with degree d decreases as d^{-3}. Power law probability distribution was observed, for instance, in the World Wide Web (BARABASI; ALBERT, 1999).

More details about the construction, structure, and dynamics of such networks can be found in (NEWMAN, 2003; BOCCALETTI et al., 2006). Illustrations of Erdös-Rényi (ER) random networks (homogeneous) and Barabási-Albert (BA) Scale-Free networks (heterogeneous) can be seen in Figure 2.3.

Regarding BA and ER networks, the main interest is the spectral radius of their Laplacian matrices, which is of major importance for synchronization conditions derived in Chapter 4. Theses networks show nice statistics properties for the maximal degree when the size of the networking is growing to infinity. Before announcing these nice properties, one state here an important lemma in spectral graph theory that relates the spectral radius of the Laplacian matrix of any connected and non-directed network to its maximal degree and the size of the network itself.

Lemma 2.2 (Ref. (BEINEKE; WILSON, 2004)). *Let* $d_{\max}$ *denote the largest degree of a non-directed network* $\mathcal{G}$ *of size* n. *Then the spectral radius* ρ_L *of the Laplacian matrix* L *of* $\mathcal{G}$ *has the following estimates:*

$$\frac{n}{n-1} d_{\max} \leq \rho_L \leq 2 d_{\max}. \tag{2.3}$$

Lemma 2.3 (Ref. (MÓRI, 2005)). *Consider a BA non-directed network of size* n *and* $d_{\max}$ *its largest degree. With probability* 1 *we have*

$$\lim_{n \to \infty} n^{-1/2} d_{\max} = \mu; \tag{2.4}$$

the limit is almost surely positive and finite.

Lemma 2.4 (Ref. (RIORDAN; SELBY, 2000)). *Consider an Erdös-Rényi network with* n *nodes, connection probability* $0 < p < 1$ *and* $q = 1 - p$. *Then, the probability that the maximum degree* $d_{\max}$ *being at most* $np + b\sqrt{npq}$, *for some constant* $b > 0$, *tends to* 1 *as* $n \to \infty$.

Figure 2.2 - A 2-regular directed graph with 12 vertices (left). It is strongly connected and cycle 4-partite (right). The eigenvalues of the adjacency matrix on the spectral circle are $2\exp(2\pi k\mathbb{i}/4)$, $k = 1, \cdots, 4$. The colored ellipses indicates the cycle partitions.

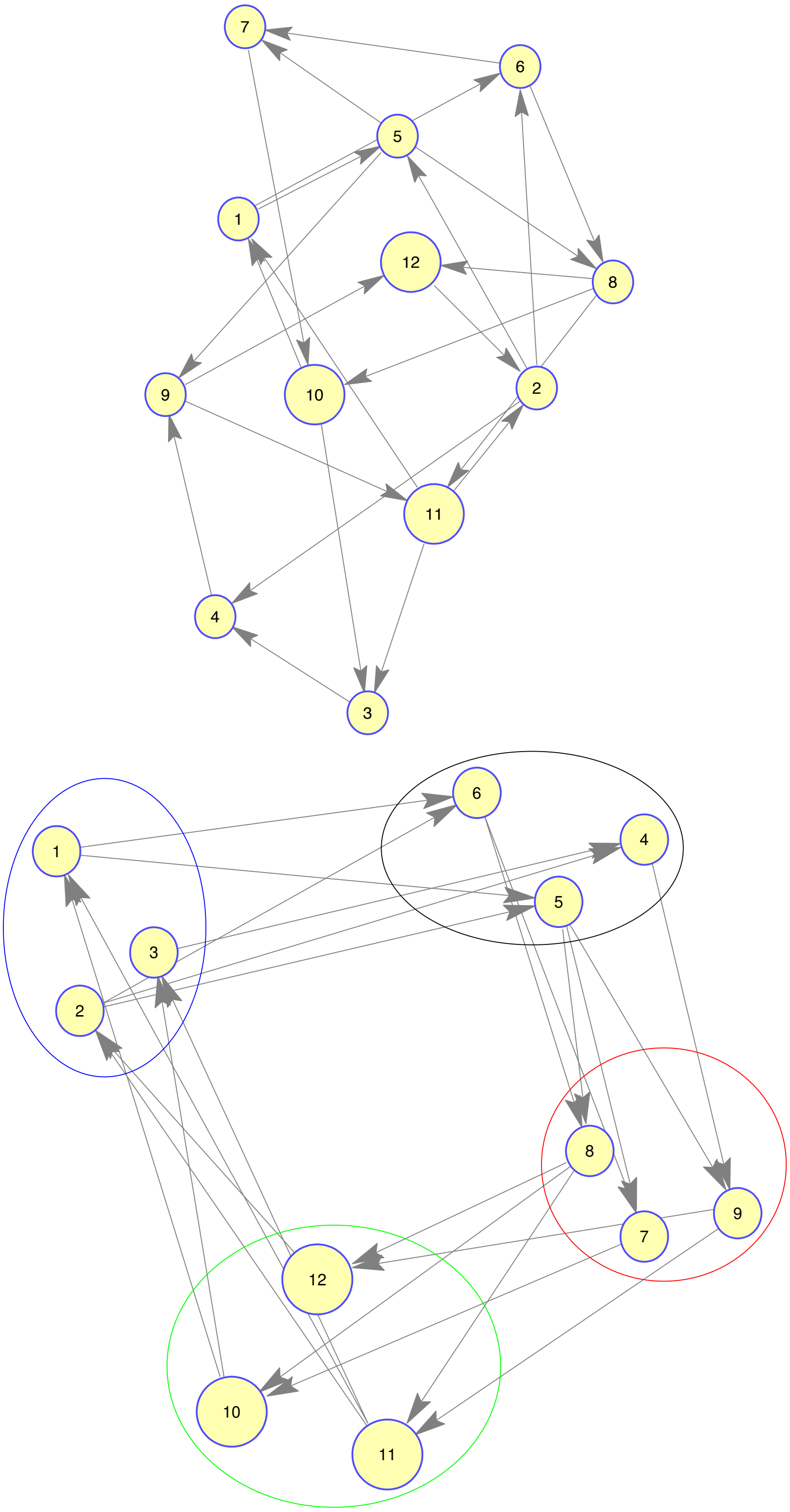
7
6
5
1
12
8
9
10
2
11
4
3
6
4
1
5
3
2
8
9
7
12
10
11

Figure 2.3 - Illustrations of a BA network (left) and an ER network (right), both with $n = 100$.

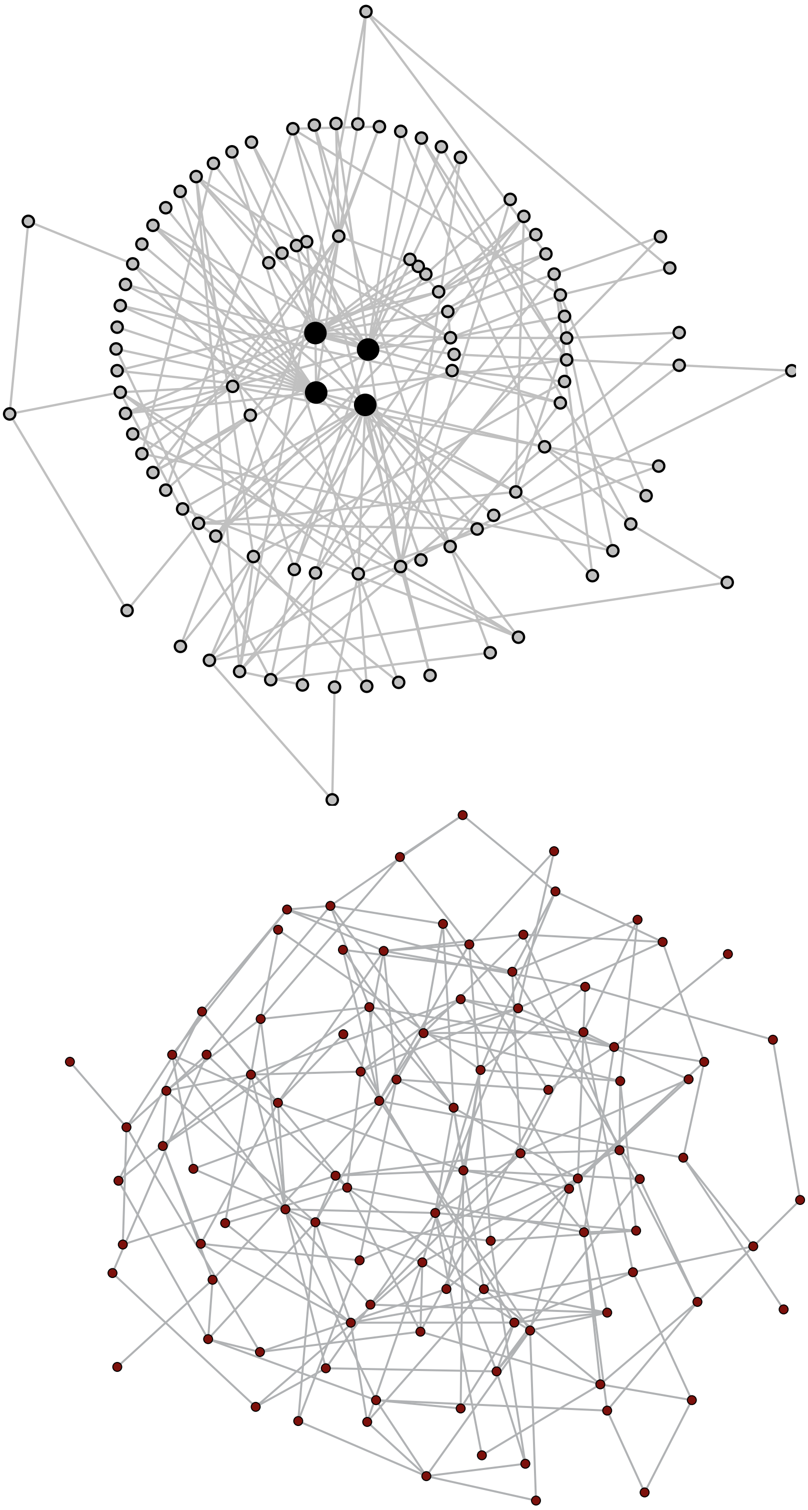

3 THEORY OF DELAY DIFFERENTIAL EQUATIONS

In this chapter one give definition of one of the main ingredients to model and study the dynamical behavior of complex networks with time-delayed interactions, namely, the Delay Differential Equation (DDE). Moreover, the main interest is centered in the local stability of the synchronization in such networks, one approach here several results from the linear theory of DDE, in particular, the theory of linear DDE for strong time delay. Here, it is closely followed the classical textbooks in the general theory of differential delay equations, namely, (SMITH, 2010; HALE; LUNEL, 1993), and well-grounded articles on DDE with large delay such as (SIEBER et al., 2013; LICHTNER et al., 2011; WOLFRUM et al., 2010; YANCHUK; PERLIKOWSKI, 2009).

3.1 The general theory of DDE

Let $C([a,b],\mathbb{R}^q)$ be the space of continuous functions from the interval $[a,b]$ to $\mathbb{R}^q$, the q-dimensional vector space over the set of real numbers. If $[a,b]=[-\tau,0]$ where $\tau>0$ represents the time-delay, then in short notation $C=C([-\tau,0],\mathbb{R}^q)$. The norm of an element x of C if defined as $\|x\|=\sup_{\theta\in[a,b]}|x(\theta)|$, where $|\cdot|$ is a norm in $\mathbb{R}^q$. With this norm, C is Banach space of infinite dimension.

A DDE is an equation of the type

$$\dot{x}(t)=f(t,x(t),x(t-\tau)), t\geq 0 \quad \text{and} \quad x(t)=\phi(t), -\tau\leq t\leq 0 \tag{3.1}$$

in which $\tau>0$ is the time delay and $f:U\to\mathbb{R}^q$, $U\subset\mathbb{R}\times C$. The right-hand of Eq. (3.1) says that the vector field of this differential equation is dependent not only on the present state of the system but also on the previous state given by τ. $x(t)$ is said to be a solution of the DDE problem (3.1) through ϕ if there exists $a>0$ such that $x\in C([-\tau,a],\mathbb{R}^q)$ and satisfies (3.1) for all $t\in[-\tau,a]$.

In order to solve a DDE problem, differently from the classical initial value problem of Ordinary Differential Equation (ODE), the knowledge of the state vector $x(t)$ itself is not enough to determine $x\left(\tilde{t}\right)$ for $\tilde{t}\geq t$. Actually, one need to know the value of all $x(s)$ for all $s\in[t-\tau,t]$. This is equivalent to know $x(t+\theta)$ for all $\theta\in[-\tau,0]$. With this notion in mind, the general element solution in C is introduced by

$$x_t(\theta):=x(t+\theta),\quad \theta\in[-\tau,0]. \tag{3.2}$$

With the notation given in (3.2), one can rewrite Eq. (3.1) as

$$\dot{x} = f(t, x_t), t \geq 0 \quad \text{and} \quad x_0 = \phi \tag{3.3}$$

where $\phi \in C$.

3.1.1 Existence and uniqueness of solutions

The basic requirement for the existence and uniqueness of a solution of (3.1) is having the function f being continuous and Lipschitz.

Definition 3.1 (Lipschitz condition)**.** *The function f is said to be Lipschitzian on each compact subset of $\mathbb{R} \times C$ if, for all $a, b \in \mathbb{R}$ and $M > 0$, there exists $K > 0$ such that*

$$|f(t,\phi) - f(t,\psi)| \leq K\|\phi - \psi\|, \quad t \in [a,b], \quad \|\phi\|, \|\psi\| < M.$$

Theorem 3.1 (Ref. (SMITH, 2010))**.** *Suppose U is an open subset of $\mathbb{R} \times C$ and $f : U \to \mathbb{R}^q$ is continuous and Lipschitzian. If $(t, \phi) \in U$ then there is $a > 0$ and a unique solution of (3.1) through ϕ defined in $[-\tau, a]$.*

Remark 3.1. *The Lipschitz constant K in Definition 3.1 may depend on the interval $[a, b]$ and M. If the function f is globally Lipschitz, that is, if K does not depends on a,b or M, then the conclusion of Theorem 3.1 is valid for all $a > 0$, that is, the solution exists for all $t \geq 0$.*

3.2 Some general properties of DDEs

This section discusses some general properties of DDE giving a non-rigorous comparative to ODE. The followed reference is (HALE; LUNEL, 1993).

- Differently from ODE, the initial condition of a DDE is not a point in $\mathbb{R}^q$ but a history function $\phi \in C^0([-\tau, 0], \mathbb{R}^q)$.

- The solution is an element of the space of continuous functions C. Consider that $x(t)$ solution of (3.1) through ϕ is an element of $\mathbb{R}^q$ could cause undesired properties. For instance, consider the scalar DDE

$$\dot{x} = -x(t - \pi/2). \tag{3.4}$$

This equation has unique solutions through any initial function ϕ since $f(x(t-\tau)) = -x(t-\pi/2)$ is smooth. But, (3.4) has solutions $x(t) = 0$, $x(t) = \sin(t)$, $x(t) = \cos(t)$. If the state space (the (t, x)) is $\mathbb{R} \times \mathbb{R}$ then the given solutions would cross each other an infinite number of time. This problem is avoided if the phase space is assigned to be $\mathbb{R} \times C$.

- Consider the solution map $T : C \to C$ given by $T_t\phi = x_t(\phi)$ where we denote $x_t(\phi)$ the solution x_t through the initial function ϕ. Then, this map may not be injective. This means that given, different past functions ϕ and ψ, one may have $T_t\phi = T_t\psi = x_t$. For instance consider the DDE

  $$\dot{x}(t) = -x(t-1)[1 - x^2(t)]$$

  and some history function ϕ with the following property: $-1 \leq \phi(t) \leq 1$ for $t \in [\tau, 0)$ and $\phi(0) = 1$. Then for any ϕ with this property the solution of the indicated DDE is $x(t) = 1$ for $t \geq 0$.

  As T_t is not injective then the uniqueness of solutions is ensured only forward in time. Fig. 3.1 depicts this example.

- Although there are several conceptual differences among DDE and ODE, for linear systems, the map T_t is described analogously. For example, in the non-autonomous ODE system $\dot{x} = Ax$, where $A \in \mathbb{R}^{q\times q}$, we have $T_t = \exp(tA)$. The matrix A is called, in the context of group theory (or semi-group for DDE), the *infinitesimal generator* of the operator T_t. The good news is that for a linear DDE the evolution operator is also characterized by the exponential of the infinitesimal generator. Moreover, it is supposed that the vector field in Eq. (3.1) is smooth, so that T_t is differentiable and the local stability of the solutions is again characterized by the infinitesimal generator of the operator. Behind this result, there is a deep mathematical background which is beyond the scope of this Thesis. The references (HALE; LUNEL, 1993; ENGEL et al., 2006) are recommended for a deeper understanding.

3.3 Linear DDE Theory for Large Delay

Consider the Eq. (3.1) and $x(t) = s(t)$ some solution. Here, one will be interested in the local stability of $s(t)$. Moreover, the analysis will be centered under two cases, namely, when $s(t) = s^*$, that is, the solution is a fixed point, and when $s(t) = s(t + T)$ for some $T > 0$, that is, the solution is a periodic orbit. These

Figure 3.1 - Solutions of the DDE $\dot{x}(t) = -x(t-1)[1-x^2(t)]$ for different history functions $\phi(t)$.

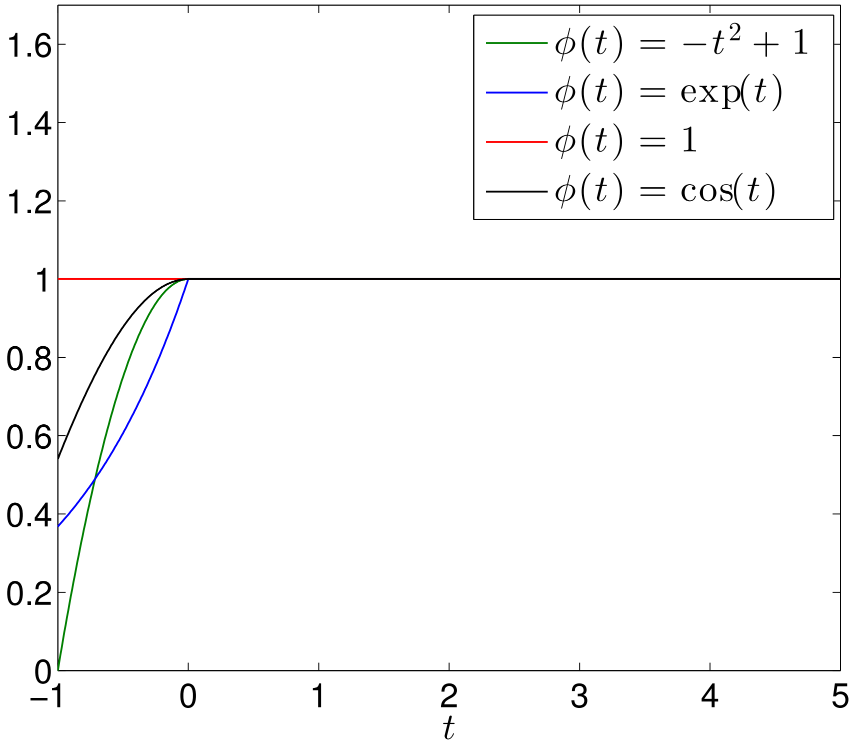

two cases are analytically tractable and the theory that is exposed in this section will cover the network dynamical models NDSF and NID studied in Chapter 4 and Chapter 5, respectively.

The variational equation (linearization) of Eq. (3.1) along $s(t)$ can be written as

$$\dot{x} = J(t)x + \sigma H(t)x(t-\tau) \tag{3.5}$$

where $\sigma \in \mathbb{C}$ is a constant that can be considered a control term and its placed in Eq. (3.5) to make it more general and adapted to the purpose of this Thesis; $J(t) = \partial_2 f\,(t, s(t), s(t-\tau))$, $H(t) = \partial_3 f\,(t, s(t), s(t-\tau))$, are $q \times q$ time-dependent matrices which are obtained by taking the partials derivatives of f on its second and third argument respectively, and evaluating them along $s(t)$.

The analysis is restricted to the case in which $H(t)$ is not time-dependent, that is $H(t) = H$.

In a general case (the periodic orbit case includes the equilibrium case), the Floquet theory can be used to study the stability of (3.5) (HALE; LUNEL, 1993). As in the case of ODE, one use the following Floquet-like ansatz

$$x(t) = y(t)\mathrm{e}^{\lambda t}, \tag{3.6}$$

where $y(t)$ is a non-trivial T-periodic function, λ and $\mathrm{e}^{\lambda T}$ are Floquet exponent and Floquet multipliers respectively. One can obtain a DDE for $y(t)$ by taking the derivative of (3.6) and replacing it in (3.5):

$$\dot{y}(t) = [J(t) - \lambda\mathbb{I}]y(t) + \sigma\mathrm{e}^{-\lambda\tau}Hy(t-\tau). \tag{3.7}$$

As the function $y(t)$ is T periodic, then $y(t-\tau)$ can be rewritten in terms of a fraction of the period T so that the large parameter τ appears only as a parameter in $\mathrm{e}^{-\lambda\tau}$. So, Eq. (3.7) reads

$$\dot{y}(t) = [J(t) - \lambda\mathbb{I}]y(t) + \sigma\mathrm{e}^{-\lambda\tau}Hy(t-l), \tag{3.8}$$

where $\eta = \tau \bmod T$ and $\mathbb{I}$ is the identity matrix in $\mathbb{R}^{q\times q}$.

To obtain Eq. (3.8) the derivative on both sides of the Floquet-like ansatz $x(t) = y(t)\mathrm{e}^{\lambda t}$ is proceeded getting

$$\dot{x}(t) = \dot{y}(t)\mathrm{e}^{\lambda t} + \lambda y(t)\mathrm{e}^{\lambda t} = (\dot{y}(t) + \lambda y(t))\,\mathrm{e}^{\lambda t}. \tag{3.9}$$

As, from Eq. (3.5)

$$\dot{x} = A(t)x + \sigma B(t)x(t-\tau) = A(t)y(t)\mathrm{e}^{\lambda t} + \sigma B(t)y(t-\tau)\mathrm{e}^{\lambda(t-\tau)}, \tag{3.10}$$

comparing Eq. (3.9) with Eq. (3.10) and canceling the common term $\mathrm{e}^{\lambda t}$ one get

$$\dot{y}(t) = [A(t) - \lambda\mathbb{I}]y(t) + \sigma\mathrm{e}^{-\lambda\tau}By(t-\tau). \tag{3.11}$$

The time delay $\tau > 0$ is large but finite, then there exists $m \in \mathbb{N}$ such $\tau = mT + \eta$ onde $\eta \in [0, T)$. Hence $\eta = \tau$ mod T and Eq. (3.8) holds.

3.3.1 Description of the Spectrum

It is shown in (YANCHUK; WOLFRUM, 2005; SIEBER et al., 2013; LICHTNER et al., 2011) that the spectrum of a DDE equation of the type of (3.8) (or (3.5)) with strong delay consists of two parts, which is introduced here following (SIEBER et al., 2013).

One defines certain objects called "instantaneous spectrum", "strongly unstable spectrum" as well as "asymptotic continuous spectrum". Strictly speaking, these objects do not belong to the spectrum of the solution of (3.5), i.e., they are not the Lyapunov exponents of system (3.5). However, they play an important role since the spectrum will be well approximated by the "strongly unstable spectrum" and "asymptotic continuous spectrum" as the delay becomes long. Another advantage of these limiting spectra is that they can be much more easily found or computed in comparison to the actual spectrum of system (3.5). See more details in (YANCHUK; WOLFRUM, 2005; YANCHUK; PERLIKOWSKI, 2009; WOLFRUM et al., 2010; LICHTNER et al., 2011; SIEBER et al., 2013; YANCHUK; GIACOMELLI, 2017).

Definition 3.2 (Instantaneous spectrum and strongly unstable spectrum). *The set Γ_I of all $\lambda \in \mathbb{C}$ for which the linear ODE system*

$$\dot{y} = [-\lambda \mathbb{I} + J(t)]y$$

has a non-trivial periodic solution $y(t) = y(t+T)$ is called the instantaneous spectrum. The subset $\Gamma_{SU} \subset \Gamma_I$ of those λ with positive real part is called the strongly unstable spectrum.

Remark 3.2. *In the case of $J(t) = J$ (does not depend on time), the instantaneous spectrum Γ_I consists of the eigenvalues of J.*

Definition 3.3 (Asymptotic continuous spectrum). *For any $\omega \in \mathbb{R}$, the complex number $\lambda = \gamma(\omega) + \mathbb{i}\omega$ belongs to the* asymptotic continuous spectrum *$\Gamma_A(\sigma)$ if the DDE*

$$\dot{y} = [J(t) - \mathbb{i}\omega\mathbb{I}]y + \sigma \mathrm{e}^{-\gamma - \mathbb{i}\phi} H y(t-\eta) \tag{3.12}$$

has a non-trivial periodic solution $y(t) = y(t+T)$ for some $\phi \in \mathbb{R}$. Here $\eta = \tau \bmod T$.

Remark 3.3. *If $J(t)$ does not depend on time, the asymptotic continuous spectrum* *can be determined from the following characteristic equation*

$$\det\left(-\mathbb{i}\omega\mathbb{I}+J+\sigma \mathrm{e}^{-\gamma-\mathbb{i}\phi}H\right)=0. \tag{3.13}$$

As follows from (YANCHUK; WOLFRUM, 2005; YANCHUK; PERLIKOWSKI, 2009; WOLFRUM et al., 2010; HEILIGENTHAL et al., 2011; LICHTNER et al., 2011; SIEBER et al., 2013; YANCHUK; GIACOMELLI, 2017), the spectrum of generic linear delay system (3.5) converges to either the strongly unstable spectrum Γ_{SU} or to the curves in the complex plane

$$\lambda=\gamma(\omega)/\tau+\mathbb{i}\omega, \quad \omega\in\mathbb{R}, \tag{3.14}$$

where $\gamma(\omega)$ is defined from the asymptotic continuous spectrum (note the division by τ). The second part of the spectrum – consisting of eigenvalues with asymptotically vanishing real parts – approaches a continuous curves asymptotically, while being still discrete for any finite τ; for this reason, it is called *pseudo-continuous spectrum.*

The union of the strongly unstable spectrum, Γ_{SU}, with the asymptotic continuous spectrum Γ_A forms the whole spectrum of Eq. (3.5), given that the instantaneous spectrum does not contain eigenvalues with zero real parts and some non–degeneracy conditions are fulfilled (LICHTNER et al., 2011; SIEBER et al., 2013). Moreover, if the set of the strongly unstable spectrum is empty ($\Gamma_{SU}=\emptyset$), and the asymptotic continuous spectrum is entirely contained on the left side of the complex plane ($\Gamma_A\subset\mathbb{C}_-$) then the trivial solution of Eq. (3.5) is exponentially asymptotically stable.

An example of a typical spectrum of the system with long delay is shown in Fig. 3.2. It illustrates a numerical spectrum of two coupled Stuart-Landau oscillators linearized in the origin and coupling function being the identity. A description of the Stuart-Landau oscillator is given in Section 4.3. The distances between neighboring eigenvalues within one curve of the pseudo-continuous spectrum scale as $2\pi/\tau$ and, in the limit of $\tau\to\infty$ they vanish and the eigenvalues fill the curve.

3.3.2 The Case of Equilibrium Solution

The following lemma gives explicit dependence of the asymptotic continuous spectrum on the coupling strength parameter σ of (3.5).

Lemma 3.1 (Ref.(YANCHUK; WOLFRUM, 2005))**.** *Consider the linear delay differ-*

Figure 3.2 - Numerically computed spectrum for the equilibrium of two Stuart-Landau oscillators (see Section 4.3) coupled as in (1.1) with identity coupling function and parameters $\alpha = 1$, $\beta = \pi$, $\tau = 20$, and $\kappa = 0.7$. The points approaching the curve on the left side of the figure belongs to the pseudo-continuous spectrum and the isolated points on the right belongs to the strongly unstable spectrum. Solid line shows the re-scaled asymptotic continuous spectrum Γ_A. The gray strip represents a break on the figure, which is necessary due to the different scales of the two parts of the spectrum.

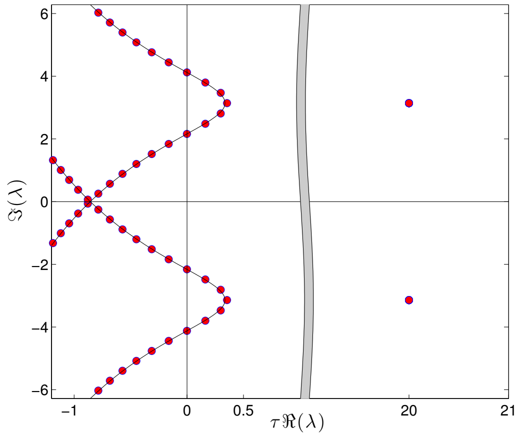

ential equation

$$\dot{\xi}(t) = J\xi(t) + \sigma H\xi(t - \tau) \tag{3.15}$$

with $J, H \in \mathbb{R}^{q\times q}$ *and* $\det(H) \neq 0$. *Then, the asymptotic continuous spectrum for (3.15) is given by the branches*

$$\{\gamma_j(\omega, \sigma) + \mathbb{i}\omega \in \mathbb{C} :\ \gamma_j(\omega, \sigma) = -\ln|g_j(\omega)| + \ln|\sigma|\}, \tag{3.16}$$

where $j = 1, \cdots, q$ *and* g_j *are complex roots of the polynomial*

$$\det\left(-\mathbb{i}\omega\mathbb{I} + J + gH\right) = 0. \tag{3.17}$$

In Eq. (3.16), the branches of the asymptotic continuous spectrum suffers a shift of the magnitude $\ln|\sigma|$. Therefore, if $|\sigma| = 1$ (no control parameter in Eq. (3.5)) the branches stays idle; If σ can be chosen so that $|\sigma| < 1$ then $\ln|\sigma| < 0$ and the branches are moved in direction to the left side of the complex plane; If σ can be chosen so that $|\sigma| < |g_j(\omega)|$ for all $j = 1, \cdots, q$ and $\omega \in \mathbb{R}$, then the branches are entirely contained on the left side of the complex plane ($\Gamma_I \subset \mathbb{C}_-$). This implies that this part of the spectrum is controlled and if, in addition, $\Gamma_{SU} = \emptyset$ then the zero solution of Eq. (3.5) is asymptotically stable.

3.3.3 The Case of Periodic Orbits

In this section it is considered the linear stability of a synchronous periodic orbit of the linearized Equation (3.5) with periodic $J(t)$. In (SIEBER et al., 2013) the authors proved results about the stability of this equation for large τ. In particular, the existence of a holomorphic function $\mathcal{H} : \Omega_1 \times \Omega_2 \subseteq \mathbb{C} \times \mathbb{C} \to \mathbb{C}$ is shown, such that λ is a Floquet exponent of the linear DDE (3.5) if and only if

$$\mathcal{H}\left(\lambda, \sigma \mathrm{e}^{-\lambda\tau}\right) = 0. \tag{3.18}$$

The function $\mathcal{H}$ in this case is analogous to the characteristic equation (3.13) for the case of equilibrium. The main difference of the periodic case is that the function $\mathcal{H}$ is not given explicitly. The asymptotic continuous spectrum is determined from the equation

$$\mathcal{H}\left(\mathbb{i}\omega, \sigma \mathrm{e}^{-\gamma}\mathrm{e}^{-\mathbb{i}\phi}\right) = 0, \tag{3.19}$$

(compare (3.19) and (3.13)). To get the asymptotic continuous spectrum, the scaling of the real part of λ given by Eq. (3.14) and large delay is considered. It is emphasized here that, in contrast to (SIEBER et al., 2013), the parameter σ is explicitly written in the argument of the function h since the dependence on σ is of interest for this study. Moreover, this parameter can be re-scaled from Eq. (3.19) by the transformation

$$\ln|\sigma| + \mathbb{i}\sigma_\theta - \gamma - \mathbb{i}\phi = -\gamma_{(1)} - \mathbb{i}\phi_{(1)}$$

and be transformed to the equation

$$\mathcal{H}\left(\mathbb{i}\omega, \mathrm{e}^{-\gamma_{(1)}}\mathrm{e}^{-\mathbb{i}\phi_{(1)}}\right) = 0 \tag{3.20}$$

which is the same as Eq. (3.19) but with $\sigma = 1$. Note that $\sigma = |\sigma|\mathrm{e}^{\mathbb{i}\sigma_\theta}$.

As a result, the following Lemma holds:

Lemma 3.2. *Consider that the non-degeneracy condition $\partial\mathcal{H}(0,0) \neq 0$ holds. The point $\gamma + \ln|\sigma| + \mathbb{i}\omega \in \mathbb{C}$ belongs to the asymptotic continuous spectrum of system (3.5) with periodic $J(t)$ if and only if the point $\gamma + \mathbb{i}\omega$ belongs to the asymptotic continuous spectrum of system (3.5) with $\sigma = 1$.*

Proof. As $\mathcal{H}$ in Eq. (3.19) is an holomorphic function on both arguments, the implicit function theorem can be used provided $\partial\mathcal{H}(0,0) \neq 0$. Hence, there is a unique continuous differentiable function $g : \mathbb{C} \to \mathbb{C}$ so that $\sigma e^{-\gamma} e^{-\mathbb{i}\phi} = g(\mathbb{i}\omega)$. As in the case of equilibrium solution, one can find $\gamma = -\ln|g(\mathbb{i}\omega)| + \ln|\sigma|$. The same approach can be applied to Eq. (3.20) having $\gamma_{(1)} = -\ln|g(\mathbb{i}\omega)|$. This implies that the different between the points of the spectrum that satifies the Eqs. (3.19) and (3.20) is the shift $\ln|\sigma|$. □

The description of the spectrum of (3.5) is concluded with the following remark:

Remark 3.4. *For both cases, namely, equilibrium and periodic orbit solutions, the main effect of the feedback strength* σ *in Eq. (3.5) for strong delays is the shift of the asymptotic continuous spectrum by the value* $\ln|\sigma|$.

3.4 Small delay versus large delay

Throughout this Thesis, new points in synchronization of networks with large delay are developed. And, beyond the reasons given at the Introduction where real dynamical systems such as lasers, neurons, ecosystems, etc, presents long delays in its models, it will be given here two mathematical reasons of why large delays are interesting:

- Firstly, large delays are analytically tractable and
- secondly, small delays are harmless.

The present chapter starts to reveal the validity of the first statement. With large but finite delay, the stability of the zero solution of a general linear DDE sums up in studying the strongly unstable and the pseudo-continuous spectrum. As the two parts of the spectrum follows different scaling properties their elements can be distinguished and analytically computed. Moreover, the positions of the points of the pseudo-continuous spectrum are analytically determined with error of order $O(1/\tau^2)$ where τ is the time-delay (details are placed in Appendix A.1) and throughout this Thesis analytic results are stated based on the knowledge of these elements.

The second statement is based on the fact that if the time-delay is small enough then the stability of the zero solution of (3.5) is not affected. The Proposition 3.1, adapted from (SMITH, 2010), make this statement precise.

Proposition 3.1. *Consider the linear DDE system* (3.5) *with* $J(t) = J$ *and its non-delayed counterpart* ($\tau = 0$)

$$\dot{x} = (J + \sigma H)x. \tag{3.21}$$

Write $g(\lambda, \tau) = \det\left(-\lambda\mathbb{I} + J + \sigma H \mathrm{e}^{-\lambda\tau}\right) = 0$ *and let* $\lambda_1, \lambda_2, \cdots, \lambda_\ell$ *be the distinct eigenvalues of* $J + \sigma H$*, let* $\delta > 0$ *and* $s \in \mathbb{R}$ *satisfy* $s < \min_j \Re(\lambda_j)$*. Then there exists* τ_0 *such that if* $0 < \tau < \tau_0$ *and* $g(\lambda, \tau) = 0$ *for some* λ *then either* $\Re(\lambda) < s$ *or* $|\lambda - \lambda_j| < \delta$ *for some* j*.*

The Proposition 3.1 says that if the delay is small enough then the solutions of $g(\lambda, \tau) = 0$ are either very close to the solutions of $g(\lambda, 0) = 0$ (eigenvalues of $J + \sigma H$) or have more negative real parts then the solutions of $g(\lambda, 0) = 0$.

The results of the Proposition 3.1 are still valid for non-autonomous systems (SMITH, 2010), that is, when $J(t)$ depends on time. Therefore, if the delay is small enough it causes no harm onto the stability of the zero solution of (3.5).

This question on how large is a large delay is intricate but one can approach it with a numerical study. Usually, the understanding of large delay is the delay that is larger than all other timescales or parameters in the system. So, typically, the large delay will depend on the dynamics which is being considered (YANCHUK; PERLIKOWSKI, 2009).

Let's consider here the simplest case, namely, the scalar equation

$$\dot{x} = ax + bx(t - \tau), \tag{3.22}$$

where $a, b \in \mathbb{R}$ are parameters. One set $a = -1$ and $b = 2$. As $a < 0$ then the strongly unstable spectrum is empty. Thus, for large delay, the spectrum of (3.22) consists only of the asymptotic continuous spectrum.

The characteristic equation of (3.22) is

$$-\lambda + a + b\mathrm{e}^{-\lambda\tau} = 0. \tag{3.23}$$

This is a transcendental equation with an infinite number of solutions. It can be solved in terms of the Lambert W function in which $z = W(z\mathrm{e}^{z})$ for $z \in \mathbb{C}$. It reads

$$\lambda = a + (1/\tau)W\left(\tau b\mathrm{e}^{-\tau a}\right). \tag{3.24}$$

See Appendix B.1 for more details on the solution of a general transcendental equation of the type (3.23) in terms of the Lambert W function. This W function has infinitely many branches and for each branch $k \in \mathbb{Z}$, Eq.(3.24) gives a different solution.

For the asymptotic continuous spectrum it is considereds, in Eq. (3.23), the scaling $\lambda = \gamma/\tau + \mathbb{i}\omega$ with $\tau \to \infty$ so that the its real part can be neglected. Hence, it is obtained that

$$- \mathbb{i}\omega + a + b\mathrm{e}^{-\gamma - \mathbb{i}\omega\tau} = 0. \tag{3.25}$$

From (3.25) it is found that

$$\gamma(\omega) = -\ln\left|\frac{\mathbb{i}\omega - a}{b}\right| = -\frac{1}{2}\ln\left(\frac{\omega^2 + a^2}{b^2}\right), \quad \omega \in \mathbb{R}. \tag{3.26}$$

For large delay, the zero solution of (3.22) is stable if $|b| < |a|$. At this moment, the stability of this solution is not the focus, so choose $b = 2$. This implies that part of the asymptotic continuous spectrum (Γ_A) is on the right side of the complex plane.

The Figure 3.3 brings part of the spectrum of (3.22) given by (3.24) for different values of τ, compared with part of the asymptotic continuous spectrum given by (3.26).

Figure 3.3 - The spectrum (red points) and the asymptotic continuous spectrum Γ_A (blue curve) for the scalar DDE (3.22). They are computed from Eq. (3.24) where each point solution is given by a branch $k \in \mathbb{Z}$ of the Lambert W function and from Eq. (3.26), respectively. Each frame brings the results for different values of τ as indicated in the title's frame. The parameters used were $a = -1$ and $b = 2$.

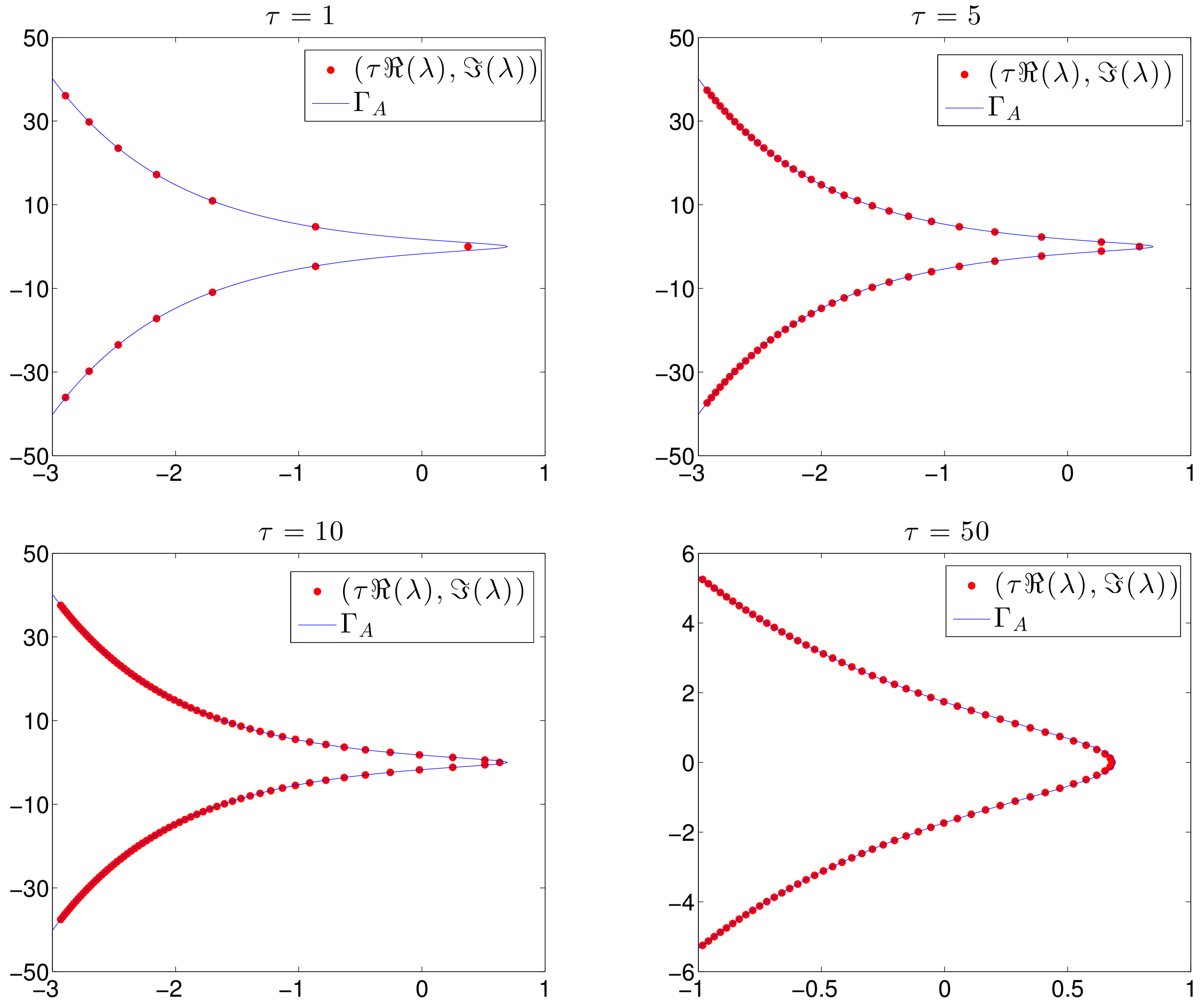

Note that, even for $\tau = 1$ most of the points (in red) of the spectrum of (3.22) are on the asymptotic curve (in blue). When τ grows, the asymptotic curve becomes more and more dense with the points of the spectrum and moreover the fitting curves of the spectrum becomes gets closer to the asymptotic one. So, two characteristics should be pointed out:

- The points of the spectrum (red points in Fig. 3.3), gets closer to each other at a rate of order $1/\tau$ (on average). More specifically, it is known (see (YANCHUK; PERLIKOWSKI, 2009)) that the distances between neighboring eigenvalues within one curve of the pseudo-continuous spectrum scale as $2\pi/\tau$ (on average) and, in the limit of $\tau \to \infty$ they vanish and the eigenvalues fill the curve. The pseudo-continuous spectrum is the approximation of the spectrum for finite τ. So, one should also expect that the distances between neighboring eigenvalues of the spectrum scale also as $2\pi/\tau$. This fact is depicted in Fig. 3.4.
- The fitting curve of the spectrum (fitting of the red point in Fig. 3.3) approximated to the asymptotic continuous curve at a rate of order $1/\tau^2$ (YANCHUK; PERLIKOWSKI, 2009). This fitting curve should have a form very close to Eq. (3.26). So, for each τ, one write a fitting the curve of the red points in Fig. 3.3 as

  $$y(\omega) = -\frac{1}{2}\ln\left(\frac{\omega^2 + \tilde{a}^2}{\tilde{b}^2}\right). \tag{3.27}$$

  where $\tilde{a}$ and $\tilde{b}$ are the fitting parameters that maximizes the goodness of the fit. Therefore, in order to check the rate of the approximation of (3.27) to (3.26) as the delay grows, for each τ one compute the following integral

  $$I = \int_{-2\pi}^{2\pi} |\gamma(\omega) - y(\omega)|\, d\omega \tag{3.28}$$

  which represents the area between the given curves and the given interval. The results are present in Fig. 3.5.

From Fig. 3.5, one can see that for $\tau = 1$ the mismatch of the spectrum to the asymptotic continuous spectrum is of the order 10^{-2}. For $\tau = 10$ it of order 10^{-4}. Therefore, the term large time-delay has a relative meaning. As was said before, the delay is large when it is larger than the other time-scales of the system. But, if a tolerance error is considered, let's say $\varepsilon > 0$ small, then the delay can be considered

Figure 3.4 - Average of $|\lambda_{k+1} - \lambda_k|$ consecutive points of the spectrum (red points in Fig. 3.3) against the time-delay τ. The blue points are the obtained numerical data for $-50 \leq k \leq 50, k \in \mathbb{Z}$ and the red curve is the fitting of the blue point which reads $y = 6.256/\tau \approx 2\pi/\tau$ as predicted.

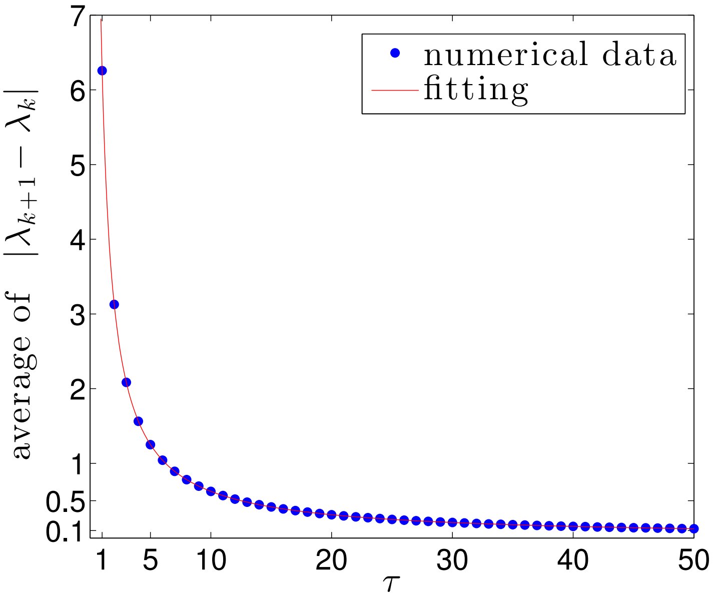

large if $\tau > \tau_0$ where $\tau_0 = \sqrt{c\varepsilon^{-1}}$ for some $c > 0$. In the case of scalar DDE (3.22), it is obtained $c = 0.043$. If $\varepsilon = 10^{-2}$ then $\tau_0 \approx 2.0736$. Hence, in this context, $\tau = 3$ can be considered large.

Figure 3.5 - Area between the fitting curve of the spectrum and the asymptotic continuous curve against τ, given by Eq. (3.28). The blue points are the computed values of Eq. (3.28) for each given τ and red curve is the fitting of these points which reads $y = 0.043/\tau^2$. The rate in which the spectrum approaches the asymptotic continuous spectrum is of order $1/\tau^2$ as expected.

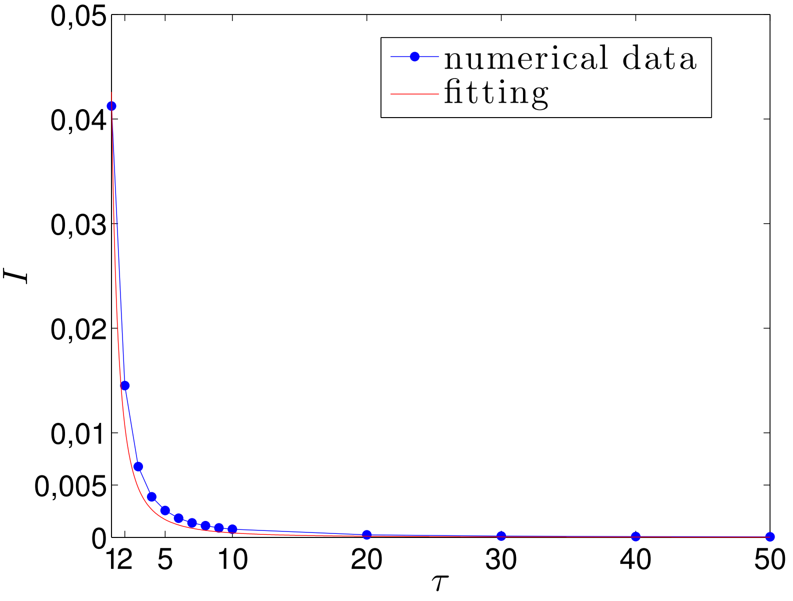

4 SYNCHRONIZATION IN NETWORKS WITH STRONGLY DELAYED COUPLINGS

Time delays appear widely in models of real networked systems where the signal propagation time is relevant. Important examples are neural systems, where the action potential velocity is taken into account, or coupled laser devices (or, more generally in coupled optical systems), where the propagation of the optical signals between the components can take a significant time comparing to the internal timescales of the lasers. In this chapter, only the network model NDSF is studied and rigorous conditions for persistence of stable equilibrium dynamics and synchronization of periodic orbits are presented, for such delay-connected networks, by investigating the properties of their spectrum. By applying these results to various networks such as scale-free, random, and regular ones, it is concluded that it is more difficult to synchronize the heterogeneous networks with long-delayed connections than the homogeneous ones. This means that the parameter interval where the synchronization takes place vanishes, in a rate proportional to the maximal degree, as the size n of the network grows. It is also discussed the possible scaling of the coupling parameter with the growth of n, that would prevent the vanishing of the synchronization interval.

4.1 Main Results

Consider the NDSF model and its assumptions. So, our problem consists of n systems coupled in a network with strongly delayed interactions. Due to Assumption 1.1, each uncoupled system have the same stable equilibrium or periodic solution $s(t)$. If the coupling parameter κ is small then, by continuity, the equilibrium solution $s(t)$ remains stable and it is expected that the network synchronizes to $s(t)$. Due to the coupling structure, the orbit $s(t)$ persists for growing κ until a maximal magnitude which depends on the network structure.

Therefore, one of the main results of this chapter, namely, Theorem 4.1, gives the interval in which the coupling parameter κ ensures that the System NDSF undergoes to stable synchronous equilibrium. More specifically, it asserts about the existence of a critical coupling parameter κ_c in which the destabilization of nodes occurs if $\kappa > \kappa_c$. Moreover, for long delay, κ_c only depends on the isolated system, the coupling function, and the network structure.

Theorem 4.1 (Persistence of equilibrium)**.** *Consider NDSF Model and Assumptions*

1.2 and 1.1. Then there is $\tau_0 > 0$ and a constant $r_0 = r_0(f, h) > 0$ such that for

$$|\kappa| < \kappa_c := \frac{r_0}{\rho_L} \tag{4.1}$$

and $\tau > \tau_0$, the synchronous equilibrium solution remains locally exponentially stable. Here, ρ_L is the spectral radius of the Laplacian matrix L.

If the condition $\kappa > \kappa_c$ is fulfilled, then there exists such $\tau_0 > 0$ that the equilibrium solution destabilizes for $\tau > \tau_0$.

As follows from Theorem 4.1, the condition $\kappa = \kappa_c$ is the strict destabilization value for $\tau \to \infty$, while the value κ_c does not depend on time delay τ. The proof of Theorem 4.1 is presented in Section 4.2. The interval $(0, r_0/\rho_L)$ of the coupling strength will be called the *synchronization window.*

Remark 4.1. *The constant r_0 from the Theorem 4.1 is given in a closed form (at least for $q \leq 3$, where q is the dimension of the isolated system). The full procedure to compute r_0 is presented in Section 4.2.*

Not only the synchronization window can be analytically determined but also the transient time towards synchronization.

Corollary 4.1 (Characteristic Time)**.** *Consider Theorem 4.1 and let $\kappa_c = r_0/\rho_L$. Then, the characteristic time ν in which the trajectories of the NDSF approach synchronization scales as*

$$\nu(\kappa) = -\tau \ln^{-1} \frac{\kappa}{\kappa_c}$$

for $\kappa \nearrow \kappa_c$ and $\tau \to \infty$.

In Section 4.3.3 the Corollary 4.1 is proved and an illustration of it is given.

In the case of the synchronous periodic solutions, the situation is more subtle. In particular, one can show that the synchronization of such periodic orbits will always be lost in the case when the interaction delay is long enough. The following theorem holds.

Theorem 4.2 (Desynchronization of periodic orbits)**.** *Consider the Network Model NDSF and Assumptions 1.2 and 1.1. Let an additional non-degeneracy assumption*

$\partial_2\mathcal{H}(0,0) \neq 0$ be fulfilled, where $\mathcal{H}$ is defined by (3.18) in Section 3.3.3. Then for any coupling parameter $\kappa > 0$, there is $\tau_0 > 0$ such that for any $\tau > \tau_0$ the synchronous periodic solution is locally orbitally exponentially unstable.

While the periodic orbits will be generically desynchronized, as stated by the Theorem 4.2, it is possible to synchronize them for an interval of values of time-delay that is bounded from above. This is the content of Theorem 4.3 and it will be exemplified in Section 4.2.2.

Theorem 4.3 (Synchronization of periodic orbits for any finite delay)**.** *Consider Network Model NDSF and the assumptions given in Theorem 4.2. Then, given τ fixed large enough, there exists $\kappa_c(\tau) > 0$ such that one of the two following statements hold:*

- *(I) The synchronous periodic solution is locally exponentially orbitally stable for $0 < \kappa < \kappa_c$ and unstable for $-\kappa_c < \kappa < 0$.*
- *(II) The synchronous periodic solution is locally exponentially orbitally stable for $-\kappa_c < \kappa < 0$ and unstable for $0 < \kappa < \kappa_c$.*

Moreover, $\kappa_c \to 0$ as $\tau \to \infty$.

Remark 4.2. *The co-dimension 1 condition $\partial_2\mathcal{H}(0,0) = 0$ may lead to isolated points, where the synchronization of the synchronous periodic orbit cannot be achieved (see example in Section 4.3.2).*

Remark 4.3. *Also, roughly speaking, the critical coupling parameter $\kappa_c(\tau)$ in Theorem 4.3, is written as $\kappa_c(\tau) = r_0(\tau)/\rho_L$.*

The main consequences of the Theorem 4.1 are presented as corollaries.

Remark 4.4. *Previous works show that condition for stable synchronization depends on the eigenvalues of the Laplacian matrix L (MAIA et al., 2016; PEREIRA et al., 2014). In particular, for general oscillators, the algebraic connectivity of the graph λ_2 (second largest eigenvalue of L) dictates the minimal contraction condition, which ensures stable synchronization. Here, it is considered stable equilibrium and strong delay interactions, then Theorem 4.1 and, in particular, the inequality (4.1) implies that the synchronization condition depends now on the spectral radius of the*

Laplacian graph matrix. It will be shown that the same synchronization condition is valid for the case of periodic orbits.

As stated in Remark 4.4, from the point of view of the network structure, the stability of the synchronization manifold is related to the spectral radius ρ_L of the Laplacian matrix. Therefore, fixing the uncoupled dynamics f, the coupling function h and time-delay $\tau > 0$ large enough, one can study the effect of the changes in the network to the synchronization.

The changes in the network that increase the spectral radius will decrease the synchronization window given by Eq. (4.1) and those changes that decrease ρ_L will increase the synchronization window. In undirected networks, the Laplacian spectral radius is non-decreasing when fixing the size of the network and adding new links to it (BEINEKE; WILSON, 2004). When the number of nodes is growing, then ρ_L is also, generally, growing depending on how the maximal degree of the network changes.

Hence, the asymptotic behavior of the synchronization window is given for two important examples of complex networks, namely, heterogeneous networks with an example of the Barabási-Albert (BA) scale-free network, and homogeneous network, with an example of the Erdös-Réniy (ER) random graph. More details about BA and ER networks are given in Section 2.3 and the proofs of the corollaries that follow are given in Section 4.4.

Corollary 4.2 (Synchronization window of large BA networks)**.** *Consider the Network Model NDSF with a BA network with n nodes. Then, for sufficiently large n, the length of the synchronization window scales as $1/\sqrt{n}$.*

Corollary 4.3 (Synchronization window of large ER networks)**.** *Consider the Network Model NDSF with a connected ER network with n nodes. Then the synchronization window is the largest possible when the connectivity threshold is crossed making the network connected. Moreover, for sufficiently large n, the length of the synchronization window scales as $1/\ln n$.*

4.2 Variational equation, conditions for synchronization

In order to find the local stability of the synchronization manifold or any synchronous solution $s(t) = x_1(t) = \cdots = x_n(t)$, the following linearized equation should be considered:

$$\dot{\xi}_j(t) = [\mathcal{D}f(s(t))]\, \xi_j(t) - \kappa\mu_j H \xi_j(t-\tau), \quad j = 2, \cdots, n. \tag{4.2}$$

Equation (4.2) is obtained by linearizing System NDSF at the synchronized solution, and then block-diagonalizing it using a change of coordinates induced by the Laplacian matrix L; the approach known as master stability function (PECORA; CARROLL, 1998). Here, μ_j are the eigenvalues of the Laplacian matrix L. $\xi_j(t)$ determines the dynamics along the eigenspaces related to μ_j near to the synchronization manifold $\mathcal{S}$, $[\mathcal{D}f(s(t))]$ is the Jacobian matrix of the vector field f along $s(t)$ and $H = \mathcal{D}h(0)$ is the Jacobian of h at 0. Details on how to obtain Eq. (4.2) are placed at Appendix B.2.

Note that $\mu_1 = 0$, and the variational equation corresponding to μ_1 is

$$\dot{\xi}(t) = [\mathcal{D}f(s(t))]\, \xi(t),$$

which describes the perturbations within the synchronization manifold.

The spectrum of a linear DDE of the type (4.2) was described in Chapter 3, Section 3.3. It consists of two parts, the instantaneous spectrum Γ_I, due to non-delayed part, and the asymptotic continuous spectrum Γ_A, which consists of the eigenvalues $\lambda = \gamma/\tau + \mathbb{i}\omega$ with vanishing real part. And, the strongly unstable spectrum, $\Gamma_{SU} \subset \Gamma_I$ consists of the elements of Γ_I with negative real part.

If the set of the strongly unstable spectrum is empty ($\Gamma_{SU} = \emptyset$), and the asymptotic continuous spectrum is entirely contained on the left side of the complex plane ($\Gamma_A \subset \mathbb{C}_-$) then the trivial solution of Eq. (4.2) is exponentially asymptotically stable. The following theorem, adapted from (SIEBER et al., 2013) makes this statement precise for the case of the stability of a periodic synchronized solution $s(t)$ with respect to desynchronized perturbations (transverse to the synchronization manifold):

Theorem 4.4. *The synchronous periodic orbit $s(t)$ of NDSF System with period T is exponentially orbitally stable with respect to perturbations transverse to the synchronization manifold for all sufficiently large τ if all of the following conditions hold:*
S-I (No strong instability) all elements of the instantaneous spectrum Γ_I have negative real parts (this implies in particular that the strongly unstable spectrum Γ_{SU} is empty), S-III (Weak stability) the asymptotic continuous spectrum $\Gamma_A(\sigma)$ is contained in $\{\lambda \in \mathbb{C} : \Re(\lambda) < 0\}$ for all $\sigma \in \{-\kappa\mu_2, \cdots - \kappa\mu_n\}$ with μ_j, $j = 2, \ldots, n$

being all nontrivial eigenvalues of the Laplacian matrix L*;*
and it is exponentially unstable with respect to perturbations transverse to the synchronization manifold for sufficiently large τ *if one of the following conditions hold:*
U-I (Strong instability) the strongly unstable spectrum Γ_{SU} *is non-empty, or*
U-II (Weak instability) a non-empty subset of the asymptotic continuous spectrum $\Gamma_A(-\kappa\mu_j)$ *has positive real part for nontrivial eigenvalue* μ_j *of the Laplacian matrix* L*.*

Proof. Although this theorem follows almost directly from Theorem 6 of (SIEBER et al., 2013), some important specific features of our setup should be pointed out.

First of all, the existence of the periodic solution $s(t)$ does not depend on time delay τ. As a result, τ can be considered as a continuous parameter here, instead of the parameter N which is an integer part of τ/T used in (SIEBER et al., 2013). Hence, the asymptotic statements with respect to N are equivalently formulated for τ in the present theorem.

Secondly, the stability of the periodic solution is determined by the variational equation (4.2) that splits into the part along the synchronization manifold with $\mu_1 = 0$ and the remaining part for the transverse perturbations with nonzero μ_j. Hence, the transverse stability is determined by the variational equation (3.7) with $\sigma \in \{-\kappa\mu_2, \cdots - \kappa\mu_n\}$. The conditions for the stability S-I and S-III guarantee that the spectrum of the corresponding variational equations is stable for large enough τ. Note that the technical non-degeneracy condition S-II from (SIEBER et al., 2013) it omitted since only to the transverse perturbations are considered here, while the trivial multiplier belongs to the direction along the synchronization manifold ($\sigma = 0$). □

In the next two subsections, the description of the spectrum of a general linear DDE (given in Section 3.3.1) is used to prove Theorems 4.1 and 4.2 for the two considered cases, persistence equilibrium solution and synchronous periodic orbit.

4.2.1 The persistence of equilibrium solution

The result obtained in Theorem 4.1 can also be proved by using Lyapunov-Kravoskii functionals (FRIDMAN, 2014). However, it is used the approach of studying the spectrum for large delay not only because it is powerful, but it also serves as a preparation to prove the result of synchronization of periodic solutions.

In this section it is specified the persistence conditions for the case when NDSF Network Modelsystem possesses a synchronous equilibrium s^*, i.e. $f(s^*) = 0$, and the Jacobian $J = \mathcal{D}f(s^*)$ is a constant $q \times q$ matrix. Note that one can write the corresponding characteristic equation explicitly as

$$\det\left(-\lambda\mathbb{I} + J + \sigma \mathrm{e}^{-\lambda\tau} H\right) = 0, \tag{4.3}$$

where $\sigma = \sigma_j = -\kappa\mu_j$, and the index j is omitted for simplicity.

The real parts of the eigenvalues λ determine the stability, and, as it was discussed, the whole spectrum converges to either the strongly unstable spectrum or pseudo-continuous spectrum. Moreover, as stated in Lemma 3.1, the asymptotic continuous spectrum is dependent of on the coupling strength parameter σ. Therefore, applying Lemma 3.1 to system (4.2), and considering Theorem 4.4, the Theorem 4.1 is proved.

Proof of Theorem 4.1 (Persistence of Equilibria). The basic idea of the proof is to show that the strongly unstable spectrum is empty and the asymptotic continuous spectrum is stable if and only if the condition (4.1) is satisfied.

The instantaneous spectrum Γ_I coincides with the spectrum of J and, by the Assumption 1.1, the equilibrium solution of the isolated system is asymptotically stable, thus there are no eigenvalues of J with positive real parts, hence $\Gamma_{SU} = \emptyset$.

Now, considering $\tau \to \infty$ one have the scaling $\lambda = \gamma/\tau + \mathbb{i}\omega$. Then, Eq. (4.3) turns to the form of Eq. (3.13). Assumption 1.2 allows using Lemma 3.1 for the variational Eq. (4.2). Then, the real part of the asymptotic continuous spectrum is

$$\gamma_{\ell,j}(\omega,\sigma) = -\ln|g_\ell(\omega)| + \ln\kappa|\mu_j|. \tag{4.4}$$

where $g_\ell(\omega)$ are the solutions of $\det(-\mathbb{i}\omega\mathbb{I} + J + gH) = 0$, with $g = \sigma\mathrm{e}^{-\gamma-\mathbb{i}\phi}$.

The condition $\gamma_{\ell,j}(\omega,\sigma) < 0$ is fulfilled if and only if

$$\kappa|\mu_j| < |g_\ell(\omega)|. \tag{4.5}$$

The asymptotic continuous spectrum lies strictly on the left side of the complex plane, if the inequality (4.5) holds for all $j = 2, \cdots, n$, $\ell = 1, \cdots, q$, and $\omega \in \mathbb{R}$. This leads to the condition

$$0 < \kappa < \frac{\min_\ell \inf_\omega |g_\ell(\omega)|}{\max_j |\mu_j|} = \frac{r_0}{\rho_L}, \tag{4.6}$$

where $r_0 = \min_{\ell=1,\cdots,q} \inf_{\omega\in\mathbb{R}} |g_\ell(\omega)|$ exists and is always bounded from zero. Indeed, if one assume the opposite, i.e., $r_0 = 0$, then it means that there exist such ℓ_0 and ω_0 that $g_{\ell_0}(\omega_0) = 0$, and hence, $\det(-\mathbb{i}\omega_0 + J) = 0$ implying that $\mathbb{i}\omega_0$ belongs to the spectrum of J. This is a contradiction since by assumption, the spectrum of J has strictly negative real parts. Moreover, $r_0 = r_0(f, h)$ since the functions $g_\ell(\omega)$ are the roots of the characteristic equation (3.17). The number $\rho_L = \max_{j=2,\cdots,n} |\mu_j|$ stands for the spectral radius of the Laplacian matrix L. Therefore, under the condition (4.1), the asymptotic continuous spectrum $\Gamma_A \subset \mathbb{C}_-$ and the zero solution of (4.2) is stable.

Having both $\mathrm{Re}(\Gamma_A) < 0$ and $\Gamma_{SU} = \emptyset$, Theorem 4.4 implies that there exists such $\tau_0 > 0$ that for all $\tau > \tau_0$ the equilibrium s^* is locally exponentially stable under the condition (4.6).

The statement about the instability of the equilibrium follows from the fact that for $\kappa > \kappa_c$ there exist such $\ell \in \{1, \ldots, q\}$, $j \in \{2, \ldots, n\}$ and $\omega \in \mathbb{R}$ that $\kappa|\mu_j| > |g_\ell(\omega)|$, and, hence the real part of the asymptotic continuous spectrum is positive $\gamma_{\ell,j}(\omega, \sigma) > 0$. Therefore, for sufficiently long time delays and $\kappa > \kappa_c$, there will be eigenvalues from the pseudo-continuous spectrum with positive real parts. $\square$

4.2.2 The case of synchronous periodic orbits

Considering the content of Section 3.3.3 (Chapter 3) one remark that

$$\mathcal{H}(\lambda, 0) = 0,$$

where $\mathcal{H}(\lambda, 0)$ is the characteristic equation of the uncoupled system, which possesses one simple trivial Floquet multiplier by Assumption 1.1. Consider now the implicit function problem

$$\mathcal{H}(\mathbb{i}\omega, g) = 0. \tag{4.7}$$

It has a unique smooth solution $g = g(\omega)$ with $g(0) = 0$ provided $\partial_2\mathcal{H}(0, 0) \neq 0$. As a result, the asymptotic continuous spectrum

$$\gamma_{(1)}(\omega) = -\ln|g(\omega)| \tag{4.8}$$

has a singularity at $\omega = 0$ and $\sup_\omega \gamma_{(1)}(\omega) = \infty$. As a result, the asymptotic continuous spectrum of (4.2), for the case of periodic solution, is singular as well

$$\sup_\omega \gamma(\omega) = \infty$$

independently of the value of σ. Hence, the asymptotic continuous spectrum possesses always an unstable part, which implies instability for large enough values of time-delays. Hence, the Theorem 4.2 has been proved.

Proof of Theorem 4.3. It is known that for $\sigma = 0$ the characteristic equation $\mathcal{H}(\lambda, 0) = 0$ possesses one simple zero root $\lambda = 0$, hence $\partial_1 \mathcal{H}(0, 0) \neq 0$. Let's study how the real parts of these eigenvalues change if σ deviates from zero using the implicit function theorem for the equation $\mathcal{H}(\lambda(\sigma), \sigma \mathrm{e}^{-\lambda(\sigma)\tau}) = 0$. Since

$$\partial_\lambda \mathcal{H}(\lambda, \sigma \mathrm{e}^{-\lambda\tau})|_{\sigma=0,\lambda=0} = \partial_1 \mathcal{H}(0, 0) \neq 0,$$

then $\lambda(\sigma)$ is the unique solution for small σ, and $\partial_\sigma \lambda|_{\sigma=0} = -\partial_2 \mathcal{H}(0, 0)/\partial_1 \mathcal{H}(0, 0)$. Here $\partial_2 \mathcal{H}(0, 0) \neq 0$ by assumption. Hence

$$\partial_\sigma \Re\left(\lambda\right)|_{\sigma=0} = -\Re\left[\frac{\partial_2 \mathcal{H}(0, 0)}{\partial_1 \mathcal{H}(0, 0)}\right] =: \alpha_P. \tag{4.9}$$

In particular, this expression shows that for $\alpha_P > 0$, the periodic solution will be destabilized for positive σ, and stabilized for negative σ. For $\alpha_P < 0$, the stabilization occurs for positive σ and destabilization for negative. It is important to notice, that the stabilization (or destabilization) occurs for all transverse modes simultaneously, since the eigenvalues $\mu_2, \ldots, \mu_n$ of the Laplacian matrix are positive and σ can admit values $-\kappa\mu_j$, which have the same sign for all μ_j, $j = 2, \ldots, n$. □

Spectrum Approximation: Note that the unique smooth solution $g = g(\omega)$ is 0 at $\omega = 0$. Note also that ω is the imaginary part of some $\lambda = \gamma(\omega)/\tau + \mathbb{i}\omega$ element of the spectrum of (4.2). If τ is large but finite, then one can approximate those elements of the spectrum (see Appendix A.1 for more details and for deduction of the following Eq. (4.10)). The approximation of ω belonging to the curve defined by the specified unique solution $g(\omega)$ is, for large τ,

$$\omega = \omega_{m,\tau} := \frac{2\pi m}{\tau} - \frac{1}{\tau}\arg g\left(w\right) + \mathcal{O}(1/\tau^2) \tag{4.10}$$

where $m \in \mathbb{Z}$. Naturally, $\omega_{m,\tau} \to 0$ as $\tau \to \infty$, but for any large fixed $\tau < \infty$, one have $\omega_{m,\tau} \neq 0$ for any $m \in \mathbb{Z}$ and therefore $g(\omega_{m,\tau}) \neq 0$. From Eq. 3.19 one get $\tau\Re(\lambda_{j,m}) = \gamma_j(\omega_{m,\tau}) = -\ln|g(\omega_{m,\tau})| + \ln|\kappa\mu_j|$. Then, an approximation for the critical coupling parameter $\kappa_c(\tau)$ is

$$\kappa_c(\tau) = \max_j \frac{1}{|\mu_j|} \min_{m\in\mathbb{Z}} |g(\omega_{m,\tau})| = \frac{1}{\rho_L} \min_{m\in\mathbb{Z}} |g(\omega_{m,\tau})| \tag{4.11}$$

where $\omega_{m,\tau}$ is given by Eq. 4.10 and g is the unique solution of Eq. 4.7 satisfying $g(0) = 0$. As $\omega_{m,\tau} \to 0$ as $\tau \to \infty$ then also $\kappa_c = \kappa_c(\tau) := (1/\rho_L) \min_{m\in\mathbb{Z}} |g(\omega_{m,\tau})| \to 0$ as $\tau \to \infty$.

4.3 Example: Coupled Stuart-Landau systems

Let us consider an example of the ring of coupled Stuart-Landau (SL) oscillators shown in Fig. 4.1.

Figure 4.1 - A directed ring network with 4 nodes.

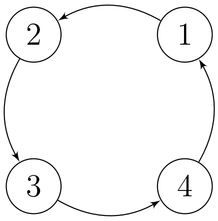

The dynamics of a node j following the NDSD Network Model is given as

$$\dot{z}_j = (\alpha + \beta\mathbb{i})z_j - z_j|z_j|^2 + \kappa \sum_{\ell=1}^{n} A_{j\ell} h(z_\ell(t-\tau) - z_j(t-\tau)). \tag{4.12}$$

where $z_j \in \mathbb{C}$. The index j may be omitted for the sake of simplicity. Throughout this section it is considered that the coupling function is $h = \sin$. In particular, $H = \mathcal{D}h(0) = 1$. So, considering the linearization on the coupling function, Eq. (4.12) is rewritten, in terms of the Laplacian matrix, as

$$\dot{z}_j \approx (\alpha + \beta\mathbb{i})z_j - z_j|z_j|^2 - \kappa \sum_{\ell=1}^{n} L_{j\ell} z_\ell(t-\tau) \tag{4.13}$$

The pure SL system is retrieved if $\kappa = 0$. Note that the SL system represents the normal form of the Hopf bifurcation, therefore, it has one equilibrium at the origin, which is asymptotically stable for $\alpha < 0$, and a stable periodic orbit (with period $T = 2\pi/\beta$) for $\alpha > 0$, which emerges from the Hopf bifurcation at $\alpha = 0$.

4.3.1 Persistence of equilibrium

Firstly, it is considered the case $\alpha < 0$ (equilibrium solution) so that the eigenvalues of the uncoupled system have negative real parts. The Jacobian matrix (considering real and imaginary parts) at zero $z = 0 + 0\mathbb{i}$ is

$$J = \mathcal{D}f(0,0) = \begin{pmatrix} \alpha & \beta \\ -\beta & \alpha \end{pmatrix}$$

with the eigenvalues $\alpha \pm \beta\mathbb{i}$.

Therefore, the strongly unstable spectrum is empty, and the whole spectrum of the zero equilibrium for the network system (4.2) consists only of the asymptotic-continuous spectrum for long delays.

The laplacian matrix of the network in Fig. 4.1 has spectral radius $\rho_L = 2$. In order to compute the value r_0 from the condition (4.1) of Theorem 4.1 the functions $g_\ell(\omega)$, $\ell = 1, 2$ is computed using Eq. (3.17):

$$g_{1,2}(\omega) = \mathbb{i}(\omega \pm \beta) - \alpha.$$

Hence, one find $r_0 = \min_\ell \inf_\omega |g_\ell(\omega)| = |\alpha|$. Therefore, the synchronization manifold for the considered network is locally exponentially stable if and only if

$$0 < \kappa < \kappa_c = \frac{|\alpha|}{2} \tag{4.14}$$

for sufficiently long time delay τ (and unstable if $\kappa > \kappa_c$).

Fig. 4.2 illustrates the convergence of the trajectories to the synchronous equilibrium (left panel) for the case when the condition (4.14) is fulfilled and the absence of convergence in the opposite case. The detailed parameter values are given in the figure's caption. Moreover, in order to compute the synchronization error, each solution is compared to a fixed one taking the norm of maximal difference, that is, the synchronization error is measured by $\max_j \|z_1(t) - z_j(t)\|$.

Figure 4.2 - (top) Solutions of Eq. (4.12) of the nodes 1 and 3 for four coupled equilibrium SL oscillators (see Fig. 4.1) in which $\kappa = 0.49$ (top, left) and $\kappa = 0.51$ (top, right). And, (bottom) time series of the synchronization error where $\kappa = 0.49$ for the down left figure and $\kappa = 0.51$ for the down right. Others parameters were $\alpha = -1$, $\beta = \pi$, $\tau = 100$ and the coupling function $h = \sin$. The hollow points stands for $z(t = 0)$ and the green squares stands for $t = 500$ (left, top and bottom) and $t = 1000$ (right, top and bottom). The history functions were taken as constant and non-zero.

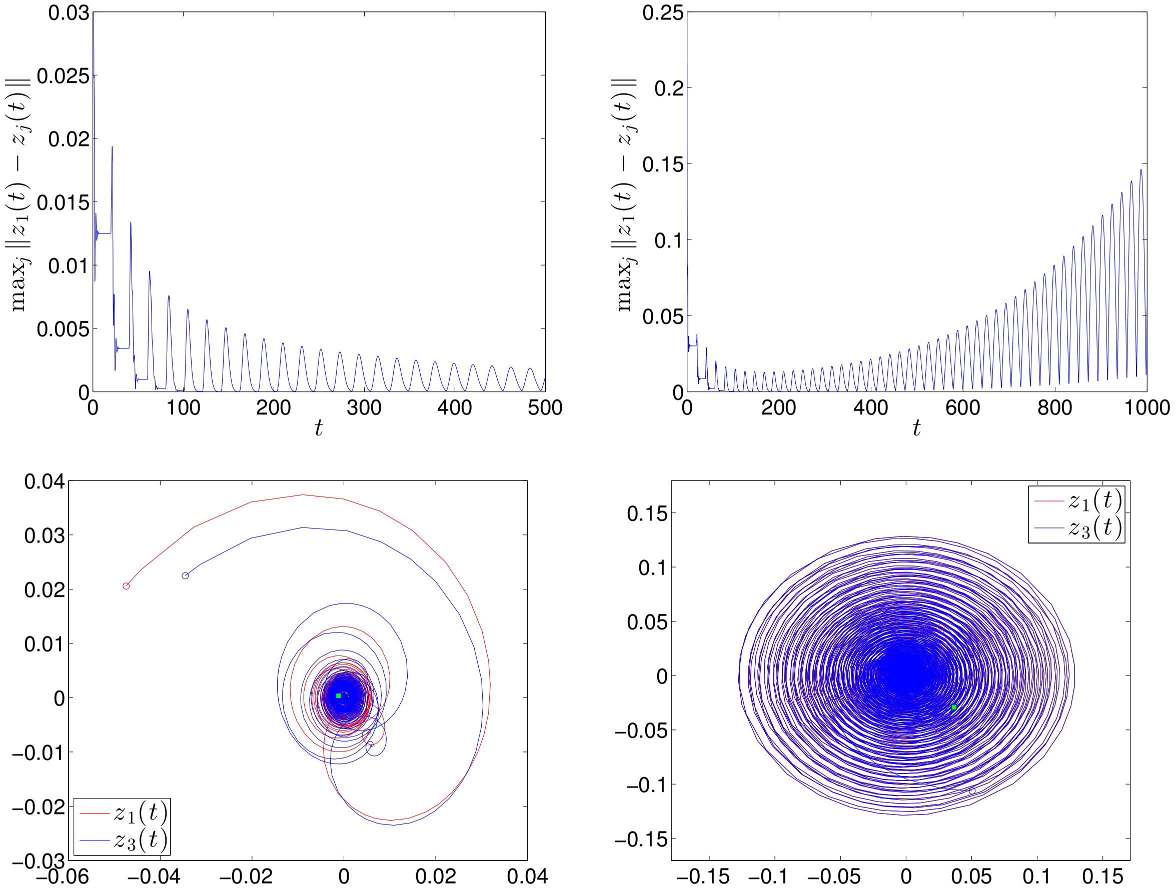

4.3.2 Synchronous Periodic Orbit

Let us consider the case $\alpha > 0$ when the synchronous periodic solution $\sqrt{\alpha}\mathrm{e}^{\mathbb{i}\beta t}$ exists.

Consider the transformation $z(t) = r(t)\mathrm{e}^{\mathbb{i}\beta t}$, then Eq. (4.13) reads, in terms of $r(t)$,

$$\dot{r}_j = \left(\alpha - |r_j|^2\right) r_j - \kappa \mathrm{e}^{-\mathbb{i}\beta\tau} \sum_{\ell=1}^{n} L_{j\ell} r_\ell(t-\tau). \tag{4.15}$$

Note that the solution $z(t) = \sqrt{\alpha}\mathrm{e}^{\mathbb{i}\beta t}$ is transformed into a family of equilibria. The variational equation of (4.15) (considering real and imaginary parts) around the equilibrium solution $r = \sqrt{\alpha}$, equivalent to (4.2), is

$$\dot{\xi}_j(t) = \begin{pmatrix} -2\alpha & 0 \\ 0 & 0 \end{pmatrix} \xi_j(t) - \kappa\mu_j \begin{pmatrix} \cos(\beta\tau) & -\sin(\beta\tau) \\ \sin(\beta\tau) & \cos(\beta\tau) \end{pmatrix} \xi_j(t-\tau). \tag{4.16}$$

where $\mu_j \geq 0$ are the eigenvalues of L. For short, Eq. (4.16) is written as $\dot{\xi}_j(t) = J_0\xi_j(t) - \kappa\mu_j\mathcal{T}\xi_j(t-\tau)$.

The instantaneous spectrum can be computed using Definition 3.2. It consists of the eigenvalues of the non-delayed part of (4.16) and reads $\Gamma_I = \{-2\alpha, 0\}$. The eigenvalue 0 in the instantaneous spectrum is associated with the trivial Floquet multiplier producing a singularity in the asymptotic spectrum. Then, as predicted by Theorem 4.2 no stable synchronization is possible for infinity delay. However, from Corollary 4.3, the synchronization interval can be computed as a decreasing function of $\tau < \infty$.

The asymptotic continuous spectrum can be computed as in the case of equilibrium solution. Using Eq. (3.13), one get $\gamma_{j,\ell}(\omega) = -\ln|g_\ell(\omega)| + \ln|\kappa\mu_j|$ where $g_\ell(\omega)$ are the solutions of

$$\det\left(-\mathbb{i}\omega\mathbb{I}_2 + J_0 + g\mathcal{T}\right) = 0 \tag{4.17}$$

Note that Eqs. (4.7) and (4.17) are the same. Hence, $\mathcal{H}(\mathbb{i}\omega, g) = \det\left(-\mathbb{i}\omega\mathbb{I}_2 + J_0 + g\mathcal{T}\right)$. More specifically,

$$\mathcal{H}(\mathbb{i}\omega, g) = g^2 - 2\cos(\beta\tau)(\alpha + \mathbb{i}\omega)g + 2\alpha\omega\mathbb{i} - \omega^2.$$

The non-degeneracy condition $\partial_2\mathcal{H}(0,0) \neq 0$ (assumption in Theorem 4.3) is satisfied since $\partial_2\mathcal{H}(0,0) = -2\alpha\cos(\beta\tau) \neq 0$ provided $\tau \neq (\pi + 2M\pi)/(2\beta)$, $M \in \mathbb{N}$. The solution of (4.17) reads

$$g_{\pm}(\omega) = (\alpha + \mathbb{i}\omega)\cos(\beta\tau) \pm \left[\alpha^2\cos^2(\beta\tau) + (w^2 - 2\alpha\omega\mathbb{i})\sin^2(\beta\tau)\right]^{1/2}. \tag{4.18}$$

From (4.18), one get $g_-(0) = 0$ and $g_+(0) = 2\alpha\cos(\beta\tau) \neq 0$ provided $\tau \neq (\pi + 2M\pi)/(2\beta)$, $M \in \mathbb{N}$. Therefore, the singularity occurs uniquely at the function $g_-(\omega)$.

In order to obtain α_P, as introduced in Eq. (4.9), one compute $\partial_1\mathcal{H}(0,0) = 2\alpha$. Hence, $\alpha_P = \cos(\beta\tau)$. As $\sigma = -\kappa\mu_j$, this implies that synchronization occurs for negative σ when $\cos(\beta\tau) > 0$ and for positive σ otherwise (positive σ is obtained if $\kappa < 0$).

Criticial coupling given by the spectrum approximation: Considering the special case in which $\tau = 2\pi M/\beta$, $M \in \mathbb{N}$ (in this case the delay τ is a multiple orbit's period which is $T = 2\pi/\beta$), one get $g_+(\omega) = 2\alpha + \mathbb{i}\omega$ and $g_-(\omega) = \mathbb{i}\omega$. Hence, the computation of an approximation for the critical coupling parameter $\kappa_c = \kappa_c(\tau)$ of Corollary 4.3 is given by Eq. 4.11. It reads, disregarding $\mathcal{O}(1/\tau^2)$ terms,

$$\begin{aligned}\kappa_c &= \frac{1}{\rho_L}\min_{m\in\mathbb{Z}}|g_-(\omega_m)| = \frac{1}{\rho_L}\min_{m\in\mathbb{Z}}\left|\mathbb{i}\left[\frac{2\pi m}{\tau} + \frac{1}{\tau}\arg g_-(\omega)\right]\right| \\ &= \frac{1}{\rho_L}\min_{m\in\mathbb{Z}}\left|\frac{2\pi m}{\tau} + \frac{\pi}{2\tau}\right| = \frac{\pi}{2\tau\rho_L}.\end{aligned}$$

Then, choosing $\beta = \pi$ and $\tau = 20$ the critical coupling parameter reads $\kappa_c = \pi/(40\rho_L)$ and for the network given in Fig. 4.1 one have $\rho_L = 2$, thus $\kappa_c = \pi/80 \approx 0.0393$.

The spectrum of 4.16 can also be computed by using Eq. (4.3). So, one get the transcendental equation

$$\lambda^2 - 2\left(\sigma\cos(\beta\tau)\mathrm{e}^{-\lambda\tau} - \alpha\right)\lambda - \sigma\mathrm{e}^{-\lambda\tau}\left(2\cos(\beta\tau) - \sigma\mathrm{e}^{-\lambda\tau}\right) = 0 \tag{4.19}$$

with $\sigma = -\kappa\mu_j$. Eq. (4.19) can be numerically solved using the Lambert W function. The solutions of (4.19) are compared to the analytical approximation.

The asymptotic spectrum (given in terms of Eq. (4.18)) and the spectrum points (solutions of Eq. (4.19)) are given in Fig. 4.3 with parameters given in the figure's caption.

Figure 4.3 - The asymptotic continuous spectrum (blue lines) and the pseudo-continuous spectrum (red dots) for the periodic Stuart-Landau system given in terms of the equations (4.18) and (4.19) respectively. The parameters considered were $\sigma = -0.08$ (with $\mu = \rho_L = 2$, the spectral radius of the Laplacian matrix of the network in Fig. 4.1, and $\kappa = 0.04$), $\alpha = 1$, $\beta = \pi$ and $\tau = 20$.

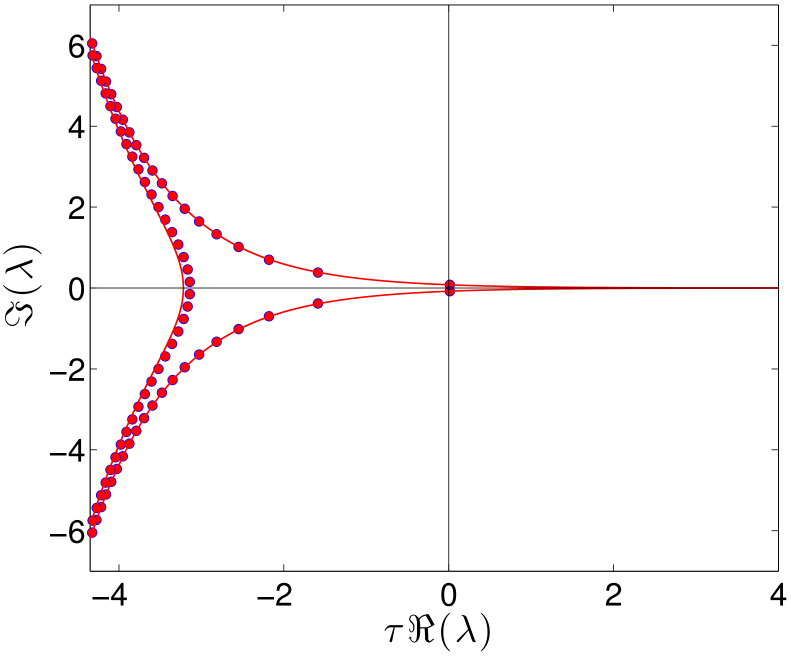

The data of Fig. 4.3 confirms the analytical approximation for the synchronization window $0 < \kappa < \pi/(2\tau\rho_L)$ with $\tau = 2\pi M/\beta$, $M \in \mathbb{N}$. Fig. 4.4 brings the results of the numerical integration of Eq. (4.12) in the periodic orbit regime for different values of κ slightly bellow and above the critical one $\kappa_c = 0.393$.

Figure 4.4 - (top) Solutions of Eq. (4.12) of the nodes 1 and 3 for four coupled periodic SL oscillators (see Fig. 4.1) in which $\kappa = 0.039$ (top, left) and $\kappa = 0.04$ (top, right). And, (bottom) time series of the norm of the difference between the cited nodes where $\kappa = 0.039$ for the down left figure and $\kappa = 0.04$ for the bottom right. Others parameters were $\alpha = 1$, $\beta = \pi$, $\tau = 100$ and the coupling function $h = \sin$. The hollow points stands for $z(t = 0)$ and the green squares stands for $z(t = 5000)$.

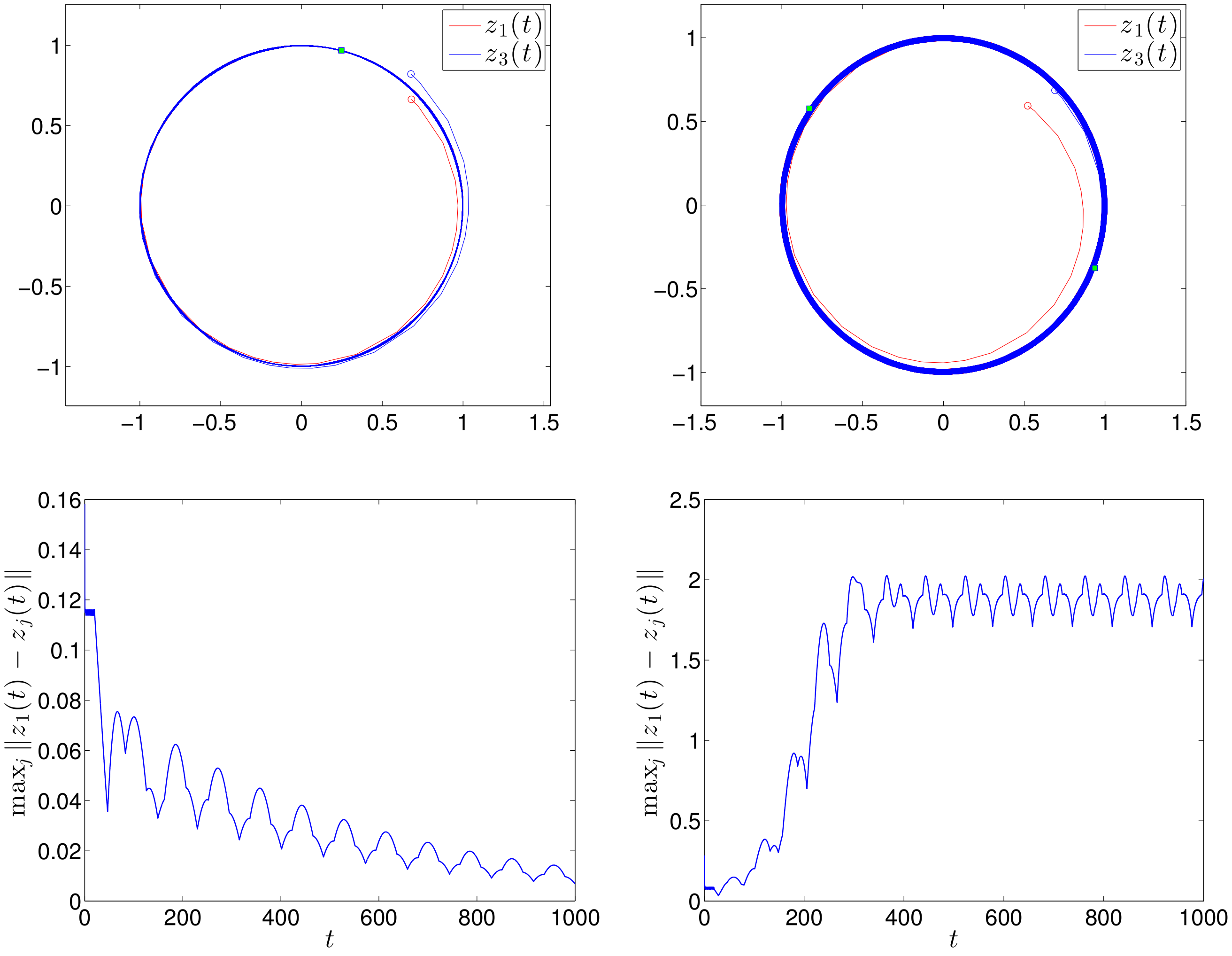

Figure 4.5 - Synchronization map in the $\sigma \times \tau$ parameter space. The color scale represents $\Re(\lambda) < 0$ in which λ is a solution of (4.19) with maximal real part. The white color stands for the instability region ($\Re(\lambda) > 0$). The parameters used were $\alpha = 1$ and $\beta = \pi$.

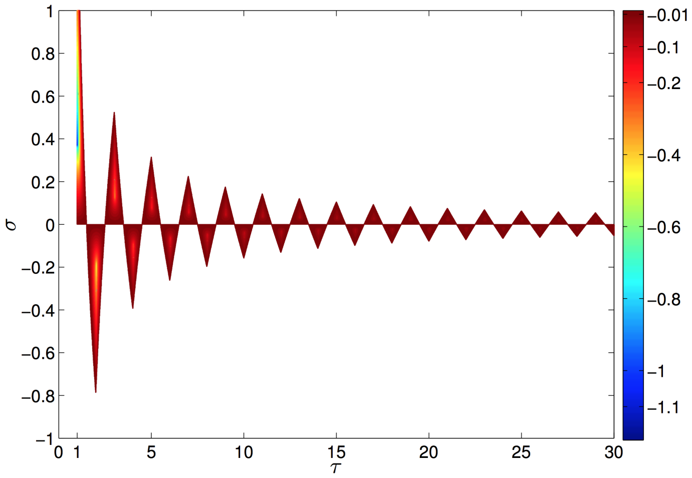

From Fig. 4.4 one can see that the critical coupling parameter obtained is indeed fair.

Now, in order to have a complete view of the stability domain, a synchronization map is produced in the parameter space $\sigma \times \tau$. The Fig. 4.5 shows such a color map presenting the values of $\max_m \Re(\lambda_m) < 0$, where λ_m, $m \in \mathbb{Z}$, is a solution of Eq. 4.19, in the $\sigma \times \tau$ parameter space. Note that $\sigma = -\kappa\rho_L$ and, as predicted by Theorem 4.3, the stable synchronization either occurs for $0 < \kappa < \kappa_c$ or for $-\kappa_c < \kappa_c < 0$ with κ_c shrinking as τ grows.

The parameter values $-1 \leq \sigma \leq 1$ of the color map in Fig. 4.5 can be related to more complicated connected network for coupling parameter values in the range $-1/\rho_L \leq \kappa < 1/\rho_L$. The interchange between stability domains occurs at the values $\tau = (\pi + 2M\pi)/(2\beta) = (2M + 1)/2$, $M \in \mathbb{N}$, where we considered $\beta = \pi$. For such values of time delays no stable synchronization is attained.

4.3.3 Characteristic time

In this section, the proof of Corollary 4.1, about the synchronization characteristic time, is discussed, that is, the order of magnitude of the time such that the trajectories enter a small vicinity of the synchronization manifold. In particular, the interest is centered in the scaling of the transient time with coupling strength κ and time delay τ.

The real parts of the eigenvalues of the linearized system can be estimated rigorously, so the characteristic time should be related to the properties of the linearized system. The decay time of the solutions $\xi(t)$ of Eq. (4.2) is

$$\|\xi(t)\| \leq C\mathrm{e}^{-\eta t} \tag{4.20}$$

with $\eta > 0$. Hence, the *characteristic time* ν is defined as

$$\nu = 1/\eta.$$

The characteristic time measures how fast the slowest solution $\xi(t)$ approaches 0. One can write $\eta = -\gamma_{\max}/\tau$ where $\gamma_{\max}$ is the maximum of the real part of the asymptotic continuous spectrum given in Eq. (4.4). It can be computed as

$$\gamma_{\max} = -\min_{\ell} \inf_{\omega} \ln |g_\ell(\omega)| + \max_{j} \ln \kappa |\mu_j| = \ln \frac{\kappa \rho_L}{r_0} = \ln \frac{\kappa}{\kappa_c}.$$

Hence, the characteristic time is

$$\nu(\kappa) = -\tau \ln^{-1} \left(\frac{\kappa}{\kappa_c} \right). \tag{4.21}$$

Clearly, $\nu \to \infty$ as $\kappa \to \kappa_c$.

Fig. 4.6 shows a test for characteristic time given by Eq. (4.21) using two coupled Stuart-Landau oscillators with parameters $\alpha = -1$, $\beta = \pi$, and $\tau = 20$. In this example, Eq. (4.21) reads $\nu(\kappa) = -20 \ln^{-1}(2\kappa)$.

4.4 Synchronization loss versus network structure

It is explored here the relationship between growing networks (with strongly delayed connection) and its synchronization window, which the main results are the corollaries 4.2 and 4.3.

Large networks such as Barabási-Albert scale-free network, Erdös-Réniy random network, and some regular graphs will be considered since the expressions for the Laplacian spectral radius ρ_L are known.

First, let us take a look at how regular graphs respond to the synchronization (considering the NDSF Network Model with long delay) in the limit of large network size. Table 4.1 lists spectral radius of the Laplacian matrix of the main regular graphs:

Figure 4.6 - Characteristic time for the synchronization of two Stuart-Landau coupled oscillators. The red curve is $\nu(\kappa) = 20\ln^{-1}(2\kappa)$. The blue dots were obtained by fixing κ and computing η, which stands for the angular coefficient of Eq. (4.20) in log scale in which $||\xi(t)|| = ||x_1(t) - x_2(t)||$, and then taking $\nu = 1/\eta$. The parameters used were $\alpha = -1$, $\beta = \pi$ and $\tau = 20$. The history functions were taken as constant and non-zero.

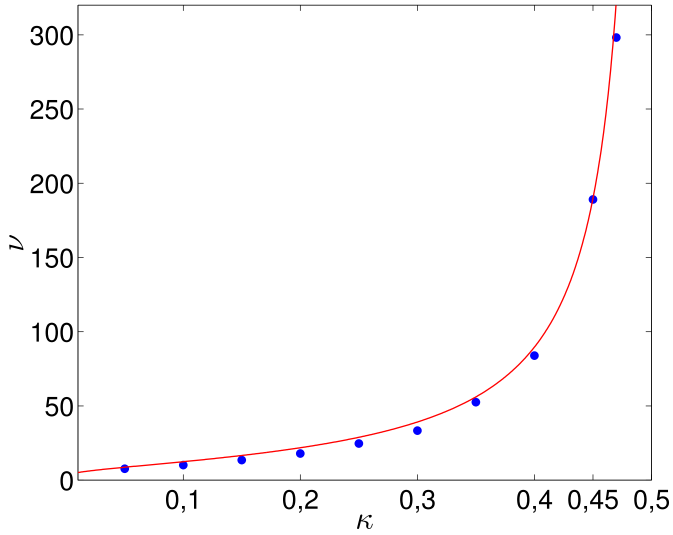

complete, ring, star, and path.

Table 4.1 - Laplacian spectral radius ρ_L and synchronization window for the coupling parameter κ (for strong delay) of some regular graphs.

Graph	ρ_L	Synchronization window
Complete	n	$(0, r_0/n)$
Ring	4 if n is even $2 + 2\cos(2\pi/n)$ if n is odd	$(0, r_0/4)$ or $(0, r_0/(2 + 2\cos(2\pi/n)))$
Star	n	$(0, r_0/n)$
Path	$2 + 2\cos(\pi/n)$	$(0, r_0/(2 + 2\cos(\pi/n)))$

The proof of the values listed in Table 4.1 for the Laplacian spectral radius can be checked in references (CVETKOVIĆ et al., 2009; LI et al., 2009; BROUWER; HAEMERS, 2011).

Using Theorem 4.1, and Table 4.1 one observe that:

- For large delay and a large network size $n \to \infty$, the synchronization manifold tends to be always unstable in networks of the types *Complete* or *Star* provided that the coupling strength κ does not scale with n.

- For large delay and a large network size $n \to \infty$, the synchronization manifold tends to be stable for a certain interval of the coupling strength $\kappa \in (0, r/4)$ in simple networks of the types *Ring* or *Path*.

Now, let us consider some complex networks. The synchronization condition will be related to the graph structure for two important examples of complex networks, namely, homogeneous and heterogeneous networks, specifically ER and BA networks. See Section 2.3 for details.

The response of the BA and ER networks to synchronization under the considered delayed model already stated in Section 4.1 and encoded in corollaries 4.2 and 4.3. Both results says that ER and BA networks tend to not have stable synchronization in the limit of large n. But, ER networks, losses stable synchronization at a slow rate compared to BA networks.

The both cited corollaries are proved here. The proof of Corollary 4.2 is based on well-known results, namely, Lemma 2.2 and Lemma 2.3.

Proof of Corollary 4.2. The Lemma 2.3 implies that the maximum degree of a BA network grows as $\sqrt{n}$ when $n \to \infty$. Therefore, using Eq. (2.3) and (2.4) one see that $\rho_L \geq \mu\sqrt{n}$ with probability 1 in the limit of large n which implies that the synchronization window, that is, the interval $(0, r/\rho_L)$ (see Theorem 4.1) shrinks and vanishes with large n. $\square$

Remark 4.5. *Corollary 4.2 shows that the synchronization manifold tends to be unstable in large and strongly delayed BA (heterogeneous) networks if the coupling strength is not scaled with* n *or* τ.

For the proof of Corollary 4.3, Lemma 2.2 and Lemma 2.4 are used.

Proof of Corollary 4.3. For large n and using the probability $p = p_0 \ln n/n$ with $p_0 > 1$ one get

$$g_{\max} \sim p_0 \ln n + O\left(\sqrt{\ln n}\right).$$

Figure 4.7 - Comparative of the critical parameter's order for the BA (blue line) and ER (red line) networks. The x-axis stands for the number of nodes in the network.

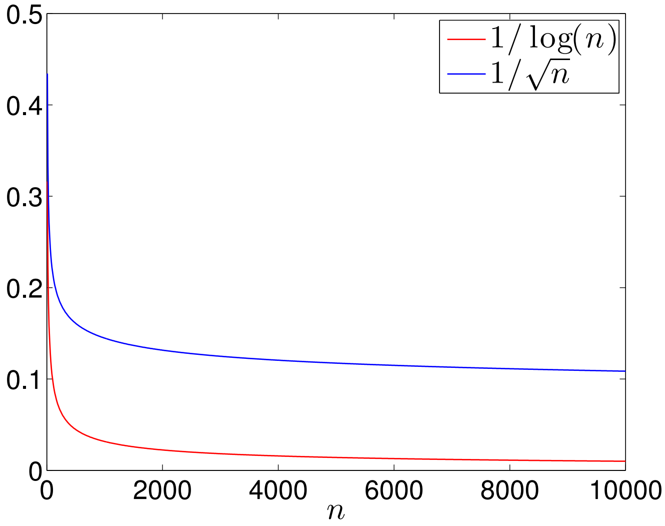

So, using Lemma 2.2, one end up with

$$\rho_L \geq \left(\frac{n}{n-1}\right)\left[p_0 \ln n + O\left(\sqrt{\ln n}\right)\right]$$

which means that $\rho_L \to \infty$ when $n \to \infty$ with a rate of order $\ln n$. The spectral radius ρ_L is the lowest possible when $p_0 \to 1^+$ maintaining the network connected, or, ρ_L is the lowest possible when the network crosses the connectivity threshold becoming connected. $\square$

Although Corollary 4.3 says that the ER random network does not allow the synchronization manifold to be stable in the limit of $n \to \infty$, the rate in which it happens is slow, making it possible to synchronize very large ER networks with long time delays. The Figure 4.7 depicts the asymptotic behavior of the critical parameter's order for these two types of network.

The properties observed for the stability of the synchronization manifold for BA and ER networks with strong delay, that is, large BA networks doesn't support strong delay interaction and relatively large ER networks supports strong delay interaction, are similar to the persistence of the synchronization when the non-delayed coupling functions are non-identical (MAIA et al., 2016).

4.4.1 Synchronization of BA and ER networks when coupling strength is scaled with n

As one has seen from the previous subsection, not only simple but also, complex networks tend to have an always unstable synchronization manifold with strong delay τ and large network size n.

In many network dynamical models, it is common to normalize the coupling parameter, in our case κ, in order to preserve certain behaviors and properties of the network, such as synchronization, mean field oscillation, community clustering, etc (ARENAS et al., 2008; RODRIGUES et al., 2016; FORTUNATO, 2010). When the network size is dynamical, for instance, the size of the network is growing with time, then this normalization becomes even more important.

With this in mind, one can see that in the regime of large network size, the coupling parameter κ should have some natural scaling depending on the network structure. If those scaling are taken into account in the network model then the stability of the synchronization manifold can always be preserved for $n \to \infty$.

For example, if it is known beforehand that a large simple network of the type Complete (or Star) is considered then the natural scaling of the coupling parameter would be

$$\kappa \to \frac{\kappa}{n}.$$

Then, further consequences of the corollaries 4.2 and 4.3 are stated when considering the scaling of the coupling parameter.

Corollary 4.4. *Consider a BA scale-free network with number of nodes equals to n. Consider the NDSF Network Model with the coupling parameter*

$$\kappa = \frac{\kappa_s}{\sqrt{n}}.$$

Then for any large enough size n and long enough delay, there is always a non-empty interval $I = (0, \kappa_{\max}(n)) \subset \mathbb{R}$ such that any synchronous periodic or steady state is locally exponentially stable for all $\kappa_s \in I$ and unstable if $\kappa_s \in \mathbb{R} \setminus \overline{I}$ (with probability 1). Moreover, the length of this interval converges to a nonzero constant with $n \to \infty$ with probability 1:

$$\lim_{n\to\infty} \kappa_{\max}(n) = \kappa_\infty, \quad 0 < \kappa_\infty < \infty.$$

Proof. Any synchronous equilibrium or periodic solution is locally exponentially stable if $0 < \kappa < r/\rho_L$ and unstable for $\kappa > r/\rho_L$ for some $r > 0$. For BA scale-free networks it is known that $\rho_L \sim \sqrt{n}$ (see Lemma 2.3). Then, if the coupling parameter is re-scaled as $\kappa \to \kappa_s/\sqrt{n}$, the new synchronization condition is $0 < \kappa_s/\sqrt{n} < r/\rho_L \approx r/\sqrt{n}$, which leads to $0 < \kappa_s < r$. ☐

Corollary 4.5. *Consider an ER random network with n nodes and the NDSF Network Model with new coupling parameter scaled as*

$$\kappa = \frac{\kappa_s}{\ln n}.$$

Then for large enough network size n and long enough time delay τ, there is an interval $I = (0, \kappa_{\max}(n)) \subset \mathbb{R}$ such that any synchronous equilibrium or periodic solution is locally exponentially stable if $\kappa_s \in I$ and unstable if $\kappa_s \in \mathbb{R} \setminus \overline{I}$ (with probability 1). Moreover, the length of the interval I converges to a nonzero constant with $n \to \infty$ with probability 1:

$$\lim_{n \to \infty} \kappa_{\max}(n) = \kappa_\infty, \quad 0 < \kappa_\infty < \infty.$$

The proof of the Corollary 4.5 follows the same steps of the Corollary 4.4 using the Lemma 2.4.

5 STABILIZATION OF STEADY STATES IN REGULAR NETWORKS

In Chapter 4 the synchronization in delayed coupled networks for stables units (having equilibrium or periodic synchronous dynamics) was studied. In that case, the assumption that the units were stable was essential to achieve stable synchronization. It was shown that when the units of the network have unstable isolated dynamics then no stable synchronization is possible (Theorem 4.4 ensures it). That is, with the NDSF Network Model, no control of the unstable dynamical units is possible.

For this reason, it has been considered in the introduction another slight different network dynamical model, namely, the NID Network Model given by Eq. (1.2). Moreover, a specific isolated dynamics is considered, which represents the normal form of the Hopf bifurcation. A specification of the dynamics is considered since the control strategy used in this chapter is based on the assumption that the dynamics of any individual node of the network is close to the mentioned bifurcation. Therefore, in this chapter, the problem of stabilization of unstable equilibrium solutions in a network scenario is approached.

5.1 Main Result

Considering Assumption 1.3, our problem formulation consists at coupling n identical systems which has an unstable equilibrium and then, due to the coupling, with an appropriated choice of coupling parameter κ and delay τ, the equilibrium is stabilized in the network. It is considered coupling with large delay, but not arbitrary large delay. The large delay is considered since the proposed problem is tackled by studying the spectrum of the linear system and it is known that this spectrum has nice asymptotic behavior, as it has been discussed in Chapter 3. Therefore, by considering a large delay, the true spectrum is approximated by the asymptotic one.

In Ref. (YANCHUK et al., 2006) the authors have shown that for a single Stuart-Landau equation with long time-delay feedback τ, successful control can be achieved periodically in τ when the parameter $\alpha > 0$ is small, that is, control occurs when the system is close to the Hopf bifurcation. Here, no self-feedback delay is considered, rather then, the delays come from the coupling with the other oscillators. However, the same ideas used in Ref. (YANCHUK et al., 2006) holds for our NID Network Model. So, the results of cited reference will be extended to regular networks.

The pair (κ, τ) that leads to the stabilization scenario depends on the spectral properties of the adjacency matrix. Hence, our main result is restricted to a family of graphs in which one can assert about a special property of the eigenvalues of the adjacency matrix A.

Assumption 5.1. *The eigenvalues* σ_j, $j = 1, \cdots, m$, *of the adjacency matrix* A, *of dimension* $n \geq m$, *that are roots of the spectral circle of* A *are equidistributed.*

The Assumption 5.1 defines that the adjacency matrix A, and consequently the graph $\mathcal{G}(A)$, with links given by A, has a special property that the eigenvalues that are roots of the spectral circle of A are the complex numbers that have the same modulus and a shift of $2\pi/m$ in their arguments. The number of the spectral roots m of A dictates the frequency of reappearance of the control region.

Theorem 5.1. *Consider the NID Model in a d-regular network satisfying Assumption 1.3 with* $0 < \alpha \ll 1$, *Assumption 1.4 with* $H = \mathbb{I}_2$ *and Assumption 5.1.*

Then, there exist $\tau_0 > 0$ *such that for all* $\tau > \tau_0$ *and*

$$\frac{\alpha}{d} < \kappa < \frac{2\pi^2}{d\alpha\tau^2 m^2} \min\{\eta_\tau, 1-\eta_\tau\}^2 + \mathcal{O}(1/\tau), \tag{5.1}$$

where

$$\eta_\tau = \frac{\beta\tau m}{2\pi} - q + \frac{m}{2\pi} \arg y\left(\frac{2\pi q}{m\tau}\right) + \mathcal{O}(1/\tau), \tag{5.2}$$

and, $q \in \mathbb{Z}$ *is chosen in such a way that* $\eta_\tau \in (0,1)$ *and* $y(\omega) = (\omega - \beta)\mathbb{i} - \alpha$, *the origin is the synchronous solution of the NID Model and it is locally exponentially stable.*

For any given τ, the maximal value that the control parameter achieve is attained for $\eta = 0.5$. Indeed, if $0 < \eta \leq 0.5$ then $\min\{\eta, 1-\eta\} = \eta \leq 0.5$ and if $0.5 < \eta \leq 1$ then $\min\{\eta, 1-\eta\} = 1-\eta \leq 0.5$. This produces

$$\kappa_{\max} := \frac{\pi^2}{2d\alpha\tau^2 m^2} + \mathcal{O}(1/\tau). \tag{5.3}$$

There are two featured cases of graphs that fulfill Assumption 5.1 (see Section 2.2 for some definitions) :

- The graph is directed and strongly connected In this case the Perron-Frobenius theory ensures the validity of Assumption 5.1.
  - If the graph is undirected then it is naturally strongly connected,

  hence the assumption is also valid. Moreover, if the undirected graph is non-bipartite then $m = 1$ and if the undirected graph is bipartite then $m = 2$.

- The graph is directed and cycle multi-partite. In this case, m is the number of the multi-partitions. As only regular graphs are considered, the special block form of A ensures the validity of Assumption 5.1 when the graph is cycle multi-partite even if it is not strongly connected.

Note that in Eq. 5.1, disregarding the $\mathcal{O}(1/\tau)$ terms, the coupling parameter is inversely proportional to the time-delay τ^2. Therefore, the interval in which the control is achieved shrinks as the delays increases. This implies that for arbitraty large delay, no control is possible. Therefore, in Sections 5.3.1 and 5.3.2 it will be shown that it is impossible to undergoes to control scenario in the case of arbitrary large delay.

Moreover if the $\mathcal{O}(1/\tau)$ terms are disregarded, then for large τ the real control region maybe empty whereas the analytical interval given by Eq. 5.1 might not be empty.

The main content of this chapter is the proof of the Theorem 5.1. It will be proved firstly for the case of two coupled oscillators (in this case $d = 1$ and $m = 2$) because this case is minimal and it gives the intuition on how the proof works. And then, the extension for the general case will be tractable.

5.1.1 Illustration

A simple example of a d-regular which is both, strongly connected and cycle multipartite graph, is the unidirectional ring of n vertices, where each vertex j connects only with the vertex $j + 1$ applying modulus n. In this case $d = 1$ and the graph is cycle n-partite. Therefore its eigenvalues are $\exp(2\pi p\mathbb{i}/n)$ with $p = 1, \cdots, n$. See Figure 5.1 (right) for an illustration.

One consequence of having a cycle m-partite graph is that the coupling parameter κ also decays quadratically with m. This can produce dramatic changes, from the control point of view, between non-directed and directed graphs. Consider for example the ring graphs as in Figure 5.1.

The non-directed ring graph with 5 nodes (left graph on Figure 5.1) is a non-bipartite regular graph (in this case one have $d = 2$ and $m = 1$) while the ring directed network (right graph on Figure 5.1) with also 5 nodes is a cycle 5-partite graph (in this case,

Figure 5.1 - A non-directed ring graph (left) and a directed ring graph (right).

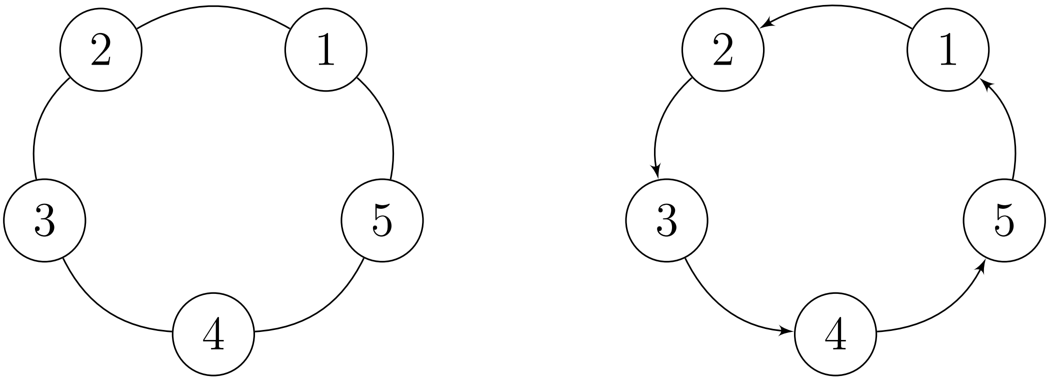

$d = 1$ and $m = 5$). The Figure 5.2 shows the huge difference between the stability regions, using the Stuart-Landau oscillator with $\alpha = 0.01$, $\beta = \pi$.

Figure 5.2 - Comparison of the stability regions for the networks from Figure 5.1. The left figure gives the stability region for the non-directed ring 2-regular graph of 5 nodes and the right figure gives the stability region of the directed 1-regular ring of 5 nodes which is cycle 5-partite. The blue area is given by Eq. (5.1) disregarding the $\mathcal{O}(1/\tau)$ terms and the red line is the maximal κ for any given τ accordingly Eq. (5.3).

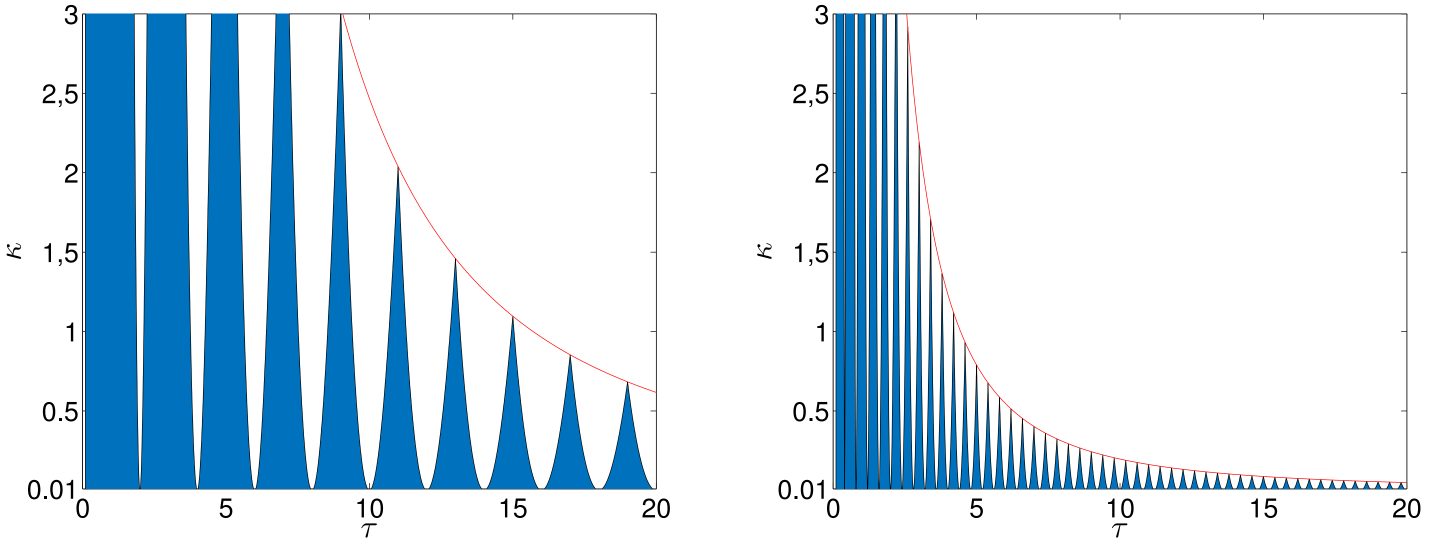

Therefore, considering the measure of area of control (blue area in Figure 5.2) one can conclude that it is easier to control the non-directed ring 2-regular ring rather than the directed 1-regular ring as illustrated in Fig. 5.1.

This example can be extended further and if the network size n grows, then, it's always possible to establish control of the unstable fixed point in a ring non-directed network whilst in the directed ring network, the unstable fixed point tends to remains always unstable for large time delay τ.

5.2 Variational equation

Consider a solution $z(t)$ near the equilibrium z^* and write $z_j(t) = z^* + \psi_j(t)$. Then, in terms of $\psi_j(t)$, Eq. (1.2), with linearization near z^*, reads

$$\dot{\psi}_j(t) = J\psi_j(t) - \kappa d_j H\psi_j(t) + \kappa \sum_{\ell=1}^{n} A_{j\ell} H\psi_l(t-\tau) + \mathcal{O}(\|\psi_j\|^2), \tag{5.4}$$

where d_j is the degree of the vertex j, $J = \mathcal{D}f(z^*)$ is the Jacobian matrix of the isolated vector field f at $z^* = 0$ and $H = \mathcal{D}h(0)$ is the Jacobian matrix of the coupling function at 0. Note that both J and H are matrices in $\mathbb{R}^{2\times 2}$ since it should be computed considering the partial derivatives with respect to real and imaginary parts of the argument.

Disregarding the superior order terms $\mathcal{O}(\|\psi_j\|^2)$ and putting Eq. (5.4) in the block form one have

$$\dot{\psi}(t) = [\mathbb{I}_n \otimes J - \kappa(D \otimes H)]\psi(t) + \kappa(A \otimes H)\psi(t-\tau) \tag{5.5}$$

where J can be explicitly computed

$$J := \mathcal{D}f(0) = \begin{pmatrix} \alpha & \beta \\ -\beta & \alpha \end{pmatrix}.$$

Remark 5.1. *Eq. (5.5) can be block-diagonalized, in the case the matrices A and D commute. The trivial case in which it happens is the case the network is d-regular, that is, all the nodes of the network has the same degree, namely, d. This implies $D = d\mathbb{I}_n$.*

Therefore, in this chapter, only regular networks are considered. Continuing with the analysis on Eq. (5.5) without making the assumption of network regularity would give no further analytical insights.

Hence, applying the change of coordinates $\xi = (R^{-1} \otimes \mathbb{I}_2)\psi$ induced by the adjacency matrix A that can be decomposed as $A = R\Lambda_A R^{-1}$ – where Λ_A is the diagonal matrix with the eigenvalues σ_l, $l = 1, \cdots, n$ on its diagonal – one get the block-diagonal system

$$\dot{\xi}(t) = [\mathbb{I}_n \otimes J - \kappa d(\mathbb{I}_n \otimes H)]\xi(t) + \kappa(\Lambda_A \otimes H)\xi(t - \tau) \tag{5.6}$$

or

$$\dot{\xi}_j(t) = [J - \kappa dH]\xi_j(t) + \kappa\sigma_j H\xi_j(t - \tau) \tag{5.7}$$

where $\xi = (\xi_1, \cdots, \xi_n)$.

5.3 More of the same: description of the spectrum

Eq. (5.7) is a linear delay differential equation with strong delay. Then, as stated in Section 3.3.1 the spectrum of (5.7) consist of the complex numbers λ that satisfies the characteristic equation

$$\det\left(-\lambda\mathbb{I}_2 + J - \kappa dH + \kappa\sigma_j H\mathrm{e}^{-\lambda\tau}\right) = 0. \tag{5.8}$$

Again, it is known (LICHTNER et al., 2011) that the spectrum of a linear DDE with large delay is split into two parts, namely,

- the instantaneous spectrum in which the eigenvalues λ are due to non-delayed terms (in our case, consisting of the eigenvalues of $J - \kappa dH$). The strongly unstable spectrum, Γ_{SU}, is the subset of the instantaneous spectrum consisting of eigenvalues with positive real part;

- the asymptotic continuous spectrum, Γ_A, in which the real part of λ is vanishing with τ, that is, $\lambda = \gamma/\tau + \mathbb{i}\omega$. In our case, they can be determined by the characteristic equation

  $$\det\left(-i\omega\mathbb{I}_2 + J - \kappa dH + \kappa\sigma_j H\mathrm{e}^{-\gamma - i\phi}\right) = 0, \tag{5.9}$$

  where $\phi \in \mathbb{R}$ is a parametrization of the oscillatory term. Estimates on this part of the pseudo-continuous spectrum, that is, the number $\lambda = \gamma/\tau + \mathbb{i}\omega$ is given in the Appendix A.1. Moreover, these estimates are an essential ingredient to prove Theorem 5.1.

Therefore, the trivial solution of (5.7) is exponentially stable if the strongly unstable spectrum is empty and the pseudo-continuous spectrum is entirely on the left side of the complex plane.

Now, by changing κ, if it is possible to control both: the strongly unstable spectrum and the pseudo-continuous spectrum, then the choice of κ leads to the control of the entire network. So, if such κ exists, it is possible to stabilize and synchronize unstable units. In such a way, the network stabilizes unstable objects. However, it will be shown in the next subsections that with arbitrary large delay ($\tau \to \infty$), there is no such κ that stabilizes the network under the model (1.2).

5.3.1 Controlling the strongly unstable spectrum

In order to control the strongly unstable spectrum of a synchronous equilibrium, one must choose $\kappa > 0$ so that the matrix $J - \kappa d H$ has all its eigenvalues with negative real part. Let's consider the assumption made in Theorem 5.1, that is, $H = \mathbb{I}_2$. As the eigenvalues of J are $\alpha \pm \mathbb{i}\beta$, then this easy criterion is fulfilled by choosing

$$\kappa > \frac{\alpha}{d}. \tag{5.10}$$

In a general case, it is not possible to assert about the eigenvalues of $J - \kappa d H$ even though the eigenvalues of J and H are known. But, if J and H are commuting matrices, the similar condition to Eq. (5.10) reads

$$\kappa > \frac{\alpha}{d \min_j \Re\sigma_j(H)},$$

where $\sigma_j(H)$ are the eigenvalues of H with $\Re\sigma_j(H) > 0$ by assumption (see Assumption 1.4).

Eq. (5.10) reveals us that if $d_{\text{min}} = 0$ then it is not possible to control the network. There are two cases where $d_{\text{min}} = 0$, namely, when the network is disconnected where there is, at least, one isolated vertex and consequently, it is not possible to control the entire network; and the second case is when in a directed network, at least one vertex is a source, that is, there are no links pointing to this vertex (or, no information arrives in this vertex).

5.3.2 Controlling the asymptotic-continuous spectrum

Consider the characteristic equation (5.9). For convenience, let us consider a simplified equation

$$\det(-\omega \mathbb{i}\mathbb{I}_2 + J + gH) = 0, \tag{5.11}$$

which is a polynomial with respect to g which also fulfills the equality $g = -\kappa d + \kappa\sigma_j \mathrm{e}^{-\gamma - \mathbb{i}\phi}$. Denote the complex roots of the polynomial (5.11) by $g_{1,2}(\omega)$.

Then for all $j = 1, \cdots, n$ the following holds

$$\sigma_j \mathrm{e}^{-\gamma-\mathbb{i}\phi} - d - \frac{g_{1,2}(\omega)}{\kappa} = 0. \tag{5.12}$$

So, considering the mentioned scaling, the asymptotic continuous spectrum of (5.7) is the set

$$\left\{ \gamma_{\ell,j}(\omega) + \mathbb{i}\omega \in \mathbb{C} : \;\; \gamma_{\ell,j}(\omega) = \ln|\sigma_j| - \ln\left| d + \frac{g_\ell(\omega)}{\kappa} \right|, \, \omega \in \mathbb{R} \right\}. \tag{5.13}$$

Note that (5.13) defines $n \times 2$ curves in the complex plane. Our aim is to choose κ in a such a way that these curves are entirely in the left side of the complex plane: $\gamma_{\ell,j}(\omega) < 0$ for all $1 \le \ell \le 2$, $1 \le j \le n$, and $\omega \in \mathbb{R}$. Note that there is one curve that majorettes all the others, namely, the one with $|\sigma_j| = \rho_A$, the spectral radius of the adjacency matrix A. Note also that the spectral radius ρ_A of a d-regular graph is $\rho_A = d$ (BROUWER; HAEMERS, 2011).

So, the condition $\gamma_{\ell,j}(\omega) < 0$ is equivalent to the inequality

$$d < \left| d + \frac{g_\ell(\omega)}{\kappa} \right|, \tag{5.14}$$

which has to hold for all $\ell = 1, 2$, and $\omega \in \mathbb{R}$.

Consider again the assumption made in Theorem 5.1, that is, $H = \mathbb{I}_2$. In this case, note that $g_\ell(\omega)$ are the solutions of Eq. (5.11) and reads $g_{1,2} = -\alpha + \mathbb{i}(\omega \pm \beta)$. Therefore, Eq. (5.14) reads as

$$d < \left| d + \frac{-\alpha + \mathbb{i}(\omega \pm \beta)}{\kappa} \right| = \left[\left(d - \frac{\alpha}{\kappa} \right)^2 + \frac{(\omega \pm \beta)^2}{\kappa^2} \right]^{1/2}.$$

After some algebraic manipulations, it is obtained

$$\kappa < \frac{\alpha^2 + (\omega \pm \beta)^2}{2d\alpha}.$$

As the last inequality has to hold for all $\omega \in \mathbb{R}$, then

$$\kappa < \kappa_2 := \inf_{\omega\in\mathbb{R}} \frac{\alpha^2 + (\omega \pm \beta)^2}{2d\alpha} = \frac{\alpha}{2d}. \tag{5.15}$$

In the case of H is not the identity but J and H are commuting matrices, one can show that the inequality similar to (5.15) reads,

$$\kappa_2 < \frac{\alpha}{2d\rho_H} \tag{5.16}$$

where ρ_H is the spectral radius of H. Indeed, in this case there is a unitary matrix U such that U^*JU and U^*HU are upper triangular matrices with the eigenvalues on the diagonal (see Ref. (HORN; JOHNSON, 1985) for more details). Then taking $\tilde{J} = U^*JU$ and $\tilde{H} = U^*HU$ one have $\det(-\mathbb{i}\omega\mathbb{I}+J+gH) = \det(U^*)\det(-\mathbb{i}\omega\mathbb{I}+J+gH)\det(U) = \det(-\mathbb{i}\omega\mathbb{I}+\tilde{J}+g\tilde{H}) = 0$. Note that the eigenvalues of a matrix do not change under a linear change of coordinates. As this last determinant is taken for upper triangular matrices, it follows that

$$g_\ell(\omega) = \frac{-\alpha + (\omega \pm \beta)\mathbb{i}}{\sigma_l(H)}$$

where $\alpha \pm \mathbb{i}\beta$ are the eigenvalues of J (also of $\tilde{J}$). So, developing Eq. (5.14) using the obtained $g_\ell(\omega)$ one get Eq. (5.16).

Remark 5.2 (Empty control interval for $\tau \to \infty$)**.** *From Eq.* (5.10) *the strongly unstable spectrum is empty if* $\kappa > \kappa_1 = \alpha/d$, *and from Eq.* (5.15) *the asymptotic continuous spectrum is controlled if* $\kappa < \kappa_2 = \alpha/(2d)$. *This makes the control interval* (κ_1, κ_2) *empty (is also empty the interval* $(\alpha/(d\min_j \Re\sigma_j(H)), \alpha/(2d\rho_H))$*. However, the above statement holds for asymptotically long time delays. That is, for any* $\alpha > 0$ *there is such* $\tau_0(\alpha)$ *such that for all* $\tau > \tau_0(\alpha)$ *the equilibrium is unstable.*

For the case when the considered system is close to the Hopf bifurcation, i.e. $0 < \alpha \ll 1$, *then the limit* $\tau_0(\alpha)$ *may become very large. As a result, near to the Hopf bifurcation, the stabilization may become possible for relatively long but finite time delays. A similar situation was shown in Ref. (YANCHUK et al., 2006).*

The Fig. 5.3 shows numerically the impossibility to control both parts of the spectrum for large enough delay and arbitrary parameter α, that is, when the system is not close enough to the Hopf bifurcation. In others words, the cited figure shows what happens to the both parts of the spectrum of (5.7) as the coupling parameter κ is increased.

Figure 5.3 - The spectrum of Eq. (5.7) for two coupled oscillators with $\tau = 20$, $\alpha = 1$, $\beta = \pi$. The blue and red dots stands for the pseudo-continuous spectrum for the two different eigenvalues of the adjacency matrix. The black lines stands for the asymptotic continuous spectrum ($\tau \to \infty$). The isolated nodes (when exists) stands for the strongly unstable spectrum. The different plots brings different values of coupling parameter κ and they are specified therein. And, the gray trip represents a break in the figure need since the different parts of the spectrum has different scaling.

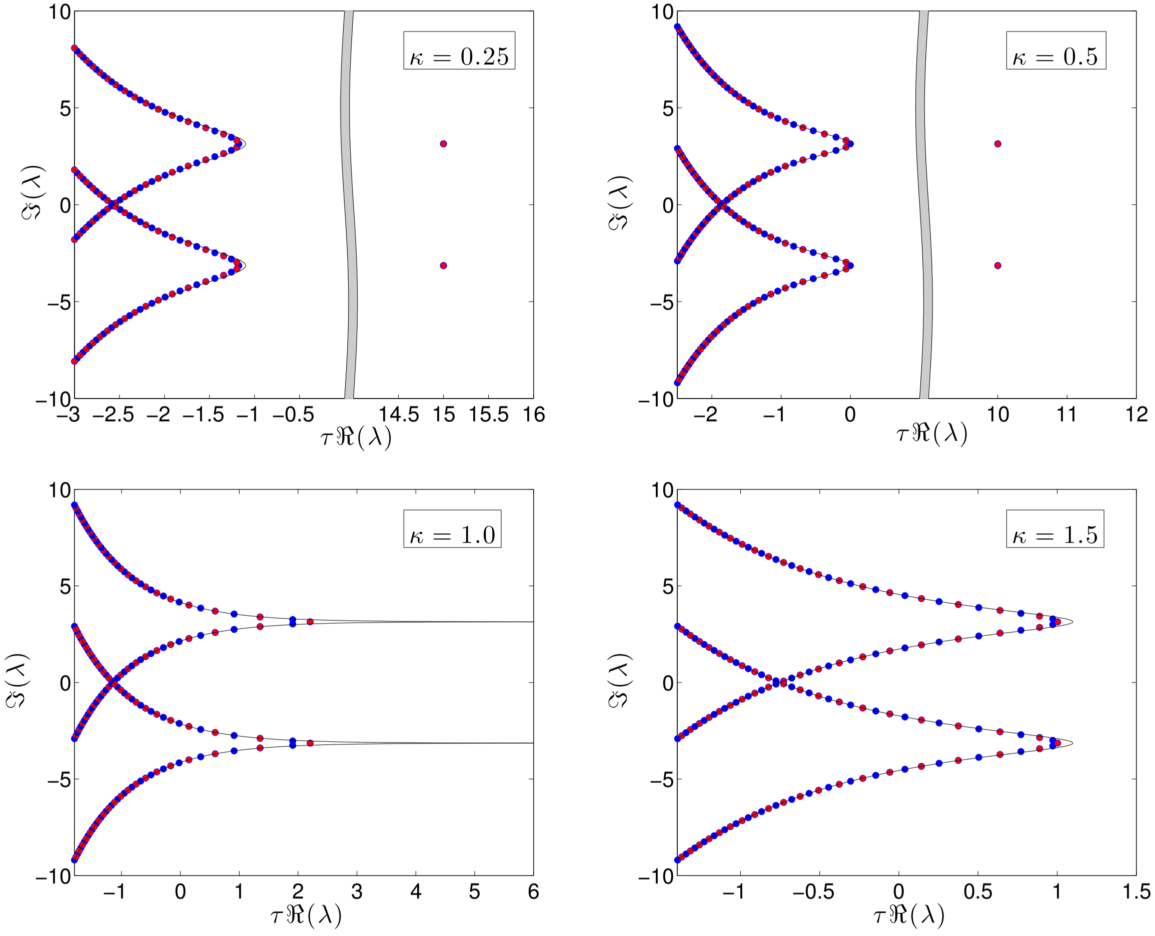

For values of $\kappa < 0.5$ the asymptotic continuous spectrum is on the left side of the complex plane but the strongly unstable spectrum is not empty. For $0.5 < \kappa < 1$ both parts of the spectrum are unstable. And, for $\kappa > 1$ the strongly unstable spectrum is empty but the asymptotic continuous spectrum has always a positive real part. Note also that for $\kappa = 1$, a bifurcation occurs, the strongly unstable spectrum becomes empty and the asymptotic continuous spectrum has singularities at $\pm\beta$. Therefore, no matter how κ is chosen, there is always a set of the spectrum with positive real parts. This confirms numerically what was derived in the current section.

5.4 Proof of Theorem 5.1: The case of two coupled oscillators

Let us consider here the case $n = 2$, that is, the case of two coupled oscillators. Then, the adjacency matrix is

$$A = \begin{pmatrix} 0 & 1 \\ 1 & 0 \end{pmatrix}.$$

It will be shown that the control also occurs periodically with τ (as in Ref. (YANCHUK et al., 2006)) but with a period two times shorter. Here, the asymptotic continuous spectrum is (see (5.13) with $d = 1$, $\sigma_{1,2} = \pm 1$) given by the branches

$$\gamma_{\pm}(\omega) = -\frac{1}{2}\ln\left[\left(1 - \frac{\alpha}{\kappa}\right)^2 + \frac{(\omega \pm \beta)^2}{\kappa^2}\right]. \tag{5.17}$$

Note that the all eigenvalues of the adjacency matrix are $\sigma_1 = -1$ and $\sigma_2 = 1$, therefore, Assumption 5.1 is satisfied. The eigenvalues have the same absolute value and this implies that the asymptotic continuous curves are overlapping each other and each γ_- and γ_+ consists of the two branches of these curves.

In order to compute the eigenvalues of the pseudo-continuous spectrum numerically, the Newton-Rhapson iterations was applied to the Eq. (5.8) considering Assumption 1.3, that is, considering the Stuart-Landau system near the Hopf-bifurcation. The result is shown in Fig. 5.4. From the same figure one can see that by fixing κ, for some values of τ all eigenvalues of the spectrum have negative real part whereas for others values of τ there are eigenvalues with positive real parts. This behavior is periodic with τ and its period is related to the number of eigenvalues of the adjacency matrix. For $\tau \to \infty$ the asymptotic curve will become dense with the pseudo-continuous spectrum. But, as it can seen from Fig. 5.4 stabilization is possible for large but finite τ.

Figure 5.4 - Position of the eigenvalues given by Eq. (5.12) with $\alpha = 0.01$ (near to the Hopf bifurcation), $\beta = \pi$, $\kappa = 1$ and $\tau = 7$ (left) and $\tau = 7.5$ (right). The blue dots are the eigenvalues obtained for $\sigma_1 = 1$ and the red ones for $\sigma_2 = -1$. The black curve is the asymptotic continuous spectrum given by the Eq. (5.17). Note that the real part is rescaled by τ in order to compare the asymptotic continuous spectrum and the actual positions of the eigenvalues.

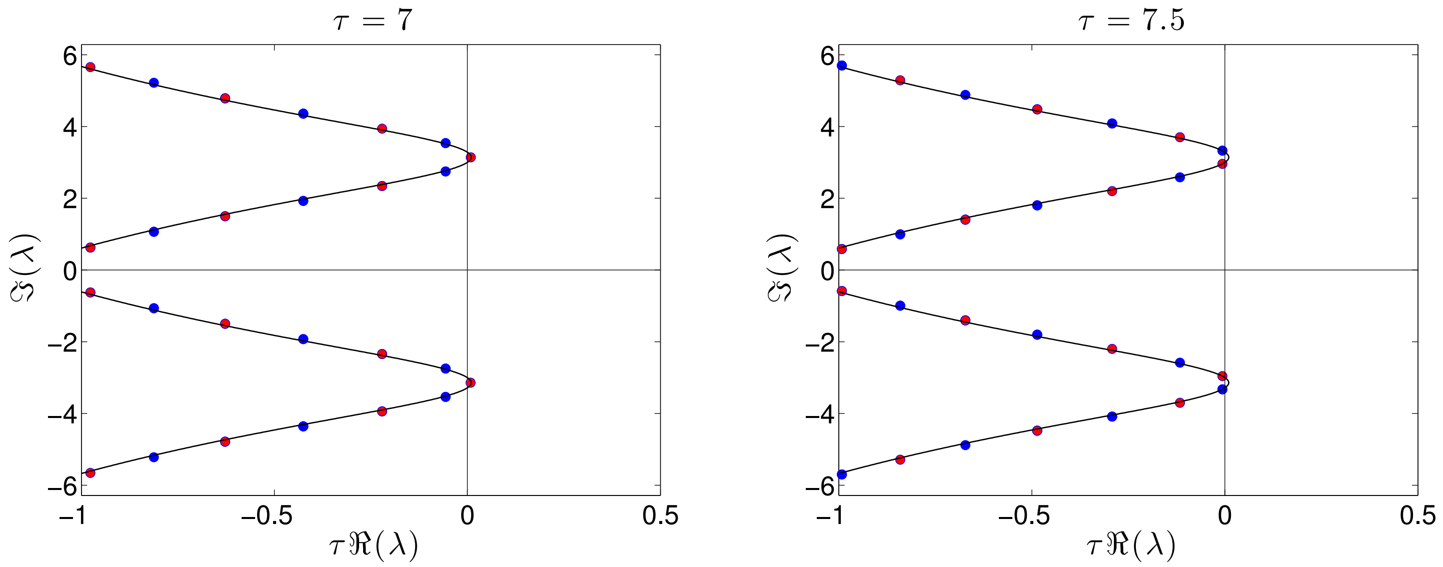

Figure 5.4 indicates how one can derive a control strategy based on the position of the eigenvalues that are close to the branches $\gamma_{\pm}(\omega)$ that may induce instabilities. The Figure 5.5 shows the control strategy that is used following Ref. (YANCHUK et al., 2006). The interval of frequencies $\omega_r < \omega < \omega_R$ corresponds to the unstable part of the asymptotic continuous spectrum, and it may induce the instability. Here,

$$\omega_{r,R} = \beta \pm \kappa \sqrt{1 - \left(1 - \frac{\alpha}{\kappa}\right)^2}$$

are the roots of the Equation (5.17). As, by assumption, $0 < \alpha \ll 1$, these roots can be approximated as

$$\omega_{r,R} \approx \beta \pm \sqrt{2\alpha\kappa} + \mathcal{O}\left(\alpha^{3/2}\right). \tag{5.18}$$

Note that, the Taylor expansion of $\sqrt{(a-x)}$ at $x=0$ is $\sqrt{(a-x)} = sqrt(a) - x/(2\sqrt{(a)}) - O(x^2)$.

Figure 5.5 - Schematic control strategy. Two consecutive eigenvalues λ_q and λ_{q+1}, have negative real parts if and only if its imaginary parts ω_q and ω_{q+1} are outside the interval in which the asymptotic curve crosses the imaginary axis. In other words, $\omega_q < \omega_r < \omega_R < \omega_{q+1}$.

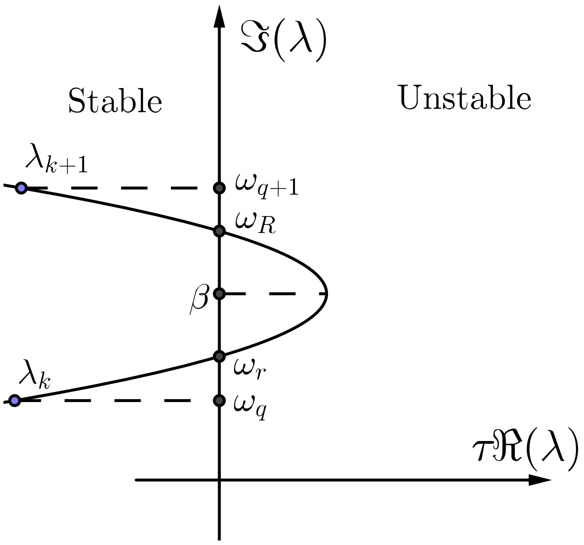

Thus, the length of the interval with unstable frequencies is $|\omega_R - \omega_r| = 2\sqrt{2\alpha\kappa} + \mathcal{O}\left(\alpha^{3/2}\right)$.

On the other hand, the the actual position of the frequencies $\omega_q \in \mathbb{R}$, $q \in \mathbb{Z}$ can be computed (see Corollary A.1 in the Appendix A.1). So, for this case of two coupled oscillators,

$$\omega_{j,q}^{(1)} = \frac{2\pi q}{\tau} - \frac{1}{\tau}\arg y_j\left(\frac{2\pi q}{\tau}\right) + \mathcal{O}(1/\tau^2) \tag{5.19}$$

and

$$\omega_{j,q}^{(2)} = \frac{2\pi q}{\tau} + \frac{\pi}{\tau} - \frac{1}{\tau}\arg y_j\left(\frac{2\pi(q+1)}{\tau}\right) + \mathcal{O}(1/\tau^2). \tag{5.20}$$

y_j are the solutions of (5.11) and they read $y_j(\omega) = (\omega \pm \beta)\mathbb{i} - \alpha$.

Eqs. (5.19) and (5.20) are related to the asymptotic continuous spectrum associated, respectively, with the eigenvalues $\sigma_1 = 1$ and $\sigma_2 = -1$ of the adjacency matrix. The curves of the asymptotic continuous spectrum in this case are the same (see Remark A.2), however, the position of the eigenvalues are shifted by $\mathbb{i}\pi/\tau + \mathcal{O}(1/\tau^2)$, as follows from Eqs. (5.19) and (5.20). Combining the two sets together, one have the approximation for the spectrum

$$\lambda_{j,q} = -\frac{1}{\tau}\ln|y_j(\omega_{j,q})| + \mathbb{i}\omega_{j,q} + \mathcal{O}(1/\tau^2), \text{ where} \tag{5.21}$$

$$\omega_{j,q} = \frac{\pi q}{\tau} - \frac{1}{\tau}\arg y_j\left(\frac{\pi q}{\tau}\right) + \mathcal{O}(1/\tau^2) \tag{5.22}$$

parametrizes Eqs. (5.19) and (5.20) for $q \in \mathbb{Z}$. Then, the distance between two consecutive eigenvalues of the pseudo-continuous spectrum is

$$|\lambda_{j,q+1} - \lambda_{j,q}| = \frac{\pi}{\tau} + \mathcal{O}(1/\tau^2).$$

Let us introduce the small parameter $\varepsilon = 1/\tau$. Then, one have $|\lambda_{j,q+1} - \lambda_{j,q}| = |\omega_{j,1+1} - \omega_{j,1}| = \pi\epsilon + \mathcal{O}(\varepsilon^2)$. As the distance between neighboring frequencies is proportional to ε then successful control is possible if α is scaled as ε^2 (see Eq. (5.18)). Therefore, it is introduced $\alpha = \alpha_0\varepsilon^2$. Thus, Eq. (5.18) reads $\omega_{r,R} = \beta \pm \varepsilon\sqrt{2\alpha_0\kappa} + \mathcal{O}(\varepsilon^3)$.

Then, in order to derive the stability condition over κ one can take a look at Figure 5.5 and see that its necessary and sufficient that in order to have consecutive eigenvalues $\lambda_{j,q}$ and $\lambda_{j,q+1}$ on the left side of the complex plane one must have

$$\omega_{j,q} < \omega_r < \omega_R < \omega_{j,k+1}$$

for all j and q or, in this case,

$$\omega_{j,q} < \beta - \varepsilon\sqrt{2\alpha_0\kappa} < \beta + \varepsilon\sqrt{2\alpha_0\kappa} < \omega_{j,q} + \pi\varepsilon. \tag{5.23}$$

Let us write β in the form $\beta = (1-\eta)\omega_{j,q} + \eta\omega_{j,q+1}$, where $0 \leq \eta \leq 1$ is some constant. Then $\beta = \omega_{j,q} + \eta(\omega_{j,q+1} - \omega_{j,q}) = \omega_{j,q} + \eta\pi\varepsilon$. As $\omega_{j,q} = \pi q\varepsilon - \varepsilon \arg y_j\,(\pi q\varepsilon) + \mathcal{O}(\varepsilon^2)$, one can find

$$\eta \coloneqq \frac{\beta}{\pi\varepsilon} - q + \frac{1}{\pi} \arg y_j\,(\pi q\varepsilon) + \mathcal{O}(\varepsilon).$$

Hence, rewriting $\beta = \omega_{j,q} + \eta_\tau \pi\varepsilon$ one have $\omega_{r,R} = \omega_{j,q} + \eta_\tau\pi\varepsilon \pm \varepsilon\sqrt{2\alpha_0\kappa}$. Substituting this expression for $\omega_{r,R}$ into (5.23), it is obtained

$$0 < \eta\pi\varepsilon - \varepsilon\sqrt{2\alpha_0\kappa} < \eta\pi\varepsilon + \varepsilon\sqrt{2\alpha_0\kappa} < \pi\varepsilon,$$

which holds up to terms $\mathcal{O}(\varepsilon^2)$. The last expression splits into two inequalities, which can be written with respect to κ as follows:

$$\kappa < \frac{\pi^2}{2\alpha_0}\eta^2 + \mathcal{O}(\varepsilon). \tag{5.24}$$

and

$$\kappa < \frac{\pi^2}{2\alpha_0}(1-\eta)^2 + \mathcal{O}(\varepsilon). \tag{5.25}$$

Considering Eqs. (5.24), (5.25), as well as the condition for the absence of the strongly unstable spectrum $\kappa > \alpha$, necessary and sufficient conditions for stability (and control) of the fixed point of the two Stuart-Landau coupled oscillators accordingly to the model (5.4) is obtained:

$$\alpha < \kappa < \frac{\pi^2}{2\alpha_0} \min\{\eta^2, (1-\eta)^2\} + \mathcal{O}(\varepsilon).$$

Rewriting $\alpha_0 = \alpha\tau^2$ and $\varepsilon = 1/\tau$ it is obtained

$$\alpha < \kappa < \frac{\pi^2}{2\alpha\tau^2} \min\{\eta^2, (1-\eta)^2\} + \mathcal{O}(1/\tau) \text{ with} \tag{5.26}$$

$$\eta = \frac{\beta\tau}{\pi} - q + \frac{1}{\pi}\arg y_j\,(\pi q/\tau) + \mathcal{O}(1/\tau), \text{ where } q \in \mathbb{Z} \text{ such that } \eta \in (0,1). \tag{5.27}$$

Remark 5.3. *As the branches are symmetric, one can choose to work with only one of them so that what is valid for one branch is also valid to the other. Therefore Eq. (5.27) does not depend on j, but the index j is kept in order to let the equations to be as general as possible. The upper branch γ_- will be considered, that is, j is then fixed, lets say $j = 1$ and $y = y_1(\omega) = (\omega - \beta)\mathbb{i} - \alpha$.*

Hence, the proof of the Theorem 5.1 is completed. The a maximal value that κ may achieve for a given τ happens when $\eta = 1/2$. It is obtained

$$\kappa_{\max} := \frac{\pi^2}{8\alpha\tau^2} + \mathcal{O}(1/\tau).$$

5.4.1 Computing the stability region for two coupled oscillators

With what was derived, it is possible to have an idea on how the proof of Theorem 5.1 is made. Note that two coupled oscillators consists of an undirected and bipartite network, therefore one get $d = 1$ and $m = 2$ in Theorem 5.1.

The control region derived in Theorem 5.1 for the case of two coupled oscillators and illustrated in Figure 5.6 (blue line) is analytic but approximated compare the blue line with the boundaries of the color map which represents the true spectrum so that $\tau\Re(\lambda) < 0$. Numerically, the region of control can be computed using the approach of the Lambert function in Eq. (5.8) to find the roots λ for which $\Re(\lambda) < 0$ for a given κ and τ. Rewriting (5.8) as

$$\det(-\lambda\mathbb{I}_2 + J + g\mathbb{I}) = 0 \tag{5.28}$$

where $g = \kappa(-d + \sigma_j e^{-\lambda\tau})$. The solution of Eq. (5.28) reads $g = g_\ell(\lambda) = \lambda - \alpha \pm \beta\mathbb{i}$. Therefore, the solution of (5.8) is

$$\lambda = (\alpha \pm \beta\mathbb{i} - d\kappa) + (1/\tau)W(\tau\kappa\sigma_j \exp(-\tau(\alpha \pm \beta\mathbb{i} - d\kappa))) \tag{5.29}$$

where W is the Lambert function that satisfies $z = W(z\exp(z))$ for $z \in \mathbb{C}$. Figure 5.6 shows a color map with the stability region given by Eq. (5.29) for the case of two coupled Stuart-Landau oscillators.

Note that in Fig. 5.6, there is a mismatch between the color points obtained from Eq. (5.29) and the analytically boundary of the control region given by Theorem 5.1 for the given experiment. This mismatch is due to the disregarding of the $\mathcal{O}(1/\tau)$ terms from Eqs. (5.1) and (5.2). In Fig. 5.7 the difference $\kappa_{\max} - \kappa_r$ is computed where $\kappa_{\max}$ and κ_r are the peaks in Fig. 5.6 from the analytically boundary and color points respectively. This difference is decaying at a rate approximately $2/\tau$ as predicted being of order $\mathcal{O}(1/\tau)$.

Figure 5.6 - Control region for two coupled Stuart-Landau oscillators, numerically computed from Eq. (5.29) with $\alpha = 0.01$, $\beta = \pi$, $d = 1$ and $\sigma_j = \pm 1$. The color scale represents the magnitude of $\Re(\lambda) < 0$ and the blue line stands for the boundary of the region control from Theorem 5.1 with $d = 1$ and $m = 2$.

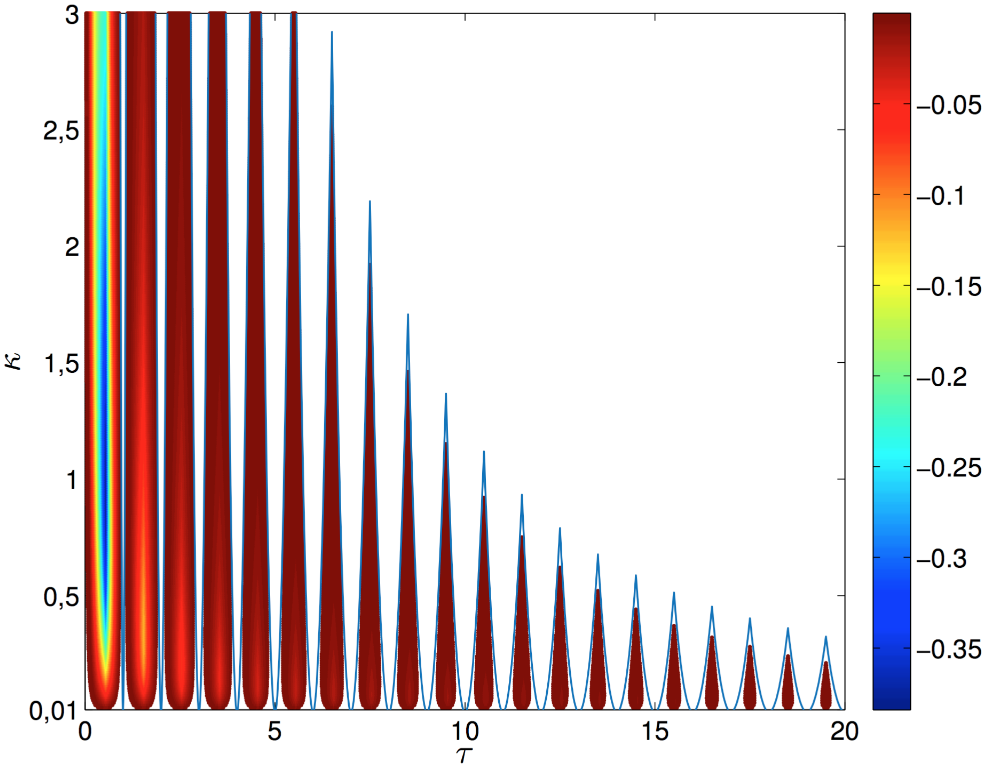

5.5 Proof of Theorem 5.1: Extension

Consider the Assumption 5.1. Algebraically, this assumptions means that the eigenvalues σ_p of the adjacency matrix that are equidistributed roots of the spectral circle of A (which the radius is d since the graph is a d-regular graph) reads

$$\sigma_p = d \exp(2\pi p \mathbb{i}/m), \quad p = 1, \cdots, m.$$

From Corollary A.2, the position of the imaginary part of the eigenvalues of the pseudo-continunous spectrum $\lambda_{j,q}$ reads

$$\omega_{j,q}^{(p)} = \frac{1}{\tau}\left[2\pi q + \frac{2\pi p}{m} - \arg y_j\left(\frac{2\pi q + 2\pi p/m}{\tau}\right)\right] + \mathcal{O}\left(\frac{1}{\tau^2}\right),$$

$q \in \mathbb{Z}, \quad q < K\tau$, for some $K > 0$ and $p = 1, \cdots, m$.

Each value of p corresponds to one curve of the asymptotic continuous spectrum.

Figure 5.7 - Values $\kappa_{\max} - \kappa_r$ (red points) where $\kappa_{\max}$ and κ_r are the peaks in Fig. 5.6 from the analytically boundary and color points respectively. The blue line is a fitting of the data with decaying rate approximately $2/\tau$.

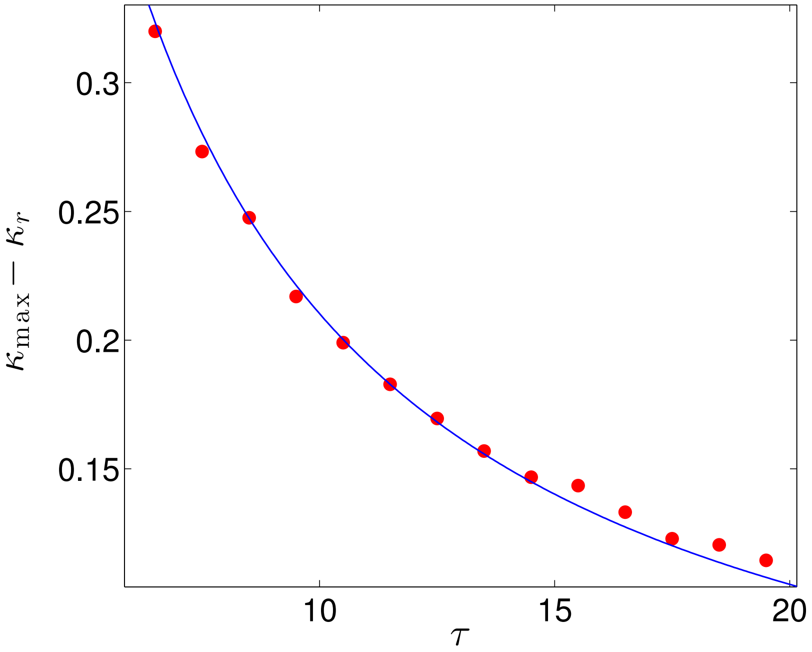

As $|\sigma_p| = d$ (the spectral radius of A), these curves are overlapping with each other (see Eq. (5.13)). The only difference between the curves is that the position of the eigenvalues of the pseudo-continuous spectrum (which is obtained for large but finite τ) are shifted by a common shift. The curves of the assimptotic continuous spectrum are now

$$\gamma_{\pm}^{(p)}(\omega) = \ln|\sigma_p| - (1/2)\ln\left[\left(d - \frac{\alpha}{\kappa}\right) + \frac{(\omega \pm \beta)^2}{\kappa^2}\right]. \tag{5.30}$$

The roots of (5.30) are $\omega_{r,R} = \beta \pm \sqrt{2d\alpha\kappa}$.

In order to stabilize the equilibrium all curves from the asymptotic continuous spectrum that are associated with the graph spectral radius σ_h must considered. A parametrization of the position of the all spectrum points on all these curves is given as

$$\lambda_{j,q} = -\frac{1}{\tau}\ln|y_j(\omega_{j,q})| + \mathrm{i}\omega_{j,q} + \mathcal{O}(1/\tau^2), \text{ where} \tag{5.31}$$

$$\omega_{j,q} = \frac{2\pi q}{m\tau} - \frac{1}{\tau}\arg y_j\left(\frac{2\pi q}{m\tau}\right) + \mathcal{O}(1/\tau^2). \tag{5.32}$$

This expression follows from the same arguments as Eqs. (5.21) and (5.22), where only two eigenvalues of the adjacency matrix were on the spectral radius. The difference of (5.31)–(5.32) from (5.21)–(5.22) is that there are now m eigenvalues on the spectral radius.

As it has be shown for the case of two coupled oscillators, the stabilization is possible when the system is close to the Hopf-bifurcation, so it is considered again $\varepsilon = 1/\tau$ and the scaling $\alpha = \alpha_0\varepsilon^2$. The distance between two consecutive spectrum points $\lambda_{j,q}$ and $\lambda_{j,q+1}$ is now $|\lambda_{j,q+1} - \lambda_{j,q}| = 2\pi/(m\tau) + \mathcal{O}(1/\tau^2)$. Therefore, a necessary and sufficient condition to have consecutive eigenvalues $\lambda_{j,q}$ and $\lambda_{j,q+1}$ on the the left side of the complex plane is similar to Eq. (5.23) but now with $\omega_{j,q}$ given by (5.32). Therefore one have

$$\omega_{j,q} < \beta - \varepsilon\sqrt{2d\alpha_0\kappa} < \beta + \varepsilon\sqrt{2d\alpha_0\kappa} < \omega_{j,q} + 2\pi\varepsilon/m.$$

Proceeding with the algebraic manipulation, the same that was made in the case of two coupled oscillators, the general stabilization condition is obtained

$$\frac{\alpha}{d} < \kappa < \frac{2\pi^2}{d\alpha\tau^2 m^2}\min\{\eta^2, (1-\eta)^2\} + \mathcal{O}(1/\tau)$$

where the left inequality controls the unstable spectrum and the right inequality controls the pseudo-continuous spectrum. Here,

$$\eta = \frac{\tau\beta m}{2\pi} - q + \frac{m}{2\pi}\arg y_j\left(\frac{2\pi q}{m\tau}\right) + \mathcal{O}(1/\tau)$$

and $q \in \mathbb{Z}$ is chosen so that $\eta \in (0, 1)$.

Again, as the branches of the asymptotic continuous spectrum are symmetric then the index j can be fixed. Therefore, one have chosen to consider the upper branch, so that one can replace y_j, without losing generality, by y which reads $y(\omega) = (\omega - \beta)\mathbb{i} - \alpha$. Hence, the Theorem 5.1 is proved.

5.5.1 Validity of Assumption 5.1 for strongly connected graphs

In the comments of the Theorem 5.1, one has stated that the strongly connected graphs fulfills the Assumption 5.1 which in it turns in an essential ingredient for our main result. The validity of this assumption lays on the Perron-Frobenius theory for non-negative matrices. It says that if the graph is strongly connected then the eigenvalues that are on the spectral circle always rise up uniformly distributed on it.

Naturally, a d-regular strongly connected graph fulfills the conditions of the Theorem 2.1 which means that the eigenvalues on the spectral circle reads accordingly with Eq. (2.1).

In a general scenario, it is not possible to assert what is the *imprimitivity index* – the number m – of the spectral radius of a strongly connected graph just by looking at its structure. Nevertheless, it has been ensured that if the graph is strongly connected, then Assumption 5.1 and therefore Theorem 5.1 hold for it.

5.5.2 Validity of Assumption 5.1 for cycle multi-partite graphs

The second characterization of the d-regular directed graph does not require the graph to be strongly connected. It is based on the number of cycle multi-partitions.

If the graph is cycle m-partite it is possible to assert about its eigenvalues in terms of the number of partitions m. Specifically, Theorem 2.2 guarantees the validity of Assumption 5.1 for cycle multi-partite graphs. In particular, the number of cycle multi-partitions is also the number of roots on the spectral circle of the adjacency matrix.

Remark 5.4. *Independently on which classification the d-regular directed graph have, namely, either strongly connected or cycle multipartite, one thing is common and important: the eigenvalues that appear on the spectral circle always comes uniformly distributed on it.*

6 CONCLUSIONS

The focus of this thesis was studying the stability of synchronization in complex networks and control of unstable steady states, given that the nodes of the network possess delayed interactions. For that two different but closely related network models were studied. Namely,

(A) the network model with a self-feedback term in the coupling function, that is, the coupling term is given as a function of the difference of the state vectors $x_\ell(t-\tau) - x_j(t-\tau)$ and

(B) the network model with a instantaneous self-feedback term in the coupling function, that is, now the coupling term is given as a function of the difference $x_\ell(t-\tau) - x_j(t)$.

With the NDSF Network Model we studied the stability of synchronization and with the NID Network Model the control of unstable steady states.

In the context of NDSF Model, we assumed that the uncoupled units of the network have an attractor, which was either an equilibrium or periodic orbit. We obtained conditions for synchronization and desynchronization which depends on the network dynamics.

(i) For the equilibrium, we showed that with strong enough delay, there is a critical coupling parameter κ_c, which depends on the dynamics, coupling function and network structure, that leads to one of the two scenarios: synchronization of the stable units if $\kappa < \kappa_c$; and the destabilization of coupled nodes if $\kappa > \kappa_c$ (this was stated in Theorem 4.1). For this case, κ_c is independent of the delay.

(ii) In the case when the uncoupled system has a stable periodic attractor, we showed that it is always desynchronized for long enough time-delay. However, for long but finite delay the synchronization of periodic orbits are attained for an interval that is shrinking as the delay grows to infinity, that is, for this case the critical coupling parameter depends also on the delay, $\kappa_c = \kappa(\tau)$, and $\kappa(\tau) \to 0$ as $\tau \to \infty$. This result was placed in Theorem 4.3.

Yet in the context of the NDSF Network Model, we have shown that fixing the vector field f, the coupling function h and the delay τ, we were able to study how the network structure affects the critical coupling κ_c. Our results elucidate this dependence and we showed that

- For Barabási-Albert scale free network, $\kappa_c \sim \mathcal{O}(1/\sqrt{n})$.
- For Erdös-Réniy (ER) random networks, $\kappa_c \sim \mathcal{O}(1/\log n)$.

The main ingredients used to study the synchronization and prove the results cited above was the spectral theory for large delay in the field on delay differential equations. And the properties of the spectrum was indeed a powerful tool.

We also showed that no control is possible for unstable steady states using NDSF Network Model since the strongly unstable spectrum is not empty and the control parameter in the refereed model does not control this part of the spectrum (see e.g. Theorem 4.4).

And, In the context of regular networks, we proved that the stabilization of fixed point in the Stuart-Landau system is not possible for arbitrary large delay whereas the stabilization is possible when the system is near to the Hopf-bifurcation. Moreover, we derived the analytical control region and showed that the control occurs periodically with the time-delay and that the frequency of this periodicity is characterized by the number of roots in the spectral radius of the adjacency matrix.

The control strategy used is specific to a system close to the Hopf-bifurcation since the Stuart-Landau system represents the normal form of this bifurcation. Therefore, the same strategy can be applied to others systems with this property (showing supercritical Hopf-bifurcation), but the derivation of the control region is system dependent.

6.1 Perspective of future research

Models extensions:

Both network models that have been studied here are simplifications of more general ones. For instance, the graph matrix considered in the NDSF Network Model is “centered at zero” meaning, for example, that the difference of the degree of a node j from the sum of the normalized weights of the links from the neighbors of j is zero. When the graph matrix is centered at zero then synchronization of chaotic systems with long-delayed interactions is not possible (FLUNKERT et al., 2010).

Therefore, with a different model, rather than NDSF, for example, considering a non-zero centered network model, the results obtained in Chapter 4 for synchronization of fixed points and periodic orbits can be extended to chaotic systems.

Extensions can also be made for the NID Model. The results obtained in Chapter 5 are valid for regular networks and for stabilization of fixed points. Hence, the natural extensions would be in the direction of considering a generic complex network and stabilization of, for example, unstable periodic solutions embedded in chaotic attractors. The stabilization of periodic orbits might be tackled by Pyragas control (PYRAGAS, 1992) using the NID Network Model, that is, in the context of regular networks. In such a case, the stabilization could be achieved for discrete values of time-delay τ, namely, the multiples of the orbit's period. The main difficulty for the extension of the results in Chapter 5 in the direction to generic complex networks is the reduction of the block variational equation to a diagonal form. An alternative to approach this problem would be using a scaling in the coupling parameter by the degree of the node j, that is $\kappa_c \to \kappa_c/d_j$ and then the condition for stability would depend on the spectral radius of $D^{-1}A$ instead of A, where $D = \mathrm{diag}(d_1, \cdots, d_n)$.

Controlling distant mobile agents:

Considering the NID Network Model, the nodes of the network can be viewed as mobile agents where an additional position term $r_j(t)$ in the complex plane is taken into account. For instance, the position of each agent $j = 1, \cdots, n$ at time t would satisfy (PALEY et al., 2007)

$$\dot{r}_j(t) = \mathrm{e}^{\mathrm{i}\phi_j(t)}, \tag{6.1}$$

where $\phi_j(t) = |z_j(t)|$ (the modulus of the solution of NID Model).

As the unstable equilibrium solution of f can be stabilized in the network by the pair (κ,τ), then, for large enough τ and appropriated choice of $\kappa = \kappa(\tau)$, we have $\phi_l(t) = |z_l(t)| \to 0$ (orbitally) exponentially fast for $t \to \infty$. Therefore, the solutions of (6.1) are such that for large t they behave as a linear function $c_j t + c_{0j}$ which means that for large enough t all agents j cease rotating and moves in the same direction like a flock. This is an example of a network stabilization to a parallel formation. We could also consider different types of desired formation patterns (circular, for instance) in which a different choice of the position equation (6.1) should be considered.

This control system may have wide application mainly in engineering system and it will be considered in a future study.

APPENDIX A

A.1 On the approximation of the eigenvalues from pseudo-continuous spectrum

The aim of this section is to give some estimations of the eigenvalues λ of the characteristic equation (5.11), which belong to the pseudo-continuous spectrum, i.e. those that converge to the asymptotic continuous spectrum as $\tau \to \infty$.

Theorem A.1. *Let $y_j(\omega)$, $j = 1, \cdots, q$, be such solutions of the polynomial*

$$\chi(\omega, y) = \det(-\mathbb{i}\omega\mathbb{I}_q + J + By) = 0 \tag{A.1}$$

where $J, B \in \mathbb{R}^{q\times q}$, that $\dfrac{\partial\chi}{\partial y}(\omega, y_j) \neq 0$ for all $\omega \in \mathbb{R}$. Assume that $\mathbb{i}\omega \notin \sigma(J)$, where $\sigma(J)$ is the spectrum of J. Then, the roots $\lambda \in \mathbb{C}$ of the characteristic equation

$$\Delta(\lambda, \tau) = \det(-\lambda\mathbb{I}_q + A + B\mathrm{e}^{-\lambda\tau}) = 0, \tag{A.2}$$

which converge to the asymptotic continuous spectrum as $\tau \to \infty$ are given by

$$\lambda = \lambda_{j,k} = -\frac{1}{\tau}\ln|y_j(\omega_{k,j})| + \mathbb{i}\omega_{k,j} \tag{A.3}$$

where

$$\omega_{k,j} = \frac{1}{\tau}\left[2\pi k - \arg y_j\left(\frac{2\pi k}{\tau}\right)\right] + \mathcal{O}\left(\frac{1}{\tau^2}\right) \tag{A.4}$$

for any $k \in \mathbb{Z}$.

Let us introduce the small parameter $\varepsilon = 1/\tau$ and the ansatz $\lambda = \varepsilon\gamma + \mathbb{i}\omega$. Then, Eq. (A.2) becomes

$$\Delta(\omega, \gamma, \varepsilon) = \det(-(\varepsilon\gamma + \mathbb{i}\omega)\mathbb{I} + A + B\mathrm{e}^{-\gamma - \mathbb{i}\omega/\varepsilon}) = 0. \tag{A.5}$$

By denoting $\phi = \omega/\varepsilon$, we consider a more general equation

$$\Delta_\varepsilon(\omega, \gamma, \phi) = \det(-(\varepsilon\gamma + \mathbb{i}\omega)\mathbb{I} + A + B\mathrm{e}^{-\gamma - \mathbb{i}\phi}) = 0. \tag{A.6}$$

Proof. Now we remark that

$$\Delta_0(\omega, \gamma, \phi) = \chi(\omega, \mathrm{e}^{-\gamma - \mathbb{i}\phi})$$

hence, given the roots y_j of the polynomial $\chi(\omega, y)$, we have $y_j(\omega) = \mathrm{e}^{-\gamma_j}\mathrm{e}^{-\mathbb{i}\phi_j}, j = 1, \cdots, q$. This implies the following explicit expressions for the solutions of $\Delta_0(\omega, \gamma, \phi) = 0:$

$$\gamma_j^{(0)}(\omega) = -\ln|y_j(\omega)|, \tag{A.7}$$

$$\phi_j^{(0)}(\omega) = 2k\pi - \arg(y_j(\omega)), \tag{A.8}$$

where $\omega \in \mathbb{R}$ plays the role of a free parameter.

Now, we show that the solutions of $\Delta_\varepsilon(\omega, \gamma, \phi) = 0$ are regular perturbations of $\phi_j^{(0)}(\omega)$ and $\gamma_j^{(0)}(\omega)$ for small ε, and can be presented as

$$\gamma_j(\omega) = \gamma_j^{(0)}(\omega) + \varepsilon\tilde{\gamma}_j(\omega) \quad \text{and} \quad \phi_j(\omega) = \phi_j^{(0)}(\omega) + \varepsilon\tilde{\phi}_j(\omega)$$

with some smooth functions $\tilde{\gamma}_j, \tilde{\phi}_j : \mathbb{R} \to \mathbb{C}$. Let us fix $\omega, j, \gamma_j^{(0)}(\omega), \phi_j^{(0)}(\omega)$, and k and expand $\Delta_\varepsilon(\omega, \gamma, \phi)$ in Taylor series in ε:

$$\begin{aligned}\Delta_\varepsilon(\omega, \gamma, \phi) &= \Delta_\varepsilon(\omega, \gamma_j^{(0)} + \varepsilon\tilde{\gamma}, \phi_j^{(0)} + \varepsilon\tilde{\phi}) \\ &= \Delta_0(\omega, \gamma_j^{(0)} + \varepsilon\tilde{\gamma}, \phi_j^{(0)} + \varepsilon\tilde{\phi}) + (\varepsilon\gamma)\frac{\partial\Delta_\varepsilon}{\partial(\varepsilon\gamma)} + O(\varepsilon^2).\end{aligned} \tag{A.9}$$

We can also expand $\Delta_0(\omega, \gamma_j^{(0)} + \varepsilon\tilde{\gamma}, \phi_j^{(0)} + \varepsilon\tilde{\phi})$ around the solutions $\gamma_j^{(0)}$ and $\phi_j^{(0)}$. We get

$$\begin{aligned}\Delta_0(\omega, \gamma_j^{(0)} + \varepsilon\tilde{\gamma}, \phi_j^{(0)} + \varepsilon\tilde{\phi}) &= \Delta_0(\omega, \gamma_j^{(0)}, \phi_j^{(0)}) + (\varepsilon\tilde{\gamma})\partial_2\Delta_0 + (\varepsilon\tilde{\phi})\partial_3\Delta_0 + O(\varepsilon^2) \\ &= \varepsilon(\tilde{\gamma}\partial_2\Delta_0 + \tilde{\phi}\partial_3\Delta_0) + O(\varepsilon^2).\end{aligned}$$

where $\Delta_0(\omega, \gamma_j^{(0)}, \phi_j^{(0)}) = 0$ since $\gamma_j^{(0)}$ and $\phi_j^{(0)}$ are solutions of Δ_0, and $\partial_2\Delta_0$, $\partial_3\Delta_0$ stand for the partial derivatives of Δ_0 with respect to the second and third arguments respectively. Now, note that $\partial_3\Delta_0 = \mathbb{i}\partial_2\Delta_0$. Then, we have

$$\Delta_0(\omega, \gamma_j^{(0)} + \varepsilon\tilde{\gamma}, \phi_j^{(0)} + \varepsilon\tilde{\phi}) = \varepsilon(\tilde{\gamma} + \mathbb{i}\tilde{\phi})\partial_2\Delta_0 + O(\varepsilon^2). \tag{A.10}$$

Substituting Eq. (A.10) in Eq. (A.9) we have

$$\Delta_\varepsilon(\omega, \gamma, \phi) = \varepsilon(\tilde{\gamma} + \mathbb{i}\tilde{\phi})\partial_2\Delta_0 + \varepsilon\gamma_j^{(0)}\frac{\partial\Delta_\varepsilon}{\partial(\varepsilon\gamma)} + O(\varepsilon^2). \tag{A.11}$$

As, by hypothesis, y_j are non-degenerate solutions of $\chi(\omega, y) = 0$ and $\dfrac{\partial\chi}{\partial y}(\omega, y_j) \neq 0$

then

$$\partial_2\Delta_0 = -\left[\frac{\partial\chi}{\partial y}(\omega, y_j)\right] y_j \neq 0$$

and therefore (A.11) can be uniquely solved for $\tilde{\gamma}$ and $\tilde{\phi}$ for small ε.

Hence, the solutions of $\Delta_\varepsilon(\omega,\gamma,\phi) = 0$ are

$$\gamma_j(\omega) = -\ln|y_j(\omega)| + \mathcal{O}(\varepsilon),$$

$$\phi(\omega) = 2\pi k - \arg y_j(\omega) + \mathcal{O}(\varepsilon).$$

The solutions of the original equations $\Delta(\lambda,\tau) = 0$ are then given by $\lambda = \varepsilon\gamma + \mathbb{i}\omega$ with an additional condition $\omega = \varepsilon\phi$. Thus we have

$$\lambda = -\varepsilon\ln|y_j(\omega)| + \mathbb{i}\omega + \mathcal{O}(\varepsilon), \tag{A.12}$$

$$\varepsilon 2\pi k - \varepsilon\arg y_j(\omega) + \mathcal{O}(\varepsilon^2) = \omega. \tag{A.13}$$

Equation (A.13) determines the values of ω that are discrete for any finite time delay. From (A.13) we have

$$\omega = \omega_{j,k} := \varepsilon 2\pi k - \varepsilon\arg y_j(\varepsilon 2\pi k) + \mathcal{O}(\varepsilon^2) \tag{A.14}$$

for all $0 < k < K/\varepsilon$ with an arbitrary K independent on ε. Substituting (A.14) into (A.12), we obtain

$$\lambda = \lambda_{j,k} = -\varepsilon\ln|y_j(\varepsilon 2\pi k)| + \mathbb{i}[\varepsilon 2\pi k - \varepsilon\arg y_j(\varepsilon 2\pi k)] + \mathcal{O}(\varepsilon^2)$$

Therefore, substituting $\varepsilon = 1/\tau$ we obtain Eq. (A.3). □

Remark A.1. *The distance between two neighboring eigenvalues is* $|\lambda_{k+1,j} - \lambda_{k,j}| = 2\pi/\tau + O(1/\tau^2)$.

Corollary A.1. *Consider the characteristic equations*

$$\Delta^{(1)}(\lambda,\tau) = \det\left(-\lambda\mathbb{I} + A + \sigma B \mathrm{e}^{-\lambda\tau}\right) = 0$$

and

$$\Delta^{(2)}(\lambda,\tau) = \det\left(-\lambda\mathbb{I} + A - \sigma B \mathrm{e}^{-\lambda\tau}\right) = 0.$$

with $\sigma \in \mathbb{R}$, $\sigma > 0$. *Then, the there are eigenvalues* $\lambda_{k,j}^{(1)}$ *and* $\lambda_{k,j}^{(2)}$ *of* $\Delta^{(1)}(\lambda,\tau)$ *and* $\Delta^{(2)}(\lambda,\tau)$ *respectively, that have the following asymptotic representation*

$$\lambda_{k,j}^{(1)} = -\frac{1}{\tau}\left(\ln\left|y_j\left(\omega_{k,j}^{(1)}\right)\right| - \ln|\sigma|\right) + \mathbb{i}\omega_{k,j}^{(1)}$$

where

$$\omega_{k,j}^{(1)} = \frac{1}{\tau}\left[2\pi k - \arg y_j\left(\frac{2\pi k}{\tau}\right)\right] + \mathcal{O}(1/\tau^2)$$

and

$$\lambda_{k,j}^{(2)} = -\frac{1}{\tau}\left(\ln\left|y_j\left(\omega_{k,j}^{(2)}\right)\right| - \ln|\sigma|\right) + \mathbb{i}\omega_{k,j}^{(2)}$$

where

$$\omega_{k,j}^{(2)} = \frac{1}{\tau}\left[2\pi k + \pi - \arg y_j\left(\frac{2\pi k + \pi}{\tau}\right)\right] + \mathcal{O}(1/\tau^2)$$

and $y_j(\omega)$ *are the non-degenerated solutions of Eq.* $\det(-\mathbb{i}\omega\mathbb{I} + A + yB) = 0$ *and* $k \in \mathbb{Z}$.

Remark A.2. *The asymptotic continuous spectrum from the characteristic equations* $\Delta^{(1)}(\lambda,\tau) = 0$ *and* $\Delta^{(2)}(\lambda,\tau) = 0$ *represents the same curve in the complex plane.*

Proof. By inspecting the proof of Theorem A.1, we observe that Eq. (A.7) is the same as

$$\gamma_j^{(0)}(\omega) = -\ln|y_j(\omega)| + \ln|\sigma|,$$

but (A.8) differ from each other by a phase shift π:

$$\phi_j^{(0)}(\omega) = 2k\pi - \arg(y_j(\omega)), \quad \text{(in case } -\sigma)$$

and

$$\phi_j^{(0)}(\omega) = 2k\pi + \pi - \arg(y_j(\omega)), \quad \text{(in case } +\sigma)$$

with y_j being the solution of the reduced polynomial $\det(-\mathbb{i}\omega\mathbb{I} + A + yB) = 0$. Therefore, using the results of the Theorem A.1 the Corollary A.1 follows. □

Corollary A.2. *Consider the characteristic equations*

$$\Delta_h(\lambda,\tau) = \det\left(-\lambda\mathbb{I} + A + \sigma_p B \mathrm{e}^{-\lambda\tau}\right) = 0$$

with $A, B \in \mathbb{R}^{q\times q}$, $\sigma_p = d \cdot \exp(2\pi p \mathbb{i}/m)$, $d > 0$ *and* $p = 1, \cdots, m$, *for some* $m \in \mathbb{N}$. *Then, the eigenvalues from the pseudo-continuous spectrum have the following asymptotic estimate*

$$\lambda_{j,k}^{(p)} = -\frac{1}{\tau}\left(\ln\left|y_j\left(\omega_{k,j}^{(p)}\right)\right| - \ln d\right) + \mathbb{i}\omega_{k,j}^{(p)},$$

where

$$\omega_{k,j}^{(p)} = \frac{1}{\tau}\left[2\pi k + \frac{2\pi p}{m} - \arg y_j\left(\frac{2\pi k + 2\pi p/m}{\tau}\right)\right] + O\left(\frac{1}{\tau^2}\right)$$

in which $k \in \mathbb{Z}$, $j = 1, \cdots, q$, *and* $y_j(\omega)$ *are the non-degenerated solutions of* $\det(-\mathbb{i}\omega\mathbb{I} + A + yB) = 0$.

Proof. Note that $|\sigma_p| = d$ and $\arg\sigma_p = 2\pi p/m$. Then, the proof is similar to the corollary (A.1). □

APPENDIX B

This appendix is dedicated to deductions of some equations that could be focus misleading in the recurrent text. Therefore, the reader that seeks for deep understanding can consult the present appendix to follow the proofs and deductions.

B.1 Deduction of the Transcendental Equation Solution

The Transcendental Equation Solution is referred to Eq. (5.29). From Eq. (5.12) and $g_\ell = \lambda - \alpha \pm \beta \mathbb{i}$, $\ell = 1, 2$ we have

$$\sigma_j \mathrm{e}^{-\lambda\tau} - d - \frac{\lambda - \alpha \pm \beta\mathbb{i}}{\kappa} = 0.$$

After some algebraic manipulation we get

$$(\alpha \pm \beta\mathbb{i} - d\kappa) - \lambda + \kappa\sigma_j \mathrm{e}^{-\lambda\tau} = 0. \tag{B.1}$$

Eq. (B.1) is of type

$$a + b\lambda + c\mathrm{e}^{-\lambda\tau} = 0. \tag{B.2}$$

with $a, b, c \in \mathbb{C}$ and $b \neq 0$. In our case, $a = \alpha \pm \beta\mathbb{i} - d\kappa$, $b = -1$ and $c = \kappa\sigma_j$. So, let's derive the solution of (B.2) in terms of the Lambert W function, which reads $z = W\left(z\mathrm{e}^z\right)$ with $z \in \mathbb{C}$, and then replace the parameters accordingly.

Consider the a first substitution $u_1 = \lambda\tau$. Then, Eq. (B.2) reads

$$a + b\frac{u_1}{\tau} + c\mathrm{e}^{-u_1} = 0.$$

Consider a second substitution $u_2 = a + bu_1/\tau$. Then, $u_1 = \tau(u_2 - a)/b$ and

$$u_2 + c\exp(-\tau(u_2 - a)/b) = u_2 + c\exp(\tau a/b)\exp(-\tau u_2/b) = 0.$$

Consider a third substitution $u_3 = \tau u_2/b$. Then, $u_2 = bu_3/\tau$ and

$$\frac{b}{\tau}u_3 + c\exp(\tau a/b)\exp(-u_3) = 0. \tag{B.3}$$

Multiplying Eq. (B.3) by $\exp(u_3)$ we get

$$u_3\exp(u_3) = -\frac{\tau c}{b}\exp(\tau a/b).$$

Applying the Lambert W function on both sides of the last inequality we have

$$u_3 = W(u_3 \exp(u_3)) = W\left(-\frac{\tau c}{b}\exp(\tau a/b)\right).$$

But,

$$u_3 = \frac{\tau u_2}{b} = \frac{\tau(a + bu_1/\tau)}{b} = \frac{\tau\left(a + \frac{b\lambda\tau}{\tau}\right)}{b} = \frac{\tau a}{b} + \lambda\tau.$$

Therefore, the solution of (B.2) is

$$\lambda = -\frac{a}{b} + \frac{1}{\tau}W\left(-\frac{\tau c}{b}\exp(\tau a/b)\right). \tag{B.4}$$

Replacing the parameters into Eq. (B.4) one get Eq. (5.29).

B.2 Deduction of the Block-diagonal Variational Equation

The Block-diagonal Variational Equation is referred to (4.2). Eq. (4.2) is obtained by the approach known as master stability equation. It consists of considering the dynamics near the synchronization manifold and then proceed with a change of basis induced by the Laplacian matrix which is diagonalizable by assumption.

Near the synchronization manifold we write $x_j(t)$, solution of (1.1), as $x_j(t) = s(t) + \eta_j(t)$ where $s(t)$ is the solution within synchronization manifold and $\|\eta_j(t)\|$ is small. Hence, considering a linearization of Eq. (1.1), we get the equations for the perturbations

$$\eta_j(t) = J(t)\eta_j(t) + \kappa \sum_{\ell=1}^{n} A_{j\ell} H[\eta_\ell(t-\tau) - \eta_j(t-\tau)] + \mathcal{O}(\|\eta_j\|^2), \tag{B.5}$$

where $j = 1, \cdots, n$, $J(t) = \mathcal{D}f(s(t))$ is the Jacobian of the vector field f along $s(t)$ and $H = \mathcal{D}h(0)$ the Jacobian matrix of h at 0. The term $\mathcal{O}(\|\eta_j\|^2)$ is small and we can disregard it (note that this is not mathematically rigorous, but is it possible to show that the stability of $\eta_j = 0$ is not affected by the superior order terms (TESCHL, 2012)).

Considering the correspondence $L = D - A$ where L is the Laplacian matrix, D is the diagonal matrix having the degree of the vertices in its diagonal and A is the Adjacency matrix. Eq. (B.5) can be written as

$$\eta_j(t) = J(t)\eta_j(t) - \kappa \sum_{\ell=1}^{n} L_{j\ell} H(\eta_\ell(t-\tau)), \quad j = 1, \cdots, n.$$

and in block form it reads

$$\dot{\eta}(t) = [\mathbb{I}_n \otimes J(t)]\eta(t) - \kappa(L \otimes H)\eta(t-\tau) \tag{B.6}$$

where $\eta(t) = (\eta_1(t), \cdots, \eta_n(t))$ is an element of $\mathbb{R}^{nq}$ for each t, and $\otimes$ stands for the Kronecker product.

Now, by hypothesis, L is diagonalizable, let's say $L = P\Lambda P^{-1}$. Then, one can make a change of coordinates projecting the vector state $\eta(t)$ onto the new coordinates induced by P. Consider the new variable $\xi := (P^{-1} \otimes \mathbb{I}_q)\eta$. Therefore, proceeding with this change of variable in Eq. (B.6) one get

$$\dot{\xi}(t) = (P^{-1} \otimes \mathbb{I}_q)[\mathbb{I}_n \otimes J(t)](P \otimes \mathbb{I}_q)\xi - \kappa(P^{-1} \otimes \mathbb{I}_q)(L \otimes H)(P \otimes \mathbb{I}_q)\xi(t-\tau).$$

Using the property of the Kronecker product, namely, $(A\otimes B)(C\otimes D) = (AC\otimes BC)$ for square matrices of same dimension, one have

$$\dot{\xi}(t) = [\mathbb{I}_n \otimes J(t)]\xi(t) - \kappa[\Lambda \otimes H]\xi(t-\tau). \tag{B.7}$$

Eq. (B.7) is block-diagonal since $\Lambda = \mathrm{diag}(\mu_1 \cdots, \mu_n)$ is a diagonal matrix in which the diagonal elements μ_j are the eigenvalues of L. Writing $\xi = (\xi_1, \cdots, \xi_n)$, the variational equation of each block of (B.7) is

$$\dot{\xi}_j(t) = J(t)\xi_j(t) - \kappa\mu_j H\xi_j(t-\tau), \qquad j = 1, \cdots, n.$$

REFERENCES

ARENAS, A.; DÍAZ-GUILERA, A.; KURTHS, J.; MORENO, Y.; ZHOU, C. Synchronization in complex networks. **Physics Reports**, v. 469, n. 3, p. 93 – 153, 2008. ISSN 0370–1573. Available from: <`http://dx.doi.org/10.1016/j.physrep.2008.09.002`>. 1, 15, 60

ARGYRIS, A.; SYVRIDIS, D.; LARGER, L.; ANNOVAZZI-LODI, V.; COLET, P.; FISCHER, I.; GARCIA-OJALVO, J.; MIRASSO, C. R.; PESQUERA, L.; SHORE, K. A. Chaos–based communications at high bit rates using commercial fibre–optic links. **Nature**, Nature Publishing Group, v. 438, n. 7066, p. 343–346, nov. 2005. ISSN 0028-0836. Available from: <`http://dx.doi.org/10.1038/nature04275`>. 2

BARABASI, A.-L.; ALBERT, R. Emergence of scaling in random networks. **Science**, v. 286, n. 5439, p. 509–512, 1999. Available from: <`http://www.sciencemag.org/cgi/content/abstract/286/5439/509`>. 20

BEINEKE, L.; WILSON, R. **Topics in algebraic graph theory**. [S.l.]: Cambridge University Press, 2004. (Encyclopedia of Mathematics and its Applications). ISBN 9780521801973. 9, 13, 20, 42

BOCCALETTI, S.; LATORA, V.; MORENO, Y.; CHAVEZ, M.; HWANG, D. Complex networks: Structure and dynamics. **Physics Reports**, v. 424, n. 4–5, p. 175–308, feb. 2006. ISSN 03701573. Available from: <`http://dx.doi.org/10.1016/j.physrep.2005.10.009`>. 19, 20

BOLLOBÁS, B. **Random graphs**. [S.l.]: Cambridge Univ Pr, 2001. 13, 19

BONDY, J.-A.; MURTY, U. S. R. **Graph theory**. New York, London: Springer, 2007. (Graduate texts in mathematics). OHX. ISBN 978-1-8462-8969-9. Available from: <`http://opac.inria.fr/record=b1123512`>. 13

BRÁZDIL, M.; JANEČEK, J.; KLIMEŠ, P.; MAREČEK, R.; ROMAN, R.; JURÁK, P.; CHLÁDEK, J.; DANIEL, P.; REKTOR, I.; HALÁMEK, J.; PLEŠINGER, F.; JIRSA, V. On the time course of synchronization patterns of neuronal discharges in the human brain during cognitive tasks. **PLoS ONE**, Public Library of Science, San Francisco, USA, v. 8, n. 5, p. e63293, 2013. Available from: <`http://www.ncbi.nlm.nih.gov/pmc/articles/PMC3655978/`>. 1

BROUWER, A.; HAEMERS, W. **Spectra of graphs**. [S.l.]: New York: Springer, 2011. (Universitext). ISBN 9781461419396. 9, 13, 15, 16, 18, 57, 71

CAMPBELL, S.; NCUBE, I.; WU, J. Multistability and stable asynchronous periodic oscillations in a multiple-delayed neural system. **Physica D: Nonlinear Phenomena**, v. 214, n. 2, p. 101 – 119, 2006. ISSN 0167-2789. 1, 2, 5

COLET, P.; ROY, R. Digital communication with synchronized chaotic lasers. **Opt. Lett.**, OSA, v. 19, n. 24, p. 2056–2058, 1994. Available from: <`http://ol.osa.org/abstract.cfm?URI=ol-19-24-2056`>. 2

CVETKOVIĆ, D.; ROWLINSON, P.; SIMIĆ, S. **An Introduction to the Theory of Graph Spectra**. [S.l.]: Cambridge University Press, 2009. (London Mathematical Society student texts). ISBN 9781107365704. 57

DAHMS, T.; LEHNERT, J.; SCHÖLL, E. Cluster and group synchronization in delay-coupled networks. **Phys. Rev. E**, American Physical Society, v. 86, p. 016202, Jul 2012. Available from: <`https://doi.org/10.1103/PhysRevE.86.016202`>. 5

DIBROV, B.; ZHABOTINSKY, A.; KHOLODENKO, B. Dynamic stability of steady states and static stabilization in unbranched metabolic pathways. **J. Math. Biol.**, v. 15, n. 1, p. 51–63, 1982. 2

ENGEL, K.; BRENDLE, S.; NAGEL, R.; CAMPITI, M.; HAHN, T.; METAFUNE, G.; NICKEL, G.; PALLARA, D.; PERAZZOLI, C.; RHANDI, A. et al. **One-parameter semigroups for linear evolution equations**. [S.l.]: New York: Springer, 2006. (Graduate Texts in Mathematics). ISBN 9780387226422. 25

ERNEUX, T. **Applied delay differential equations**. [S.l.]: Springer, 2009. 204 p. (Surveys and Tutorials in the Applied Mathematical Sciences, v. 3). 1

FIEDLER, B.; YANCHUK, S.; FLUNKERT, V.; HÖVEL, P.; WÜNSCHE, H.-J.; SCHÖLL, E. Delay stabilization of rotating waves near fold bifurcation and application to all–optical control of a semiconductor laser. **Phys. Rev. E**, APS, v. 77, n. 6, p. 066207, 2008. Available from: <`http://link.aps.org/abstract/PRE/v77/e066207`>. 1

FIEDLER, M. Algebraic connectivity of graphs. **Czechoslovak Mathematical Journal**, Institute of Mathematics, Academy of Sciences of the Czech Republic, v. 23, n. 2, p. 298–305, 1973. Available from: <`http://eudml.org/doc/12723`>. 9

FLUNKERT, V.; YANCHUK, S.; DAHMS, T.; SCHÖLL, E. Synchronizing distant nodes: A universal classification of networks. **Phys. Rev. Lett.**, American Physical Society, v. 105, n. 25, p. 254101, 2010. Available from: <`https://doi.org/10.1103/PhysRevLett.105.254101`>. 2, 5, 10, 86

FORTUNATO, S. Community detection in graphs. **Physics Reports**, v. 486, n. 3–5, p. 75 – 174, 2010. ISSN 0370–1573. Available from: <`http://dx.doi.org/10.1016/j.physrep.2009.11.002`>. 60

FOSS, J.; MILTON, J. Multistability in recurrent neural loops arising from delay. **J Neurophysiol**, v. 84, p. 975–985, 2000. Available from: <`http://jn.physiology.org/content/84/2/975`>. 1

FRIDMAN, E. Tutorial on lyapunov-based methods for time-delay systems. **European Journal of Control**, v. 20, n. 6, p. 271 – 283, 2014. ISSN 0947-3580. 44

GOLUBITSKY, M.; STEWART, I. Synchrony versus symmetry in coupled cells. In: DUMORTIER, F.; BROER, H.; MAWHIN, J.; VANDERBAUWHEDE, A.; LUNEL, S. V. (Ed.). **Equadiff 2003: Proceedings of the International Conference on Differential Equations**. [S.l.]: World Scientific, 2005. p. 13–24. 1

GRZYBOWSKI, J.; MACAU, E.; YONEYAMA, T. The lyapunov-krasovskii theorem and a sufficient criterion for local stability of isochronal synchronization in networks of delay-coupled oscillators. **Physica D: Nonlinear Phenomena**, v. 346, p. 28 – 36, 2017. ISSN 0167-2789. 6

GRZYBOWSKI, J. M. V.; MACAU, E. E. N.; YONEYAMA, T. On the formulation and solution of the isochronal synchronization stability problem in delay-coupled complex networks. **Chaos**, v. 22, n. 3, 2012. 2, 6

HALE, J. K.; LUNEL, S. M. V. **Introduction to functional differential equations**. [S.l.]: Springer–Verlag, 1993. 447 p. 9, 23, 24, 25, 27

HART, J. D.; PADE, J. P.; PEREIRA, T.; MURPHY, T. E.; ROY, R. Adding connections can hinder network synchronization of time-delayed oscillators. **Phys. Rev. E**, American Physical Society, v. 92, p. 022804, Aug 2015. Available from: <`https://link.aps.org/doi/10.1103/PhysRevE.92.022804`>. 2, 5

HEILIGENTHAL, S.; DAHMS, T.; YANCHUK, S.; JÜNGLING, T.; FLUNKERT, V.; KANTER, I.; SCHÖLL, E.; KINZEL, W. Strong and weak chaos in nonlinear networks with time-delayed couplings. **Phys. Rev. Lett.**, American Physical Society, v. 107, p. 234102, 2011. Available from: <http://link.aps.org/doi/10.1103/PhysRevLett.107.234102>. 29

HORN, R.; JOHNSON, C. **Matrix analysis**. [S.l.]: Cambridge Univ. Press, 1985. 72

HÖVEL, P.; SCHÖLL, E. Control of unstable steady states by time-delayed feedback methods. **Phys. Rev. E**, American Physical Society, v. 72, p. 046203, Oct 2005. Available from: <https://link.aps.org/doi/10.1103/PhysRevE.72.046203>. 4

IZHIKEVICH, E. M. Polychronization: Computation with spikes. **Neural Computation**, v. 18, p. 245–282, 2006. Available from: <https://dx.doi.org/10.1162/089976606775093882>. 1

JAVALOYES, J.; MANDEL, P.; PIEROUX, D. Dynamical properties of lasers coupled face to face. **Phys. Rev. E**, v. 67, p. 036201, 2003. Available from: <http://journals.aps.org/pre/abstract/10.1103/PhysRevE.67.036201>. 1

KINZEL, W.; ENGLERT, A.; REENTS, G.; ZIGZAG, M.; KANTER, I. Synchronization of networks of chaotic units with time–delayed couplings. **Physical Review E (Statistical, Nonlinear, and Soft Matter Physics)**, APS, v. 79, n. 5, p. 056207, 2009. Available from: <http://link.aps.org/abstract/PRE/v79/e056207>. 2, 5

LEHNERT, J. **Controlling synchronization patterns in complex networks**. [S.l.]: Springer International Publishing, 2015. (Springer Theses). ISBN 9783319251158. 18

LI, J.; SHIU, W. C.; CHAN, W. H. The laplacian spectral radius of some graphs. **Linear Algebra and its Applications**, v. 431, n. 1, p. 99 – 103, 2009. ISSN 0024-3795. Available from: <http://www.sciencedirect.com/science/article/pii/S0024379509000901>. 57

LICHTNER, M.; WOLFRUM, M.; YANCHUK, S. The spectrum of delay differential equations with large delay. **SIAM J. Math. Anal.**, v. 43, p. 788–802, 2011. Available from: <http://dx.doi.org/10.1137/090766796>. 10, 23, 28, 29, 69

LÜCKEN, L.; PADE, J. P.; KNAUER, K.; YANCHUK, S. Reduction of interaction delays in networks. **EPL (Europhysics Letters)**, v. 103, n. 1, p. 10006, 2013. Available from: <`http://stacks.iop.org/0295-5075/103/i=1/a=10006`>. 1

MAIA, D. N. M.; MACAU, E. E. N.; PEREIRA, T. Persistence of network synchronization under nonidentical coupling functions. **SIAM J. Appl. Dyn. Syst.**, v. 15, n. 3, p. 1563–1580, 2016. Available from: <`http://epubs.siam.org/doi/10.1137/15M1049786`>. 8, 15, 41, 59

MEYER, C. **Matrix analysis and applied linear algebra book and solutions manual**. [S.l.]: Society for Industrial and Applied Mathematics, 2000. ISBN 9780898714548. 17

MILLER, N.; GARNIER, S.; HARTNETT, A. T.; COUZIN, I. D. Both information and social cohesion determine collective decisions in animal groups. **Proceedings of the National Academy of Sciences**, v. 110, n. 13, p. 5263–5268, 2013. Available from: <`http://www.pnas.org/content/110/13/5263.abstract`>. 1

MIROLLO, R. E.; STROGATZ, S. H. Amplitude death in an array of limit–cycle oscillators. **Journal of Statistical Physics**, v. 60, n. 1, p. 245–262, 1990. ISSN 1572–9613. Available from: <`http://dx.doi.org/10.1007/BF01013676`>. 3

MóRI, T. F. The maximum degree of the barabási–albert random tree. **Comb. Probab. Comput.**, Cambridge University Press, New York, NY, USA, v. 14, n. 3, p. 339–348, may 2005. ISSN 0963–5483. Available from: <`https://doi.org/10.1017/S0963548304006133`>. 20

NEWMAN, M. E. J. The Structure and Function of Complex Networks. **SIAM Review**, SIAM, v. 45, n. 2, p. 167–256, 2003. Available from: <`http://dx.doi.org/10.1137/S003614450342480`>. 19, 20

OGUCHI, T.; NIJMEIJER, H.; YAMAMOTO, T. Synchronization in networks of chaotic systems with time-delay coupling. **Chaos: An Interdisciplinary Journal of Nonlinear Science**, v. 18, n. 3, p. 037108, 2008. Available from: <`http://dx.doi.org/10.1063/1.2952450`>. 2, 4, 6

OROSZ, G.; WILSON, R. E.; STEPAN, G. Traffic jams: dynamics and control. **Phil. Trans. R. Soc. A**, v. 368, p. 4455–4479, 2010. 1

PALEY, D. A.; LEONARD, N. E.; SEPULCHRE, R.; GRUNBAUM, D.; PARRISH, J. K. Oscillator models and collective motion. **IEEE Control Systems**, v. 27, n. 4, p. 89–105, Aug 2007. ISSN 1066-033X. 9, 87

PECORA, L. M.; CARROLL, T. L. Master stability functions for synchronized coupled systems. **Phys. Rev. Lett.**, v. 80, p. 2109–2112, 1998. Available from: <`http://journals.aps.org/prl/abstract/10.1103/PhysRevLett.80.2109`>. 43

PENG, M.; YUAN, Y. Synchronization and desynchronization in a delayed discrete neural network. **International Journal of Bifurcation and Chaos**, v. 17, n. 03, p. 791–803, 2007. Available from: <`http://www.worldscientific.com/doi/abs/10.1142/S0218127407017550`>. 1

PEREIRA, T.; ELDERING, J.; RASMUSSEN, M.; VENEZIANI, A. Towards a theory for diffusive coupling functions allowing persistent synchronization. **Nonlinearity**, v. 27, n. 3, p. 501, 2014. Available from: <`http://stacks.iop.org/0951-7715/27/i=3/a=501`>. 8, 15, 41

PETSCHE, H.; BRAZIER, M. **Synchronization of EEG activity in epilepsies: a symposium organized by the Austrian Academy of Sciences, Vienna, Austria, September 12–13, 1971**. [S.l.]: New York: Springer-Verlag, 2012. ISBN 9783709183069. 1

PIKOVSKY, A.; ROSENBLUM, M.; KURTHS, J. **Synchronization: a universal concept in nonlinear sciences**. [S.l.]: Cambridge University Press, 2003. (Cambridge Nonlinear Science Series). ISBN 9780521533522. 1

PRIVAT, Y.; TRELAT, E. Control and stabilization of steady-states in a finite-length ferromagnetic nanowire. **ESAIM: COCV**, v. 21, n. 2, p. 301–323, 2015. Available from: <`https://doi.org/10.1051/cocv/2014028`>. 2

PYRAGAS, K. Continuous control of chaos by self-controlling feedback. **Physics Letters A**, v. 170, n. 6, p. 421 – 428, 1992. ISSN 0375-9601. Available from: <`http://www.sciencedirect.com/science/article/pii/037596019290745 8`>. 4, 87

RAMIREZ, J. P.; OLVERA, L. A.; NIJMEIJER, H.; ALVAREZ, J. The sympathy of two pendulum clocks: beyond huygens' observations. **Scientific Reports**, v. 6, n. 23580, p. 23580 EP –, 03 2016. Available from: <`http://dx.doi.org/10.1038/srep23580`>. 1

REDDY, D. V. R.; SEN, A.; JOHNSTON, G. L. Time delay induced death in coupled limit cycle oscillators. **Phys. Rev. Lett.**, American Physical Society, v. 80, p. 5109–5112, Jun 1998. Available from: <`http://link.aps.org/doi/10.1103/PhysRevLett.80.5109`>. 3

RIAL, J. A.; OH, J.; REISCHMANN, E. Synchronization of the climate system to eccentricity forcing and the 100,000-year problem. **Nature Geosci**, Nature Publishing Group, v. 6, n. 4, p. 289–293, 04 2013. Available from: <`http://dx.doi.org/10.1038/ngeo1756`>. 1

RIORDAN, O.; SELBY, A. The maximum degree of a random graph. **Comb. Probab. Comput.**, Cambridge University Press, New York, NY, USA, v. 9, n. 6, p. 549–572, nov. 2000. ISSN 0963–5483. Available from: <`http://dx.doi.org/10.1017/S0963548300004491`>. 20

RODRIGUES, F. A.; PERON, T. K. D.; JI, P.; KURTHS, J. The kuramoto model in complex networks. **Physics Reports**, v. 610, p. 1 – 98, 2016. ISSN 0370–1573. Available from: <`http://dx.doi.org/10.1016/j.physrep.2015.10.008`>. 60

ROSENBLUM, M.; PIKOVSKY, A. Synchronization: from pendulum clocks to chaotic lasers and chemical oscillators. **Contemporary Physics**, v. 44, p. 401–416, may 2003. 1

SIEBER, J.; WOLFRUM, M.; LICHTNER, M.; YANCHUK, S. On the stability of periodic orbits in delay equations with large delay. **Discrete Contin. Dyn. Syst. A**, v. 33, p. 3109–3134, 2013. 10, 23, 28, 29, 31, 43, 44

SINGER, W. Synchronization of cortical activity and its putative role in information processing and learning. **Annu. Rev. Physiol.**, v. 55, p. 349–374, 1993. 2

SMITH, H. L. **An introduction to delay differential equations with applications to the life sciences**. [S.l.]: Springer Science+ Business Media, 2010. 9, 23, 24, 32, 33

SORIANO, M. C.; GARCIA-OJALVO, J.; MIRASSO, C. R.; FISCHER, I. Complex photonics: Dynamics and applications of delay–coupled semiconductors lasers. **Rev. Mod. Phys.**, American Physical Society, v. 85, p. 421–470, 2013. Available from: <`http://link.aps.org/doi/10.1103/RevModPhys.85.421`>. 1, 5

STEUR, E.; MICHIELS, W.; HUIJBERTS, H.; NIJMEIJER, H. Networks of diffusively time–delay coupled systems: Conditions for synchronization and its relation to the network topology. **Physica D**, v. 277, p. 22–39, 2014. Available from: <`http://dx.doi.org/10.1016/j.physd.2014.03.004`>. 5

TESCHL, G. **Ordinary differential equations and dynamical systems**. [S.l.]: Amer Mathematical Society, 2012. (Graduate Studies in Mathematics Series). ISBN 9780821883280. 96

THOMPSON, M. J. Fundamentals and advancements in generator synchronizing systems. In: ANNUAL CONFERENCE FOR PROTECTIVE RELAY ENGINEERS, 65., 2012, Istanbul, Turkey. **Proceedings...** Istanbul, 2012. p. 203–214. 1

TRONCIU, V. Z.; WÜNSCHE, H.-J.; WOLFRUM, M.; RADZIUNAS, M. Semiconductor laser under resonant feedback from a fabry-perot resonator: Stability of continuous-wave operation. **Phys. Rev. E**, American Physical Society, v. 73, p. 046205, Apr 2006. Available from: <`https://link.aps.org/doi/10.1103/PhysRevE.73.046205`>. 2

WOLFRUM, M.; YANCHUK, S.; Hövel, P.; Schöll, E. Complex dynamics in delay–differential equations with large delay. **Eur. Phys. J. Special Topics**, v. 191, p. 91–103, 2010. Available from: <`http://dx.doi.org/10.1140/epjst/e2010-01343-7`>. 10, 23, 28, 29

WU, J. Symmetric functional differential equations and neural networks with memory. **Transactions of the American Mathematical Society**, American Mathematical Society, v. 350, n. 12, p. 4799–4838, 1998. ISSN 00029947. Available from: <`http://www.jstor.org/stable/117746`>. 1

YANCHUK, S.; GIACOMELLI, G. Spatio-temporal phenomena in complex systems with time delays. **Journal of Physics A: Mathematical and Theoretical**, v. 50, n. 10, p. 103001, 2017. ISSN 1751–8121. Available from: <`http://stacks.iop.org/1751-8121/50/i=10/a=103001`>. 1, 5, 10, 28, 29

YANCHUK, S.; PERLIKOWSKI, P. Delay and periodicity. **Phys. Rev. E**, APS, v. 79, n. 4, p. 046221, 2009. Available from: <`http://link.aps.org/abstract/PRE/v79/e046221`>. 23, 28, 29, 33, 36

YANCHUK, S.; WOLFRUM, M. Instabilities of equilibria of delay–differential equations with large delay. In: ENOC, 5., 2005, Eindhoven, Netherlands. **Proceedings...** Eindhoven, 2005. p. 1060–1065. 28, 29

YANCHUK, S.; WOLFRUM, M.; HÖVEL, P.; SCHÖLL, E. Control of unstable steady states by long delay feedback. **Phys. Rev. E**, v. 74, p. 026201, 2006. 2, 4, 10, 63, 72, 75, 77